Determinants of *IL7* Expression in B cells of Patients with Metastatic Melanoma

Akin-Adigun Oluwafemi

Supervisor: Prof. Benjamin P. Fairfax

A thesis submitted for the degree of Master of Science (by Research) in Oncology

Michaelmas Term 2024





Department of Oncology

St. Catherine's College

University of Oxford

Abstract

Background: Immune checkpoint blockade (ICB) has revolutionized the care of metastatic melanoma. However, they are frequently associated with autoimmune side effects referred to as immune-related adverse events (irAEs) that complicates their use. For which there is currently no biomarker to identify patients at risk. Previous work from the group has shown that allelic variation at rs16906115, a single nucleotide polymorphism (SNP) intronic to *IL7* (encoding IL-7) was predictive of high grade irAEs in melanoma patients receiving ICB. Carriers of the minor allele at this locus were shown to have higher levels of *IL7* expression in their B cells compared to non-carriers. It was also noted that melanoma patients' B cells significantly upregulated *IL7* compared to B cells isolated from healthy donors. Furthermore, in patients, *IL7* was found to be predictive of irAEs independent of genotype. This suggests a causal link between B cell *IL7* and irAEs with melanoma inducing this effect. However, the mechanism whereby melanoma leads to induction of *IL7* in B cells is unclear. This thesis aims to explore the determinants of *IL7* expression in B cells of patients with melanoma and characterise the role of antibodies in the anti-tumour response.

Methods: Healthy B cells were cultured in plasma from patients with metastatic melanoma as well as in melanoma conditioned media. Plasma concentrations of 92 proteins with immunological relevance were determined using a proximity extension assay, these data were integrated with bulk RNA and single cell data to explore correlates of B cell *IL7* expression. Durable responders were identified and re-sampled to explore the long-term effects of ICB on B cells. Finally, plasma concentrations of immunoglobulin isotypes were determined using a bead-based approach and integrated with flow cytometry assessment of immune cell composition to characterise the humoral response to metastatic melanoma.

Results: Melanoma secretome induces B cell *IL7* expression, although this response is highly heterogeneous. Plasma IL-6 and IL-10 are potential regulators of B cell *IL7* expression. B cell interactions with $CD4^+$ T cells via CD40LG/CD40 ligand-receptor pairing might be a potential stimulator of *IL7* expression. Finally, plasma IgD is a predictor of poor clinical outcome in metastatic melanoma patients and is associated with significant differences in $CD8^+$ T cell subset composition.

Conclusion: Taken together, the results from this research might provide further insights into the B cell response to melanoma and the impact on oncological outcomes and the development of irAEs.

Acknowledgements

I would like to extend my profound gratitude to my supervisor, Prof. Benjamin Fairfax for his invaluable guidance, unwavering support and constructive feedback throughout every stage of the research journey. He has given me the opportunity to form and explore my own ideas. I am immensely grateful to every member of the Fairfax group, past and present: Dylan Muldoon, Julia Bremke and Sophie Mackay for teaching me good experimental techniques and assisting with wet lab work; Gusztav Milotay and Martin Little for their ongoing feedback to ensure the success of this work; Shawn Sun, Lea Cohen and Guangyi Niu for their guidance and support with bioinformatic analyses; Chelsea Taylor, Orion Tong, and Robert Watson whose hard work laid the foundation for this thesis.

I would like to appreciate my Mum and Dad, for the unshakable emotional and financial support; my siblings, Tosin and Iyanu; my friends – Olayinka and Charles – who walked this journey with me.

Finally, I am grateful to God almighty for the incredible grace to come this far.

Table of Contents

1. Introduction

1.1. Melanoma……..1
1.1.1. Epidemiology…….....1
1.1.2. Risk Factors…….....1
1.1.3. Common mutations in Melanoma…..……...2
1.1.4. Management of Melanoma……4
1.2. Immune Checkpoint Blockade……..5
1.2.1. Overview……....5
1.2.2. Classification and Mechanism of Action…….....5
1.2.3. The burden of immune related adverse events……..6
1.2.4. Biomarkers of immune related adverse events……..7
1.3. The Genetic biomarker of irAEs……...8
1.3.1. B cell *IL7* expression.……8
1.3.2. What is Interleukin 7?…….....8
1.4. The role of B cells in Melanoma……10
1.5. Thesis aims and objectives……..11
1.5.1. Aims and objectives……11
1.5.2. Justification……....……..11

2. Materials and Methods…….……**12**

2.1. Samples……...12
2.1.1. Patient Cohort……...……...12
2.1.2. Clinical outcome data……...……...12
2.1.3. Laboratory blood count……...12
2.1.4. Survival Analyses……...……12
2.2. Peripheral blood sample processing……13
2.2.1. Ficoll Density Gradient Centrifugation……...……13
2.2.2. Plasma Collection……...……13
2.2.3. Peripheral blood mononuclear cell collection……...……..13
2.2.4. Magnetic-activated cell sorting separation……...……...14
2.2.5. RNA extraction……....14
2.2.6. Blood cone……...14
2.3. Cell culture……..14
2.3.1. Tumour cell lines……...……...14
2.3.2. B cell induction with Plasma……...15
2.3.3. B cell induction with melanoma-conditioned media……...15
2.4. Quantitative polymerase chain reaction (qPCR) ……15
2.4.1. RNA extraction……..15
2.4.2. Complementary DNA generation…….……...16
2.4.3. Primer design and validation……...16
2.4.4. qPCR reaction……..……....16
2.5. Flow Cytometry……..……17
2.6. Measurement of Plasma Immunoglobulin……..……18
2.7. Proteomic analyses……..……19
2.7.1. Sample preparation……...……...19
2.7.2. Normalisation and quality control……...19
2.8. Transcriptomic analyses……..……19
2.8.1. Bulk RNA sequencing……..……...19
2.8.1.1. Library preparation……...……..19
2.8.1.2. Sequencing and upstream data analysis……...……..19
2.8.1.3. Differential gene expression……...19

2.8.1.4. Pathway analysis……20
2.8.2. Single Cell RNA sequencing……...20
2.8.2.1. Sample preparation……..……..20
2.8.2.2. Pre-processing, QC and cell filtering……...……...20
2.8.2.3. Clustering and Annotation……..20
2.8.2.4. NicheNet Analysis……..20
2.8.2.4.1. Sender Agnostic Approach……..……21
2.8.2.4.2. Sender Focused Approach……..…21

3. Results

3.1. Immune related adverse events and Patient outcome……..…22
3.1.1. Introduction…….……....22
3.1.2. Baseline characteristics of patients and irAEs…….……....22
3.1.3. The occurrence of any grade irAEs is associated with improved patient outcome……22
3.1.4. Sub-section summary……...……....27
3.1.5. Sub-section acknowledgements……...……....27
3.2. Induction of *IL7* in B cells……..……28
3.2.1. Introduction……..……....28
3.2.2. Healthy B cells in Plasma……....28
3.2.3. B cell *IL7* expression by Melanoma-conditioned media…….……....30
3.2.4. B cell *IL7* expression and patient characteristics…….……....31
3.2.5. Sub-section summary……...……....32
3.3. Plasma Proteins and B cell *IL7* expression…….……33
3.3.1. Introduction……..……....33
3.3.2. Normalisation and Quality control……...……...33
3.3.3. Plasma IL-6 and IL-10 concentration anti-correlates with B cell *IL7* expression ……..……....34
3.3.4. Pre-treatment monocyte count interacts with B cell *IL7*……..……...35
3.3.5. Sub-section summary……...……....37
3.3.6. Sub-section acknowledgements……...……....37
3.4. Cell-cell interaction using NicheNet……...……38
3.4.1. Introduction……..……....38
3.4.2. Selection of gene set of interest and background genes……...……...38
3.4.3. Sender Agnostic method……..……....38
3.4.4. Sender Focused method……...……....40
3.4.5. *CD40LG*/*CD40* correlates with B cell *IL7* in single cell and bulk RNA data.. ……..42
3.4.6. Sub-section summary……...……....43
3.4.7. Sub-section acknowledgements……..……....43
3.5. *IL7* dynamics in Durable Responders…….……43
3.5.1. Introduction……..……....43
3.5.2. Batch Effects Correction……..……....43
3.5.3. Long term B cell transcriptomic changes…….……...44
3.5.4. Sub-section acknowledgements……...……....46
3.6. The Humoral response and impact on outcome in patients with metastatic melanoma ……47
3.6.1. Introduction……..……....47
3.6.2. Immunoglobulin concentration and patient outcome……...……...47
3.6.3. B cell *IL7* and Plasma Immunoglobulin concentration……...48
3.6.4. Differences in immune cell composition by Plasma Immunoglobulin D concentration……49
3.6.5. Low Immunoglobulin D correlates with genes in $CD8^+$ T cell involved in the production of pro-inflammatory cytokines……..…..51
3.6.6. Sub-section summary……...……....52

3.6.7.Sub-section acknowledgements……...……....52
4. Discussion……..…….53
4.1. Discussion……...……..……53
4.2. Limitations……..…….54
4.3. Future directions…….…….55
4.4. Executive summary…….55
Appendix A – Optimizing the B cell culture……..57

Appendix B – Supplementary Images…….……..59

Bibliography…….…….62

Chapter 1: Introduction

1.1 Melanoma

Melanoma is a form of skin cancer, arising from the malignant transformation of melanocytes, the pigment producing cells of mainly neural crest origin, which are present in the basal layer of the skin[1]. However, melanocytes are not limited to the skin and can also be found in the retinal pigment epithelium of the eyes, the stria vascularis of the cochlea, the leptomeninges, the heart as well as the mucosal linings[2-5]. Hence, there are various forms of the disease: cutaneous melanoma, uveal melanoma, mucosal melanoma etc. In this chapter, I describe the current knowledge of the biology of melanoma and its management strategies.

1.1.1 Epidemiology

Cutaneous melanoma is the most common form of melanoma with a global incidence of 15 – 25 per 100, 000[6]. It occurs mostly in Caucasians and despite accounting for less than 10% of all skin cancers, it is the most aggressive form, responsible for up to 90% of all skin-cancer related deaths[7]. Median overall survival is 6 months in patients with distant metastatic disease who receive no treatment. In the United Kingdom (UK), cutaneous melanoma is the 3rd most prevalent cancer with a continuously rising incidence, related to changing leisure-time habits e.g., intermittent sun exposure and episodes of sunburn from tanning. Globally, it is deemed one of the fastest growing cancers[1, 7, 8].

1.1.2 Risk Factors

Like every cancer, melanoma arises from the complex interplay between genetic and environmental risk factors[9]. Several epidemiological studies have shown that sun exposure/ultra-violet radiation (UVR) is the most important of the environmental risk factors implicated[10]. Ultraviolet (UV) light has three different wavelengths: UV-A (315nm-400nm), UV-B (280nm-315nm) and UV-C (100–280 nm)[11]. UV-B and C are highly absorbed by DNA and can directly induce DNA damage; UV-A, on the other hand, is poorly absorbed but can indirectly induce DNA damage through the production of reactive oxidative species (ROS)[12]. The damage to the DNA occurs through the formation of cyclobutene pyrimidine dimers and 6-4 pyrimidine-pyrimidone photoproducts, interfering with the DNA structure and causing alterations in transcription[12, 13]. Usually, these so called “DNA adducts” are identified and removed by the nucleotide excision repair (NER) system. However, impairment in any component of this system can lead to inability to repair DNA damage and increase the risk of melanoma. This is typified by the autosomal recessive disease – Xeroderma pigmentosum (XP)[14]. Individuals with XP have a deficiency in the NER system and their susceptibility to skin cancer is increased by 1000-fold[15, 16]. This suggests that the underlying mechanism behind melanoma formation is the lack of complete repair of skin cancer-associated mutations.

Perhaps, arguably more important are host risk factors for melanoma. While UVR exposure is critical for the formation of melanoma, genetic susceptibility sets the stage. Genetic polymorphisms in *MC1R* are responsible for ethnic differences in constitutive pigmentation and for different responses to UVR exposure[17]. In response to UVR exposure, α-Melanocyte-stimulating hormone (α-MSH) production is increased from both keratinocytes and melanocytes[18]. This binds to melanocortin 1 receptor (MC1R), present on the cell membranes of melanocytes and leads to the activation of protein kinase A (PKA)[19]. PKA in turn activates

cyclic adenosine monophosphate (cAMP) responsive element binding protein (CREB), a transcription factor that regulates the expression of melanocyte inducing transcription factor (*MITF*)[20, 21]. This leads to increased proliferation of melanocytes and synthesis of melanin. Melanin is stored in vesicles and transferred to surrounding keratinocytes, where it is arranged strategically over the sun-exposed region of the DNA[21, 22]. Individuals with non-functional polymorphisms in the *MC1R* gene (such as 'red-head' phenotype) are unable to initiate this process and are prone to sunburn and melanoma[23, 24]. The differences in the degree of pigmentation, which is determined by the ratio between the more UV-protective eumelanin and the less UV-protective pheomelanin, have been identified as a risk factor for melanoma. Faired-skinned populations such as Caucasians with low eumelanin/pheomelanin ratio, have a higher incidence of melanoma compared to dark-skinned populations with higher eumelanin[25]. A genome-wide association (GWAS) meta-analyses by Landi *et al* identified 68 single nucleotide polymorphisms in 54 loci associated with increased risk of melanoma. Many of these genes were enriched in pathways associated with skin pigmentation and nevi count[26]. Other polymorphisms involve genes active in telomere maintenance. In melanocytes carrying oncogenic mutations, longer telomeres are associated with delayed senescence. This leads to an increased risk of acquiring further mutations associated with malignant transformation. Telomerase is a ribonuclease consisting of RNA template (TERC) and reverse transcriptase catalytic subunit (TERT) and is responsible for elongation of the telomere, by synthesizing new DNA[27]. Two independent studies have identified an association between activating polymorphisms in the promoter region of *TERT* and increased risk of melanoma[28, 29]. Others have reported an association between melanoma and pathogenic variants in *POT1*, *ACP* and *TER2IP*[30-32].

The presence of precursor lesions such as the melanocytic nevus is another risk factor for melanoma. Melanocytic nevi are benign overgrowths of melanocytes and lead to hyperpigmented spots on the skin. This can be congenital or acquired and the sudden accumulation of several of these lesions in later life or the change in phenotypic features is a risk factor for melanoma. A study by Gandani *et al* 2005 showed that individuals with ≥100 melanocytic naevi carry a sevenfold increased risk for lifelong melanoma development[33]. Advanced age is a risk factor for melanoma and a predictor of poor outcomes. One reason for this is believed to be the reduced immunosurveillance associated with increasing age. Although melanoma has a median age at onset of 67 years, there have been several reports of the disease in the young. In the United States, cutaneous melanoma is one of the most common cancer in adults aged 20 – 39 years[34].

1.1.3 Common mutations in Melanoma

Mutations leading to melanoma can either be sporadic or germline. Familial melanoma which accounts for less than 10% of all melanomas is associated with low frequency and high penetrance mutations. The most common of these include mutations in the *CDKN2A* locus, found in 40% of all familial melanomas and encodes two different tumour suppressor proteins – $p16^{INK4A}$ and $p14^{ARF}$ – produced via alternative promoters and translation through different reading frames. Wild-type $p16^{INK4A}$ regulates cell-cycle progression from G1-S phase by inhibiting the phosphorylation of the retinoblastoma (RB) protein by the cyclin-dependent kinases, CDK4 and CDK6. In contrast, $p14^{ARF}$ stabilizes and prevents the ubiquitylation of p53 thereby causing cell arrest in both G1/S and G2/M phase[1, 35, 36]. Therefore, inactivating mutations in *CDNK2A* gene promotes uncontrolled cellular proliferation and increase the risk

of cancers. Other genes associated with familial melanomas involve rare mutations in *CDK4* involved in cell cycle control or *BAP1* involved in the DNA damage response[1].

Sporadic melanomas on the other hand account for 90% of all melanomas and are frequently driven by mutations that have high prevalence and low penetrance[1]. Many of these mutations are enriched in the mitogen-activated protein kinase (MAPK) pathway and the phosphatidyl inositol-3-kinase AKT pathway (Figure 1.1). The MAPK pathway is a key signal transduction pathway that regulates critical molecular processes involved in cell proliferation, cell differentiation and cell survival[37]. The MAPK pathway is otherwise known as the RAS-RAF-MEK-ERK pathway, indicating the proteins activated sequentially in the pathway. *BRAF* mutations are found in approximately 40 – 60% of all melanoma and the most common (approximately 90%) is the V600E missense mutation (transversion of T to A at nucleotide 1799) which results in the conversion from the hydrophobic amino acid, valine into the hydrophilic amino acid, glutamic acid[38]. Because V600E mutation is also found in >80% of acquired melanocytic nevi, it is believed that this might represent a first step in the cell transformation i.e. senescence and additional mutations are required for the development of overt malignancy[1]. With an incidence that vary between 10 – 30%, the V600K is second most common *BRAF* mutation and results in the conversion of valine into the hydrophilic amino acid lysine. A study by Zengarini *et al* comparing patients with V600E to the V600K mutation revealed that although there was no significant difference in the tumour morphology between the two, the V600K mutation was associated with higher frequency of metastasis and disease progression[39].

The most commonly mutated RAS protein in melanoma is the Neuroblastoma RAS (NRAS) proto-oncogene found in approximately 15 – 20% of all melanomas. The dimerization and auto-phosphorylation of receptor tyrosine kinases (RTKs) leads to the activation of NRAS, which then promotes the activity of downstream RAF[36, 40]. Activating mutations are commonly found in Q60/61 and G12/13 codons[8]. Interestingly, mutations in *BRAF* and *NRAS* are usually mutually exclusive in single cell[41]. The reason for this has been linked to hyperactivation of the MAPK pathway which eventually leads to self-induced apoptosis of the cell[42]. Suggesting that mutation in only one of these genes is required for malignant transformation. *Neurofibromin 1 (NF1)* is a tumour suppressor gene and a negative regulator of the RAS-RAF pathway. Wildtype *NF1* exerts its control on cell cycle by converting the active RAS guanosine triphosphate (RAS-GTP) to its inactive form, RAS guanosine diphosphate (RAS-GDP), thereby inhibiting downstream RAS signalling[43]. Loss of function mutations in *NF1* leads to unchecked signalling of the MAPK pathway and is associated with a 3.6-fold increase in the risk of melanoma[44]. Melanomas with *NF1* mutations are usually found on skin with chronic sun exposure or in older adults[43]. *NF1* mutations are enriched in desmoplastic melanoma, a rare form of melanoma characterised by diverse activation of the RAS/MAPK pathway and distinct clinical and histopathological features[43, 45]. Melanoma lacking mutations in either of *BRAS*, *NRAF* or *NF1* are referred to as the triple-wild type melanomas[46]. These melanomas are associated with low-frequency driver mutations in *GNA11*, *GNAQ*, *KIT*, *CTNNB1*, *EZH2*[46]. Triple-wild type melanomas are characterised by low mutational burden, lack of UV signature and usually associated with mucosal and uveal melanomas[46-48].

The PI3K-AKT pathway plays a pivotal role in transmitting signals for cellular growth and proliferation and is often activated in melanoma because of inactivating mutations in the

tumour suppressor gene *PTEN* and activating mutations in *AKT*[37]. *PTEN* encodes a phosphatase that negatively regulates PIP3, an intermediate in the PI3K-AKT pathway. Loss of function mutation in *PTEN* thus lead to constitutive activation of the PI3K pathway and increase in AKT activity[49]. *PTEN* mutations are found to be enriched in individuals with metastatic melanoma compared to individuals with primary disease and therefore suggests a role in melanoma progression[50]. The predominant isoform of AKT protein in melanoma is AKT3 which is found in 70% of all melanomas and drives progression to a more aggressive cancer[36]. Other commonly mutated genes in melanoma include genes involved in pigmentation such as the melanocortin-1 receptor (*MC1R*), microphthalmia-associated transcription factor (*MITF*), tyrosinase (*TYR*), tyrosinase-related protein-1 (*TYRP1*), SRY-box transcription factor 10 (*SOX10*) and paired box 3 (*PAX3*)[51]. Functional deficiencies in any of the aforementioned genes lead to imbalances in the eumelanin/pheomelanin ratio, thereby increasing the risk of melanoma[36].

Melanoma carries the highest mutational burden of all human tumours[52, 53]. In a whole genome sequencing (WGS) study by Hayward *et al.*, it was reported that melanomas have an average rate of 38.23 mutations per megabase of DNA[48]. This property of melanoma leads to the production of a large repertoire of tumour antigens which can interact with the immune system. This makes melanoma highly immunogenic and very susceptible to treatments that manipulates the immune system[54].

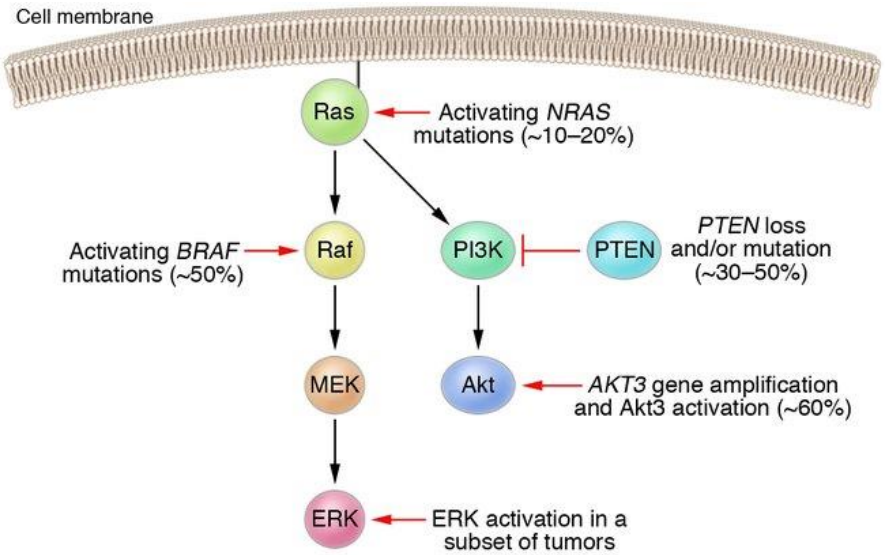


Figure 1.1: Genetics of Melanoma. Image obtained from[55]

1.1.4 Management of Melanoma

The clinical management of melanoma requires adequate staging of the disease at the time of diagnosis to guide therapy decisions. Of the several available forms of staging, the American Joint Committee on Cancer (AJCC) is the most clinically relevant, the eight edition of which was implemented in 2018 and is based on tumour size and degree of spread in the body[56]. Simplistically, it divides melanoma into 4 distinct stages from Stage 1 through to IV in order

of increasing severity. While early-stage disease (stage I and II) is associated with a comparatively better overall survival, stage IV disease is associated with precarious prognosis and stage III disease has a more heterogenous prognosis[57]. Stages I, II and early-stage III disease, together referred to as resectable melanoma are managed with surgical excision with curative intent. Whereas, late-stage III and stage IV, also known as unresectable/metastatic melanoma are managed with systemic anti-cancer therapy (SACT).

SACT for melanoma comes in various forms: chemotherapy (e.g. Dacarbazine), targeted therapies (e.g. BRAF/MEK inhibitors) and immunotherapy (e.g. immune checkpoint blockade). Prior to the introduction of immune checkpoint blockade (ICB), dacarbazine was the first agent approved for the management of malignant melanoma with an objective response rate (ORR) of 10 – 20% [58, 59]. However, melanoma is chemo-resistant and for many years, Dacarbazine was the only single-agent chemotherapy approved for the treatment of melanoma. Several other systemic agents were tried singly or in combination with dacarbazine but showed no significant benefit for patients[60, 61]. Currently the standard of care for the management of metastatic melanoma involves the use of ICB or molecular targeted therapies.

Since the introduction of ICB for the treatment of metastatic melanoma in 2010, the outlook in melanoma care has greatly improved. Median overall survival (OS) was less than 6 months in 2013 for patients with metastatic melanoma. However, median OS has improved to 72 months for patients receiving combination treatment and 36.9 months for patients taking single agent ICB[62].

1.2 Immune Checkpoint Blockade

1.2.1 Overview

The discovery of immune checkpoint blockade (ICB) changed the narrative in the treatment of metastatic melanoma. By removing the so-called ‘brakes’ and consequently unleashing the power of the immune system on cancers, ICB are able to induce a strong immune response against tumours[63]. These “brakes” under normal conditions serve to prevent collateral damage on the ‘self’ while the immune system attacks the ‘non-self’. In other words, immune checkpoints serve to preserve self-tolerance. However, one of the hallmarks of cancer is immune evasion, and these so called “brakes” can be co-opted by the cancer cells to evade immune surveillance and effector functions[64]. These “brakes” thus provide potential druggable targets in cancer therapy design.

1.2.2 Classification and Mechanism of Action

The immune checkpoint blockade/inhibitors are classified based on the checkpoint molecule they interact with. CTLA-4 was the first immune checkpoint that was discovered and plays a central role in T cell activation, by acting as a competitive inhibitor of CD28. Engagement of CD28 by its ligands CD80/86 on antigen presenting cells (APCs) leads to generation of costimulatory signals necessary for the amplification and maintenance of T cell activation[65]. However, engagement of CTLA-4 leads to dampening of T cell activation in normal states. In cancer, chronic antigen stimulation drives T cells into an exhaustive phenotype characterised by the upregulation of CTLA-4 and loss of T cell effector functions. In addition, CTLA-4 causes sequestration of CD80/86 from the cell membrane of antigen presenting cells, via trans-

endocytosis, further impairing the costimulatory effect of CD28[66]. Monoclonal antibodies against CTLA-4 such as Ipilimumab has been designed to cause reversal of T cell exhaustion frequently observed in the immune system of cancer patients, thereby restoring the ability of these cells to kill the tumour[67].

PD-1/PD-L1 system is another well studied immune checkpoint in humans. In contrast to CTLA-4, PD-1 can be thought of as an identifier of 'membership'. That is cells bearing the ligands (PD-L1 and PD-L2) for the receptor are spared from cytotoxic activity of effector T cells. It thus plays a central role in the maintenance of immune tolerance[68]. Monoclonal antibodies against PD-1 such as Nivolumab and Pembrolizumab are approved for use in the management of metastatic melanoma.

Relatlimab, a monoclonal antibody against checkpoint molecule Lymphocyte-activation gene 3 (LAG-3) was recently approved in combination with nivolumab for the management of metastatic melanoma following a phase III trial (Relativity-047) which showed a longer progression-free survival of 10.1 months in patients receiving combination Relatlimab/Nivolumab versus 4.6 months in patients taking Nivolumab alone[69, 70].

1.2.3 The burden of Immune related adverse events

Despite the significant success of these medications in the management of metastatic melanoma, a major Achilles heel to the use of these medications is their potential to cause off-target autoimmune-like side effects otherwise referred to as immune related adverse events (irAEs)[71]. They are characterised by varying degrees of organ damage and associated with infiltration of cytotoxic T cells into the organs. irAEs are perversive and can affect any organ in the body at varying onset and severity[72]. This heterogeneity can be based on the class or dose of ICB administered or patient-related factors[73]. The median time to first toxicity is within 4 months of commencing ICB with peak onset within the first 4 weeks of therapy. However, irAEs have been reported within a few days of ICB initiation and after 1 year of ICB discontinuation[74]. irAEs are defined and graded based on the Common Terminology Criteria for Adverse Effects (CTCAE) into grades 1 through to 5: mild, moderate, severe, life-threatening and death. Mild to moderate toxicities are frequent and management can simply involve close monitoring of patient to withholding therapy for a few weeks until symptoms resolve. Grade 3 or 4 disease require high dose corticosteroids or other immunosuppressants and the permanent discontinuation of therapy[75].

The onset and management of irAEs is a subject of major dilemma in clinical practice and goes beyond the high incidence and potential disruption of anti-cancer therapy. In some cases, the organ damage caused by irAEs can have irreversible long-term side effects requiring lifelong therapy[76]. For example, hypopituitarism requiring hormonal supplementation or kidney failure requiring renal replacement therapy. In addition, while ICB can be said to "switch on" the immune system against cancer, the management of irAEs is centred around treatment with medications that dampen the immune response. It is unclear the effects of these medications on the long-term patient outcome. Although several studies have reported that there is no effect of immunosuppressants on survival[77, 78], some studies have identified a potential negative role of steroids on survival[79, 80].

More interestingly, the occurrence of irAEs have been reported to associate with better outcome in cancer patients being treated with ICB[74, 81]. It is perhaps intuitive to find an outcome benefit

for the occurrence of irAEs as the activated immune system against cancer can also lead to increased risk of autoimmunity. However, many of the studies evaluating this relationship are retrospective and did not account for the immortal time bias of irAEs[82]. Recent studies looking at this relationship used the landmark analyses method to account for this bias. However, this approach is limited by heterogeneity in the onset of irAEs which makes the selection of a landmark time particularly challenging. In addition, there are studies that have reported a negative role of irAEs on patients' response[83]. In this thesis, I used the time-dependent covariate analyses to address this immortal time bias, and is reported in the first section of chapter 3. Taken together, the high burden of irAEs highlights an urgent need for biomarkers for risk stratification of patients.

1.2.4 Biomarkers of Immune Related Adverse Events

According to the FDA, a biomarker is defined as a characteristic that is measured as an indicator of biological or pathogenic processes or responses to an intervention[84]. In the context of irAEs, there is no currently approved biomarker for routine use in the clinic[85]. However, several categories of biomarkers have been evaluated for their predictability of irAEs. Many of these biomarkers, double as biomarkers of anti-tumour response and might suggest more of immune fitness rather than predict irAEs. Decoupling the "anti-tumour" response and the "anti-self" response in the context of ICB would indeed be transformative in cancer immunology.

The peripheral blood is of particular importance to clinicians due to ease and accessibility of samples. Baseline absolute neutrophil count (ANC) has been reported to negatively correlate with irAEs[85, 86]. In a study by Liu *et al*, it was reported that a 1.11×10^9/L decrease in ANC was associated with increased risk of grade 3 or higher irAEs[86]. On the other hand, high absolute lymphocyte count associates with increased risk of irAEs[87-89]. Peripheral blood derived marker such as the Neutrophil-Lymphocyte ratio (NLR) and the Lymphocyte-Monocyte ratio (LMR) have also been shown to correlate with risk of irAEs. In a meta-analysis by Zhang *et al* of 47 studies published between 2018 and 2023 they observed that patients with NLR less than 3 were at higher risk of irAEs[90]. For other immune cell subsets, high baseline absolute eosinophil count (AEC) has been reported to correlate with increased risk of irAEs[91, 92]. In one study, high AEC was found to associate with increased risk of endocrine irAEs in melanoma patients[93].

Cytokines form an important group of mediators of the immune response and as such their role in predicting irAE has been extensively explored. In particular, lower levels of IL-6[94] and TNF-α at baseline have been reported to associate with increased risk of irAEs. In contrast, higher levels of IL-17 have been associated with severe colitis in patients on anti-CTLA-4[95]. Given studies that have reported that the mechanism behind irAEs is a breakdown of self-tolerance, autoantibodies have been evaluated as potential biomarkers of irAEs. The presence of organ-specific autoantibodies has been reported to increase the risk of irAEs in that organ. For example, several studies have found that the presence of antithyroid antibodies at baseline was associated with an increased risk of thyroiditis secondary to ICB[96-98]. In addition, high levels of generic autoantibodies such as rheumatoid factor and anti-nuclear antibodies was correlated with increased risk of irAEs in any organ[99]. More recent studies have found that it is not just the presence of these autoantibodies at baseline that is important, but also a change in levels following the commencement of ICB[100, 101].

1.3 The Genetic biomarker of irAEs

1.3.1 B cell *IL7* expression

The heterogeneity in the onset and severity of immune related adverse events suggests that there might be an underlying genetic component. It has been shown recently that genetic variation may influence response to ICB and potentially the risk of irAEs[102]. Groha *et al* in 2021 performed a genome-wide association study of 1751 patients with various cancers managed with ICB and identified three genomic loci associated with any grade immune related adverse events: *IL22RA1, LINCO2484, IL7*[103]. The allelic variation at rs16906115, a single nucleotide polymorphism (SNP) in *interleukin 7 (IL7)* has been replicated in 3 independent cohorts, including a study by Taylor *et al* where it was shown that melanoma patients who carried the minor allele at this locus (~8% European population) had increased likelihood of developing severe irAEs requiring corticosteroid treatment before the fifth cycle of ICB[104]. Mechanistically, it was shown that carriers of the *IL7* SNP expressed more *IL7* in their B cells compared to non-carriers. This effect was found to be significantly higher in peripheral blood isolated B cells from patients with metastatic melanoma compared to B cells from healthy donors. Interestingly, this effect was not found in other immune subsets and was independent of the ICB class received by the patient. However, independent of the SNP, *IL7* expression in melanoma patients' B cells was found to correlate with increased risk of irAEs, suggesting a causal link. It does however seem like the effect of *IL7* expression in B cells is context-dependent. While it increases the likelihood of irAEs in patients exposed to ICB, the carriage of the risk allele was associated with prolonged progression free survival in patients not treated with ICB[104]. Suggesting a wider role of *IL7* and B cells in the evolution of melanoma.

1.3.2 What is Interleukin 7?

IL7 is a protein coding gene located on the long arm of chromosome 8. It encodes the cytokine, IL-7 which has been described as the most extensively studied cytokine, likely because of its pervasive effects on almost all immune cells at multiple stages of their developmental process. The active form of IL-7 is a 24kDa globular protein which is folded into four alpha helices with a hydrophobic core. IL-7 is produced mainly by stromal cells in the bone marrow, thymus and secondary lymphoid organs. It has also been reported to be produced by cells in the intestines, ovaries, liver, skin and brain[105, 106]. It is generally believed that IL-7 is not produced by lymphocytes nor other members of the immune system. While little is known about the constitutive production of IL-7, IL-7 has been reported to be inducible by interferon gamma (IFN) in intestinal epithelial cells[105] and salivary gland epithelial cells[107]. In addition, Weitzmann *et al* showed that IL-1 and TNF-α can induce *IL7* expression in stromal cells[106, 108]. On the other hand, Tang *et al* reported that TGF-beta leads to reduced expression of *IL7* in stromal cells[106, 109].

IL-7 signals through the IL-7 receptor (IL7R), a heterodimer consisting of IL7R alpha (otherwise referred to as CD125) and the common cytokine receptor gamma chain (CD132). Engagement of IL-7 to its receptor leads to downstream signalling involving PI3K and JAK-STAT pathways, supplying cells with anti-apoptotic and proliferative signals. IL-7 plays an important role in T cell development and homeostasis. IL7R is expressed on double negative (DN) thymocytes where it provides necessary proliferative signals and directly instructs the recombination of the TCR gamma locus through DNA demethylation and histone

acetylation[110]. IL7R expression is lost on double positive cells, but reappears on single positive T cells. Post development, IL7R expression is maintained on mature T cells by transcription factors forkhead box protein 01 and Ets-1[111]. IL-7 is important for maintaining the survival of naïve T cell populations. However, following T cell activation, T cells downregulate IL7Rα and this prevents further response to IL-7. IL7R is then re-expressed on memory T cells where it is involved in the homeostasis of this cell population. Indeed, there is an inverse correlation between plasma IL-7 concentrations and T cell populations, specifically, $CD4^+$ T cells[112, 113]. The high IL-7 concentration in lymphopaenic conditions is believed to be a result of decreased consumption by T cells and levels usually return to normal following the restoration of $CD4^+$ T cell numbers. This regulatory pattern is described to be reminiscent of the relationship between erythropoietin and red blood cell counts. The vital role of IL7/IL7R axis on T cells is exemplified by the patients with severe combined immunodeficiency (SCID). These patients have reduced numbers or total absence of T cells. IL-7 also plays a vital role in B cell maturation. IL7R is expressed on common lymphoid progenitors (CLPs) and B cell progenitors through the pro-B cell stage, then downregulated on pre-B cells. However, unlike mature T cells, IL7R is not re-expressed by mature B cells[110, 114]. Suggesting that IL-7 has no direct effects on mature B cells. However, Sammicheli *et al* reported that IL-7 can maintain B cell survival and proliferation indirectly via the induction of CD70 and BAFF in resting T cells[115].

Considering the massive effect of IL-7 on T cells, recombinant IL-7 (rhIL7) has been developed for use in patients with lymphopenia. IL-7 is particularly useful in these settings because of its capacity to enhance immune reconstitution of both $CD4^+$ and $CD8^+$ T cells[110]. In the tumour microenvironment, IL-7 has been reported to inhibit the proliferation of regulatory T cells, and promote the development of interleukin-17-producing $CD4^+$ T cells (T_H17) which enhances the anti-tumour activity of effector T cells[116, 117]. In addition, IL-7 stimulation leads to the production of pro-inflammatory cytokines such as IL-6, IL-1 and TNF-α[118].

In the first clinical trial of rhIL7, 11 patients with metastatic melanoma were administered different doses of rhIL7 every 3 days for 21 days. Although there was no clinical benefit observed, there was a marked increase in naïve T cell population and a decrease in $FoxP3^+$ $CD4^+$ T cells[116]. The absence of observable clinical benefit might be because rhIL7 was administered in the absence of anti-PD1. While it might enhance the benefit of anti-PD1, IL-7 will not reverse T cell exhaustion. Currently, there are several studies exploring the potential benefits of combining IL-7 with other anti-cancer therapies such as tumour vaccines, oncolytic viruses, CAR-T cell therapy[118].

1.4 The role of B cells in Melanoma

This discovery of B cell gene expression having significant impact on the natural history of melanoma and the body's response to therapy opens up the conversation further on the role of B cells in the immunoediting of melanoma. Compared to T cells, the B cell function in the anti-tumour response have been less studied[119]. Meanwhile, B cells form the second arm of the adaptive immune response and are mainly involved in the production of antibodies. Following formation in the bone marrow, B cells migrate to the secondary lymphoid organs as transitional B cells ($CD24^{hi}$ and $CD38^{hi}$) where they differentiate to naïve B cells ($CD19^+$, IgM^+, IgD^+,

CD27$^-$) and lie in-wait for foreign antigen[120, 121]. Naïve B cells through their B cell receptor (BCR) identify and bind to a foreign antigen. This antigen is internalized through endocytosis, digested and then a component of the antigen is displayed on the MHC class II complex. Antigen specific CD4$^+$ T follicular cells interact with B cells through direct contact involving CD40LG-CD40, ICAM1-LFA1 and SLAM family members and through the production of various cytokines such as IL-4 and IL-21. Thereby supplying B cells with much needed co-stimulatory signals. Consequently, activated B cells then undergo a two-step differentiation process to produce short-lived plasmablasts (CD38^{hi}, CD27^{hi}, CD138$^-$), long-lived plasma cells (CD38^{hi}, CD27^{hi}, CD138$^+$) and memory B cells[122]. In the first phase, activated B cells differentiate into germinal centre (GC) B cells, which go into the GC reaction and short-lived plasma cells that generate low affinity antibodies. In the second phase, GC B cells migrate into the germinal centre where they undergo class switching and somatic hypermutation to produce memory B cells and long-lived plasma cells capable of producing high affinity antibodies. Although interactions with CD4$^+$ T helper cells are critical for the development of memory B cells in both phases, memory B cells can also be produced through T cell-independent and GC-independent approaches. These memory cells are usually produced in response to polysaccharide antigens and unmethylated CpG DNA[122]. Although antibody production by these B cells is rapid, they have low affinity and mostly of class IgM.

Antibodies are made of two identical heavy chains and two identical light chains, joined together at the hinge region by disulphide bonds. The heavy and light chains combine to form the antigen binding region of the antibody, otherwise referred to as the Fab arm. The heavy chains form the effector region of the antibody molecule, otherwise referred to as the Fc region. Based on the Fc region, antibodies can be divided into different isotypes: IgG, IgA, IgM, IgD, IgE. Through these antibodies, B cells are able to induce antibody-dependent cell-mediated cytotoxicity (ADCC), antibody-dependent cellular phagocytosis (ADCP), complement-dependent cytotoxicity.

There are controversies regarding the composition and role of B cells in cancers. This has been attributed to the high variation in markers used to describe B cells and its subsets. In a review by Rodgers *et al*, it was shown that while some studies defined B cells as CD19$^+$, others have defined B cells as CD20$^+$[123]. This introduces challenges when trying to make sense of the entire literature on B cell function in cancer. Having said that, B cells are a component of the TME, and found usually in the tumour stroma margin[124]. B cells make up approximately 25% of the cell infiltrate in the tumour microenvironment (TME) and have been shown to not just be by-standers in the TME, but can modulate the T cell effector functions[125, 126]. Griss *et al* reported that B cell inflammation was necessary for the anti-tumour activity of T cells[127]. B cells in the TME aggregate into structures known as tertiary lymphoid structures (TLS), with morphology similar to that of secondary lymphoid organs. The TLS is believed to serve as an immunomodulatory outpost close to the tumour where B cells undergo somatic hypermutation and class switching and also present antigens to effector T cells. The presence of TLS in the TME has also been correlated with improved patient outcome to immunotherapy in metastatic melanoma patients[128, 129]. On the other hand, B cells have also been shown to correlate with poor survival[130]. A subset of B cells, regulatory B cells (Bregs) have been shown to produce IL-10 and TGF-beta which creates an immunosuppressive TME potentially supporting tumour progression. Furthermore, Bregs can also convert CD4$^+$ T cells into regulatory T cells. Yet, other studies have found no correlation between B cells infiltrates in the TME and survival.

This suggests that the B cell function might be context-dependent. Finally, very few studies have explored the effect of the different immunoglobulin subtype on patient outcome.

1.5 Thesis aims and objectives:

1.5.1 Aims and Objectives

Considering the significant impact of B cell *IL7* expression on the natural history of melanoma and the response to ICB, this warrants further evaluation to uncover the factors responsible for *IL7* expression in B cells.

The main aims of this thesis are to:

i. Explore the determinants of *IL7* expression in B cells of metastatic melanoma patients

ii. Characterise humoral response to melanoma and the impact on patient outcome

1.5.2 Justification

Work from this thesis can potentially shed more light into the pathways responsible for the development of irAEs in patients with cancer receiving ICB. This can also potentially serve as a biomarker for irAEs. In addition, work from this study can potentially shape the *IL7* therapy design and approach to the clinical management of patients with irAEs.

Chapter 2: Materials and Methods

2.1 Samples

2.1.1 Patient Cohort

Patient cohort consist of adults being managed for metastatic melanoma at the Oxford University NHS Foundation Trust (OUHFT) with immune checkpoint blockade (ICB). Patients were treated with anti-PD-1 monoclonal antibodies as single agent (sICB), pembrolizumab (2mg/kg every 3 weeks) or nivolumab (480mg every 4 weeks) or received combination therapy consisting of either the anti-CTLA-4, ipilimumab (3mg/kg) plus nivolumab (1mg/kg) every 3 weeks for the first four cycles, followed by maintenance nivolumab (480mg every 4 weeks). Samples were collected at baseline (C1), prior to receiving the first dose of ICB and after the first cycle of treatment (C2). Additional samples were collected from patients who were identified to be radiologically and clinically cancer free with at least five years of post-treatment follow-up. For every patient that volunteered to take part in the study, a written informed consent was obtained by Clinicians prior to sample collection. Ethical approval was obtained with REC number 06/Q1605/55.

2.1.2 Clinical Outcome Data

Patient cohort were followed up and data on the occurrence of immune related adverse events (irAEs), disease progression and death were obtained from the patients' electronic medical record. Disease progression was examined using immune-related Response Evaluation Criteria in Solid Tumors v1.1 (irRECIST.1.1)[131] and irAEs evaluated using the common terminology criteria for adverse events (CTCAE). Progression-free and overall survival were defined as time from commencement of therapy to the time progression was first identified or death from any cause occurred respectively. Additional data on patients' previously received therapy, performance status at start of treatment, weight, and height were also recorded.

2.1.3 Laboratory Blood Count

Results from full blood count tests performed on the patient as part of their work-up before treatment were obtained from their electronic medical record. Sample was valid if taken within 30 days before receiving ICB. Blood count was generated using Sysmex XN series analysers (Sysmex corporation).

2.1.4 Survival Analyses

Kaplan-Meier and log-rank test were used in univariate analysis to understand the effect of irAEs on patient outcome. To account for the immortal time bias of irAEs, a time-dependent covariate analysis was performed. First, time to toxicity was defined as the time from the start of treatment to the time of occurrence of the first toxicity regardless of grade or organ involved. A special dataset was then created with multiple time intervals for the different covariate values for each patient using *tmerge(data1, data2, event(), tdc())* from the *Survival* package[132]. The *event (months-to-death, death indicator)* creates the new event indicator to go with the newly created time intervals and the tdc *(time to toxicity, toxicity indicator)* creates the time-dependent covariate indicator to go with the newly created time intervals. In evaluating system-specific irAEs on patient outcome, irAEs were grouped according to the organ-system involved as shown in table 2.1. Unless otherwise stated, all cox proportional hazards regression analysis

were performed using *coxph* function[133], controlling for age, sex, prior exposure to ICB, prior exposure to BRAF inhibitors, performance status and treatment type.

System	Pathology
General Systemic	Pyrexia, infusion reaction, SIRS response
Rheumatology	Arthritis, myalgia, arthralgia
Respiratory	Pneumonitis
Ophthalmology	Anterior uveitis, conjunctivitis
Neurology	Encephalitis, Meningitis, Autonomic neuropathy, Peripheral neuropathy, Mononeuritis multiplex, Bell's palsy, Myasthenia gravis
Haematology	Neutropoenia, Anaemia, Thrombocytopaenia, Autoimmune haemolytic anaemia (AIHA)
Genito-urinary (GU)	Nephritis, Cystitis
Gastro-intestinal (GI)	Colitis, Gastritis, Hepatitis, Xerostomia, Mucositis, Pancreatitis, Coeliac disease
Endocrine	Thyroiditis, Hypophysitis, Adrenalitis, type 1 diabetes mellitus (T1DM)
Dermatology	Rosacea, Lupus pernio, pruritus, bullous pemphigoid, erythema nodosum, urticaria, erythema multiforme, vitiligo
Cardiac	Myocarditis

Table 2.1: Classification of irAEs by system

2.2 Peripheral Blood Sample Processing

2.2.1 Ficoll Density Gradient Centrifugation

Approximately 30 - 50 mL of whole blood was collected from every patient into Ethylenediaminetetraacetic acid (EDTA)-coated tubes (BD Vacutainer System) prior to the administration of ICB. Samples were diluted 1:2 in Hanks Balanced Salt Solution (HBSS). Diluted blood was then split four ways and layered carefully unto 12.5 mL of Ficoll-Plaque (cytiva) in a 50 mL Falcon tube. Samples were centrifuged at 400 g for 30 minutes at room temperature with acceleration set to 'slow' and deceleration turned off.

2.2.2 Plasma Collection

Plasma was gently collected using a stripette from the top layer of the centrifuged samples. The plasma was further processed by spinning at 16000 g for 20 minutes at 4°C to remove contaminating platelets and cellular debris. Processed plasma was stored in aliquots at -80°C for use in downstream experiments.

2.2.3 Peripheral Blood Mononuclear Cell Collection

Peripheral blood mononuclear cells (PBMCs) were collected from the PBMC layer using a Pasteur pipette into a 50 mL Falcon tube. PBMCs were washed twice with HBSS and then counted using Countess™ III Automated Cell Counter. Approximately 2.0 x 10^6 cells were

lysed in 500 µL of RLT buffer (Qiagen) supplemented with 2M Dithiothreitol (DTT), henceforth referred to as RLT buffer, and then stored at -80°C. Approximately 10 - 20 x 10^6 cells per positive selection were taken for magnetic-activated cell sorting (MACS) and the rest of the PBMCs were resuspended in freeze media (made up of 90% foetal bovine serum [FCS] plus 10% Dimethyl sulphoxide [DMSO]), split into 5 – 10 x 10^6 cells/mL per cryovial and stored in liquid nitrogen.

2.2.4 Magnetic-Activated Cell Sorting Separation

The number of cell selections performed per sample depended on the total amount of PBMCs recovered. Routinely, $CD8^+$ cells, $CD19^+$ cells and occasionally $CD14^+$ cells were sorted for using positive selection. Isolation was performed using MACS. For each selection, cells were first re-suspended in 80 µL of MACS buffer per 10^7 PBMCs. Then, 20 µL of cell specific microbeads was added and the samples were incubated at 4°C for 15 minutes. Cells were washed in 1 mL of MACS buffer, centrifuged at 300 g for 10 minutes, then re-suspended in 500 µL MACS buffer. While the cells were spinning, the MS column was equilibrated and samples were added to the column and allowed to run through completely. The MS columns were washed three times with 500 µL MACS buffer. To extract cells bound to the column which formed the cells of interest, the MS column was taken off the separator, 1 mL of MACS buffer was added and the fluid was flushed out using the plunger provided. The resulting number of cells were counted using a Countess Automatic Cell Counter and then resuspended in 350 µL of RLT. Samples were stored in -80°C prior to use for bulk RNA sequencing.

2.2.5 RNA extraction

Samples in RLT were homogenised using QIAshredder columns (Qiagen). This was followed by RNA extraction using the AllPrep DNA/RNA/miRNA kit (Qiagen) adhering to manufacturer guidelines. The concentration of extracted RNA was determined using Qubit 4 fluorometer (Thermo Fisher Scientific) and samples were immediately frozen at -80°C prior to RNAseq library preparation.

2.2.6 Blood cone

Blood cones from healthy donors were obtained from the NHS blood and transplant. PBMCs were extracted using Ficoll density centrifugation and stored in liquid nitrogen as described above. Approximately 35 – 50 million cells were frozen per vial.

2.3 Cell Culture

2.3.1 Tumour Cell lines

Tumour cell lines, outlined in Table 2.2, were derived from human melanoma cells and described using information from ExPASy. Melanoma cell lines were revived from liquid nitrogen and maintained in Dulbecco's Modified Eagle's Medium (DMEM; Gibco) supplemented with 10% FBS and 1% Penicillin/Streptomycin. Cells were incubated at 37°C and 5% CO_2. Melanoma conditioned media (MCM) was prepared by culturing stably replicating cells until 80% confluence, the entire media was then replaced with fresh media and MCM was extracted 48 hours later. The MCM was sterile filtered then ultracentrifuged at

16000g, 4°C for 20 minutes. MCM was stored in aliquots at -80°C. Control media was prepared in the same way but without melanoma cells.

Cell line	Passage number	Disease origin	Sex	Resource Identification Initiative (ExPASy)
501-Mel	7	Melanoma metastatic site, BRAF+	Female	501-mel (RRID:CVCL_4633)
A375P	36	Amelanotic melanoma	Female	A375-P (RRID:CVCL_6233)
CHL1	10	Melanoma metastatic site,	Female	CHL-1 (RRID:CVCL_1122)
SKMEL-28	12	Cutaneous melanoma	Male	SK-MEL-28 (RRID:CVCL_0526)
ME	21	Mucosal melanoma (oral)	Female	ME [Human melanoma] (RRID:CVCL_C666)
Na8	18	Melanoma		NA8-MEL (RRID:CVCL_S599)
SKMEL2	17	Melanoma	Male	SK-MEL-2 (RRID:CVCL_0069)

Table 2.2: Characteristics of melanoma cell line used, including passage number at extraction of MCM.

2.3.2 B cell induction with Plasma

Healthy human B cells were magnetically sorted from PBMCs obtained from blood cones. 3 - 5 x 10^5 B cells were then cultured at a concentration of 1 x 10^6 cells/mL in media consisting of 50% B cell medium (complete RPMI 1640 medium supplemented with 10% FBS, 1% L-Glutamine, 1% Penicillin/Streptomycin, 50 ng/mL IL-2 (RD Systems), 50 ng/mL IL-21 (BioLegend), 50 ng/mL soluble CD40 ligand (BioLegend)) and 50% plasma from patients with metastatic melanoma. Details of B cell media optimisation with cytokines can be found in Appendix A. The cells were maintained at 37°C and 5% CO_2 for 72 hours. Prior to use, plasma was ultracentrifuged for 20 minutes at 16000g, 4°C to remove any contaminating platelets or cellular debris. For control, B cells were cultured in B cell medium alone for the same duration of time. 50% of the media was replaced every 24 hours with fresh media consisting of 50% B cell medium and 50% patient's plasma.

2.3.3 B cell induction with melanoma-conditioned media

3 x 10^5 healthy human B cells were cultured at a concentration of 1 x 10^6 cells/mL in media consisting of 50% B cell medium and 50% melanoma-conditioned media (MCM). The cells were maintained at 37°C and 5% CO_2 for 72 hours. 50% of the media was replaced every 24 hours with fresh media consisting of 50% B cell medium and 50% MCM.

2.4 Quantitative Polymerase Chain Reaction

2.4.1 RNA Extraction

Cultured B cells were extracted and lysed in 75 µL of RLT buffer (if number of cultured B cells were less than 1 x 10^5) or 350 µL of RLT buffer (if number of cultured B cells were greater than 1 x 10^5). Samples were first homogenised by vortexing for 1 minute (if number of cultured B cells were less than 1 x 10^5) or using QIAshredder columns (Qiagen) (if number of cultured

B cells were greater than 1 x 10^5). RNA extraction was then performed using the AllPrep DNA/RNA micro kit (Qiagen) adhering to manufacturer guidelines. RNA was eluted into 14ul of RNAse free water and the concentration of extracted RNA was determined using Qubit 4 fluorometer (Thermo Fisher Scientific) and samples were immediately frozen at -80°C prior to cDNA generation.

2.4.2 Complementary DNA generation

Complementary DNA (cDNA) generation was performed on RNA samples using Superscript III/IV first-strand synthesis system (ThermoFisher Scientific). The concentration of the cDNA was determined using the Nanodrop spectrophotometer (ThermoFisher Scientific).

2.4.3 Primer design and validation

Primers were designed using Primer3Plus software. Specifically, primers were designed to span exon-exon junction to prevent the amplification of genomic DNA with GC content of 40 – 60%, GC clamp at the end to increase specificity of target binding. Primer specificity was determined using NCBI primer blast[134] and UCSC in silico PCR tool[135]. Primers were further validated in an end-point PCR and amplicons visualised by 2% agarose gel.

Target	Forward Primer	Reverse Primer
IL7	CGCAGACCATGTTCCATGTTTC	CGATGCTGACCATTAGAACACTC
POU2AF1	CAGTGTTGACCTATGCCTCTCC	GAGGTGGGTAGTGTGGAAAGG
IKZF3	TCTGTGCCCGCAGAAAGTG	TCTTCATTGGCTGGGCCTTC
TFE3	GAAGGAACGGCAGAAGAAAGAC	CTGGACTTAGGGATGAGAGTGC
GAPDH	TCAAGGCTGAGAACGGGAAG	CGCCCCACTTGATTTAGGAG

Table 2.3: Sequences of primer pairs used

2.4.4 qPCR Reaction

Quantitative polymerase chain reaction (qPCR) was performed using SYBR Green JumpStart Taq ReadyMix. 25 µL reaction was set up in triplicates using buffer provided, 100 ng of cDNA and final concentration of 200 nM forward primer and 200 nM reverse primer. qPCR analysis was performed using a StepOnePlus real-time PCR machine (ThermoFisher Scientific) for 40 cycles with cycling steps shown in the table 2.4. Melt curve analysis was performed at the end of every qPCR analysis to ensure amplification of the right product. GAPDH was selected as the housekeeping gene. Target gene expression was calculated in Excel using the comparative Ct method described by Livak[136], detailed below.

ΔCt = Ct (gene of interest) – Ct (housekeeping gene)

$\Delta\Delta Ct$ = ΔCt (treated sample) - ΔCt (untreated sample)

Gene expression = $(2^{-\Delta\Delta Ct})$

Step	Temperature	Duration	Cycles
Initial denaturation	94	120 seconds	1
Denaturation	94	15 seconds	40
Annealing, extension and fluorescence reading	60	60 seconds	

Table 2.4: Cycling parameters of qPCR reactions

2.5 Flow Cytometry

Flow cytometry was performed to investigate the subset composition of both B cells and T cells. All aspects of this experiment were performed by Chelsea Taylor, a previous DPhil student in the laboratory. Firstly, panel B1 was used to investigate the PBMC composition, panel T2 was used to investigate the subset composition of $CD4^+$ and $CD8^+$ T cells and panel B5 was used to investigate the subset composition of B cells. Each panel is described in detail in Table 2.5.

Target/Stain	Fluorochrome	Antibody clone	Dilution	Source	Panels
Live/Dead cell stain kit	Near-IR	n/a	1000	Thermo Fisher Scientific	B1, T2, B5
CD3	BV785	UCHT1	25	BioLegend	B1, T2
CD56	BV421	5.1H11	50	BioLegend	B1, T2
CD19	AF700	HIB19	50	BioLegend	B1
CD14	PE/Cy7	M5E2	50	BioLegend	B1
CD16	FITC	3G8	50	BioLegend	B1, B5
CD8a	BV510	RPA-T8	25	BioLegend	B1, T2,
CD21	PE	Bu32	50	BioLegend	B1
MHCI	APC	W6/32	50	BioLegend	B1
PD1	BV650	EH12.2H7	50	BioLegend	B1, T2
CD4	APC	RPA-T4	50	BioLegend	T2
CD27	AF700	M-T271	50	BioLegend	T2
CD45RA	FITC	HI100	50	BD BioSciences	T2
Pan gb TCR	PE	B1	50	BioLegend	T2
CD3	FITC	UCHT1	25	BioLegend	B5
CD56	FITC	HCD56	50	BioLegend	B5
IgD	BV421	IA6-2	50	BioLegend	B5
CD27	APC	M-T271	25	BioLegend	B5
CD38	PE/Cy7	HB-7	50	BioLegend	B5
CD24	B785	ML5	50	BioLegend	B5
CD138	PE	DL-101	50	BioLegend	B5
CD24	BV785	ML5	50	BioLegend	B5
CD11c	BV605	3.9	50	BioLegend	B5
CD71	PE/Dazzle594	CY1G4	100	BioLegend	B5

Table 2.5: Flow cytometry panel summary

PBMC samples were recovered from liquid nitrogen and thawed at 37°C followed by centrifugation at 400G for 10 minutes at 4°C. Cells were counted and 1 x 10^6 cells (or 3 x 10^6 for panel B5) were aliquoted per 5 mL FACS polystyrene tube and washed with HBSS. Aliquots were also taken for fluorescence minus one (FMO) and isotype controls. The cells were incubated with fixable amine reactive viability dye at 1/1000 in HBSS for 30minutes, 4°C in the dark. Samples were then washed and stained with extracellular antibodies at the appropriate dilution for 30 minutes. The cells were then washed in HBSS to remove excess and unbound antibodies. The cells were then fixed in 100 µL 2% formaldehyde (Merck) for 10 minutes and subsequently washed in HBSS. Finally, the cells were resuspended in staining buffer. Flow cytometry was performed using the BD Fortessa LSRII and FACS DIVA software. Compensation controls were obtained from fresh cells and performed for every batch. Data was analysed using FlowJo software version 10.7.1.

T cells were identified as $CD3^+CD56^{\pm}$. Based on CD4/CD8 positivity, T cells were further divided into $CD4^+CD8^-$, $CD4^-CD8^+$, $CD4^-CD8^-$ (double negatives), $CD4^+CD8^+$ (double positives). In addition, T cell subsets were defined using canonical markers: naïve T cells ($CD45RA^+$, $CD27^+$), central memory T cells ($CD45RA^-CD27^+$), effector memory T cells ($CD45RA^-CD27^-$), and effector memory T cells re-expressing CD45RA ($CD45RA^+CD27^-$). B cells were identified as $CD19^+$, additionally, to capture plasma cells which tend to downregulate the expression of CD19, a dump channel was created consisting of CD3/CD56/CD16 and whole B cells were selected from dump- cells, effectively keeping both $CD19^-$ and $CD19^+$ cells. B cell subsets were then defined as follow: Naïve B cells were identified as IgD^+CD27^-, switched memory B cells as $CD27^+IgD^-$, unswitched memory B cells as $CD27^+IgD^+$, transitional B cells were identified by high expression of CD24 and CD38.

2.6 Measurement of Plasma Immunoglobulin Concentration

Plasma concentration of immunoglobulin isotypes was measured using bead-based assay kit from LegendPlex adhering to the manufacturer's guidelines. To measure the concentration of IgA, IgM and the IgG isotypes, the plasma was diluted 1:100,000, for IgD, plasma was diluted 1:5000 and for IgE, plasma was diluted 1:100. To a 96-well v-bottom plate, 25 µL of assay buffer, 25 µL of diluted plasma and 25 µL of multiplex beads were combined in duplicates into each well. The plate was sealed and placed on a plate shaker for 2 hours at 800rpm room temperature. The plate was then centrifuged at 1050rpm for 5 minutes using a swinging bucket rotor and washed twice with 200 µL of the wash buffer provided. 25 µL of detection antibodies was added to each well and the plate was then placed on a plate shaker at 800rpm for 1 hour. 25 µL of SA-PE was then added and the plate placed on the plate shaker for additional 30 minutes. The beads were washed again and re-suspended in 150 µL of wash buffer. Samples were run on a Attune NxT flow cytometer (Thermo Fisher Scientific). Fcs files were uploaded unto the online bioinformatic tool provided by LegendPlex and concentration of immunoglobulins was determined. Initial batches of experiments were performed by Chelsea Taylor. I then performed further immunoglobulin measurement in 20 more paired samples at a dilution of 1:50,000.

2.7 Proteomics Analyses

2.7.1 Sample Preparation

Plasma samples were thawed on ice and ultracentrifuged at 16000g for 5 minutes. 40 µL of patients' plasma were loaded randomly onto a 96-well PCR plate. Olink proteomics proximity extension assay was used for the determination of the concentration of 92 plasma proteins on the Immuno-oncology panel (performed by Technology platforms group). Samples were sent in 2 batches across 3 plates: two plates were sent in the first batch and one plate was sent in the second batch.

2.7.2 Normalisation and Quality Control

Normalisation was performed in R using the package *OlinkAnalyze*[137]. Inter-plate normalisation was performed with the median as the normalisation factor. First, samples on plate 2 were normalised to samples on plate 1. Then, samples on plate 3 were normalised to combined normalised protein expression values of plate 1 and 2. This step was performed by Dylan Muldoon and I was assured of the quality of the result. Quality control was performed by the Olink team and samples identified as not passing QC were filtered out.

2.8 Transcriptomic Analyses

2.8.1 Bulk RNA Sequencing

2.8.1.1 Library Preparation

RNA samples were thawed on ice prior to mRNA isolation using the NEBNext® Poly(A) mRNA Magnetic Isolation Module kit (New England Biolabs). Libraries were created from approximately 600ng of RNA sample using NEBNext® Ultra II Directional RNA Library Prep Kit for Illumina® (New England Biolabs). Samples were indexed using NEBNext® Multiplex Oligos for Illumina® (New England Biolabs).

2.8.1.2 Sequencing and Upstream data analysis

Sequencing was performed in batches. First set of batches were performed on an Illumina HiSeq4000 (75bp paired end). Subsequent sequencing was performed on either NovaSeq6000 (150bp paired end) or NovaSeqX (150bp paired end) at the Oxford Genome Centre (Wellcome Trust Centre for Human Genetics). Reads were aligned to the Homo sapiens GRCh38/hg38 genome build with HISAT2[138] and read counts table generated using HTSeq[139] version 1.0. High quality reads were selected by MAPQ score using Bamtools[140] and duplicate reads excluded using Picard[141]. Laboratory work and bioinformatic pre-processing of bulk RNAseq were performed by others.

2.8.1.3 Differential Gene Expression

Differential expression gene analysis was performed in R using the package DESeq2[142]. After filtering the count data to include unique genes and samples of interest, a DESeq object was created using *"DESeqDataSetFromMatrix(countData = Gene count data, colData = Sample metadata, design = ~ Confounding variables + Testing variable)"*. Genes that are lowly expressed i.e. had low count numbers across all samples were filtered out using

"rowSums(counts matrix) > 10", retaining only those genes that have more than 10 counts in total across all samples. Differential gene analysis was then performed using the wrapper function "*DESeq (DESeq object)"* which consists of three main steps: estimation of size factors, estimation of dispersion and negative binomial generalised linear model fitting with hypothesis testing using the Wald test and correction for multiple testing using Benjamini-Hochberg procedure. Results table of the analysis was extracted using the *"results(DESeq2 object)".* Ensemble gene IDs were converted to gene symbols using *"mapIDs ()"* form the AnnontationDBi package[143]. Normalised counts were obtained using *getVarianceStabilizedData (DESeqDataSet object)* from DESeq2.

2.8.1.4 Pathway Analysis

Pathway analysis was performed on gene sets that are significantly expressed within a condition of interest using *"enrichGO()"* from clusterProfiler[144, 145] and org.Hs.eg.db[146]. Upregulated genes or downregulated genes were evaluated as a group.

2.8.2 Single Cell RNA Sequencing

2.8.2.1 Sample Preparation

PBMC samples were recovered from liquid nitrogen and thawed at 37°C for approximately 45 seconds. The cells were washed in HBSS and counted. Dead cells were removed from the PBMC pool by running the samples through a MACS live:dead column (Miltenyi), adhering to the manufacturer's protocol. The cells were counted and 60,000 live PBMCs were loaded into a partitioning reaction. Sequencing was performed on an Illumina NovaSeq 6000 S4 flow cell (150bp PE).

2.8.2.2 Pre-processing, QC and cell filtering

Cellranger (v6.0.1)[147] was used to align FASTQ for gene expression (GEX) libraries. EmptyDrops[148] was used to identify empty droplets (false discovery rate (FDR) ≤ 0.01). Barcodes called as empty by both Cellranger and EmptyDrops were excluded. CellSNP-lite[149] was used to pile-up genotyping data from single-cell reads, and vireo subsequently used to deconvolute individual sample from pools. Doublet identification was performed during sub-clustering by identifying cells with mixed transcriptomes of canonical markers using Scrublet[150]. Cells with <300 transcripts and >20% of mitochondrial-encoded genes were removed.

2.8.2.3 Clustering and Annotation

Clustering was performed based on nearest neighbour graph using 30 latent dimensions obtained from scVI[151, 152] and scArches[153]. Automated cell-type annotation was first performed on embeddings produced by scVI with Celltypist using the pre-trained classifier, "Immune_All_Low.pkl". Marker genes were then identified by performing a t-test based differential expression analysis (using log-normalised counts from Scanpy). Highly similar cell clusters were merged based on hierarchical dendrograms generated using scVI-derived neighbourhood graphs.

2.8.2.4 NicheNet Analysis

NicheNet[154] was used to perform ligand-receptor-target analysis between immune cells using a modification to the standard workflow described in the vignette. First, the Seurat[155] object

was filtered to include only cells from melanoma patients prior to commencement of therapy. Doublets were also removed. B cells were identified as the receiver cell. Genes expressed in receiver cell was determined using *"get_expressed_genes(receiver, Seurat_object, pct = 0.05)"*. Genes expressed in greater than 5% of all B cells were defined as the background genes. Genes of interests was determined by first performing a differential gene analysis between B cells that have at least one read count for *IL7* transcript (*IL7* positive) and cells that have no transcript read (*IL7* negative) using the *"FindMarkers(object = Seurat_object_Bcells, ident.1 = 'IL7+', ident.2 = 'IL7-', group.by = "IL7_status", min.pct = 0.05)"*. The first 30 significantly upregulated genes were selected as the genes of interest.

2.8.2.4.1 Sender Agnostic Approach

Potential ligands were defined as ligands whose cognate receptors are expressed on the receiver cell. Potential ligands were then ranked using area under precision recall curve generated using *predict_ligand_activities(geneset_of_interest, background_expressed_genes, NicheNet prior model, potential_ligands)*. The first 30 ligands were selected for further analysis. Ligand target prediction analysis was performed using *get_weighted_ligand_target_links(best_ligands, geneset_of_interest, NicheNet prior model)* and the first 250 targets with the highest interaction potential were selected. Receptors with the highest interaction potential with the prioritised ligands were identified using get_weighted_ligand_receptor_links*(best_ligands, expressed_receptors, NicheNet prior model).*

2.8.2.4.2 Sender Focused Approach

I defined sender cells as all cells in the dataset i.e. $CD4^+$ T cells, $CD8^+$ T cells, Monocytes, NK cells and B cells. The entire pipeline for the sender agnostic approach was repeated, however, potential ligands were defined as the ligands expressed by at least one of the sender cells and whose cognate receptor is expressed on the receiver cell. To identify the source of the ligands, the function *assign_ligands_to_celltype()* was used.

Chapter 3: Results

3.1 Immune related adverse events and Patient Outcome

3.1.1 Introduction

The occurrence of immune related adverse events (irAEs) and the impact on patient outcome remains a subject of debate amongst researchers. First, I wanted to replicate the previously observed association between irAEs and patient outcomes. One of the pitfalls of previously published studies on this association is the failure to account for immortal time bias of irAEs. Therefore, in my analysis, a time-dependent cox proportional hazards model was used to adjust for this bias.

3.1.2 Baseline characteristics of patients and irAEs

A total of 303 patients with metastatic melanoma were prospectively recruited in this study. Patients were managed with standard of care single agent anti-PD1 (sICB) or combination anti-PD1 and anti-CTLA4 (cICB). Over the course of their treatment, information on the occurrence of any grade adverse events were recorded according to the guidelines set out by CTCAE. Median age for all patients in the cohort was 67 years and the incidence of any grade irAEs was 74.3%. Median follow-up was 53.4 months and patients with at least 6 months of follow-up were included in the analysis.

The baseline characteristics of patients with irAEs are summarised in Table 3.1. Briefly, individuals who experienced any grade irAEs were observed to be significantly younger (median age = 66 years) than patients without irAEs (median age = 71.5 years). This can be because younger and perhaps fitter patients are more likely to be administered cICB which has a higher risk of causing toxicities compared to sICB[156]. Indeed, of the patients that received cICB, 73.8% of them developed irAEs, while only 26.2% of patients taking sICB developed toxicities. This difference in the choice of treatment type might also explain why significantly more patients who developed irAEs had performance status less than or equal to 1 (96% vs 84%, $p = 0.0015$). There were no significant differences in the sex or body mass index (BMI) of the patients. When compared to the patients without irAEs, significantly smaller proportion of patients with irAEs had had a previous malignancy. All other parameters were equal between both groups.

Gastrointestinal-related irAEs were observed to have the highest incidence in the dataset, most of which were grade 3. This is followed by skin-related toxicities, most of which were mild toxicities. Ophthalmologic, haematologic and cardiac toxicities were the least observed, with incidence rate of 1.3%, 2.2% and 2.2% respectively (Figure 3.1a and 3.1b).

3.1.3 The occurrence of any grade irAEs is associated with improved patient outcome

Kaplan-Meier analysis, showed prolonged overall survival (OS) in patients with any grade irAE (median OS = 78 months versus 11 months in patients without irAE, $p < 0.0001$) and prolonged progression-free survival (PFS) (median PFS = 20 months versus 2.8 months, $p < 0.0001$, Figure 3.2 a and b). The survival benefit of irAEs was also observed after a 12-week landmark Kaplan-Meier analysis (Supplementary Figure B.1). A time-dependent cox proportional hazard model showed that the occurrence of any grade irAE was associated significantly with improved OS (HR = 0.40, 0.27, 0.60, $p < 0.0001$) and PFS (HR = 0.58 (0.39

– 0.84, p = 0.005) (Figure 3.2c and 3.2d). I then explored the impact of organ-specific toxicities on patient outcome.

Parameter		**irAEs**		**P value**
		Yes (%) (n = 225)	**No (%)** (n = 78)	
Age	Median (IQR)	66 (46 – 86)	71.5 (50.5 – 91.5)	0.003*
Male		125 (55.8)	42 (51.6)	0.793
BMI	<18.5	1 (0.4)	1 (1.3)	0.827
	18.5 – 24.9	64 (28.4)	21 (26.9)	
	25.0 – 29.9	90 (40.0)	32 (41.0)	
	>30	70 (31.1)	24 (30.8)	
Performance Status	0 – 1	216 (96.0)	66 (84.6)	0.0015*
	2+	9 (4.0)	12 (15.4)	
Treatment type	cICB	166 (73.8)	29 (37.2)	<0.001**
	sICB	59 (26.2)	49 (62.8)	
Prior Chemotherapy	Yes	15 (6.7)	8 (10.2)	0.324
Prior Malignancy	Yes	16 (7.1)	14 (17.9)	0.008*
Prior ICB	Yes	27 (12.0)	15 (19.2)	0.129
Prior BRAFi	Yes	24 (10.7)	15 (19.2)	0.075
BRAF Status	Mutant	73 (33.0)	27 (36.0)	0.673
	Wild-type	148 (67.0)	48 (64.0)	
***IL7* SNP (rs16906115)**	Yes	24 (10.7)	6 (7.7)	0.51
Steroids	Yes	167 (74.2)	0 (0)	
Second line	Yes	56 (24.9)	0 (0)	

Table 3.1: Baseline characteristics of patients with irAEs. P value computed using Wilcoxon rank sum test for continuous variables and Fisher's exact test for categorical variables.

(a) (b)

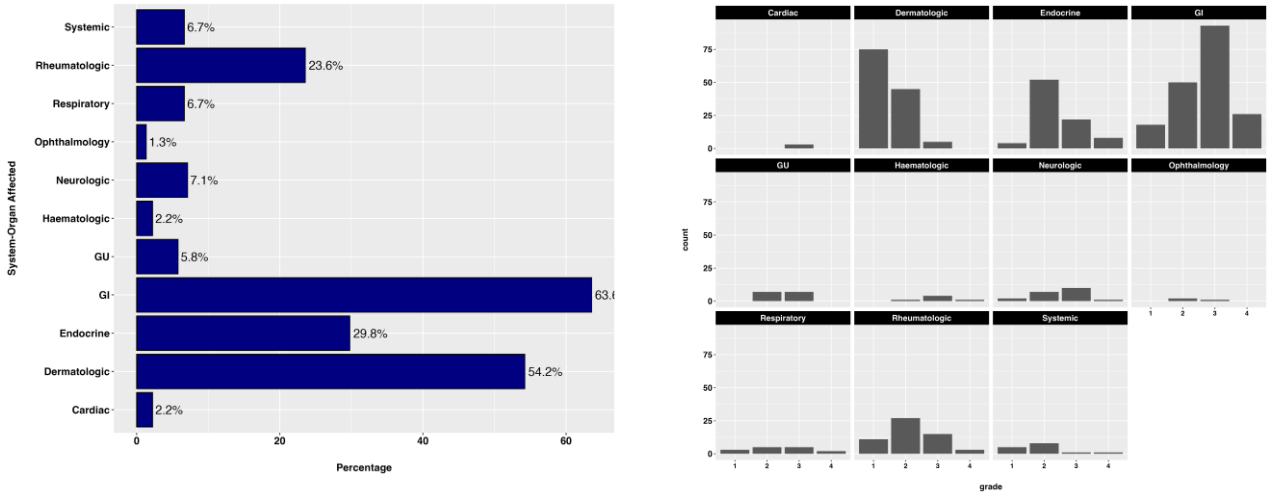


Figure 3.1: (a) Frequency of System irAEs in patients with any grade irAEs (n = 225). (b) Frequency plot of irAEs grade by system.

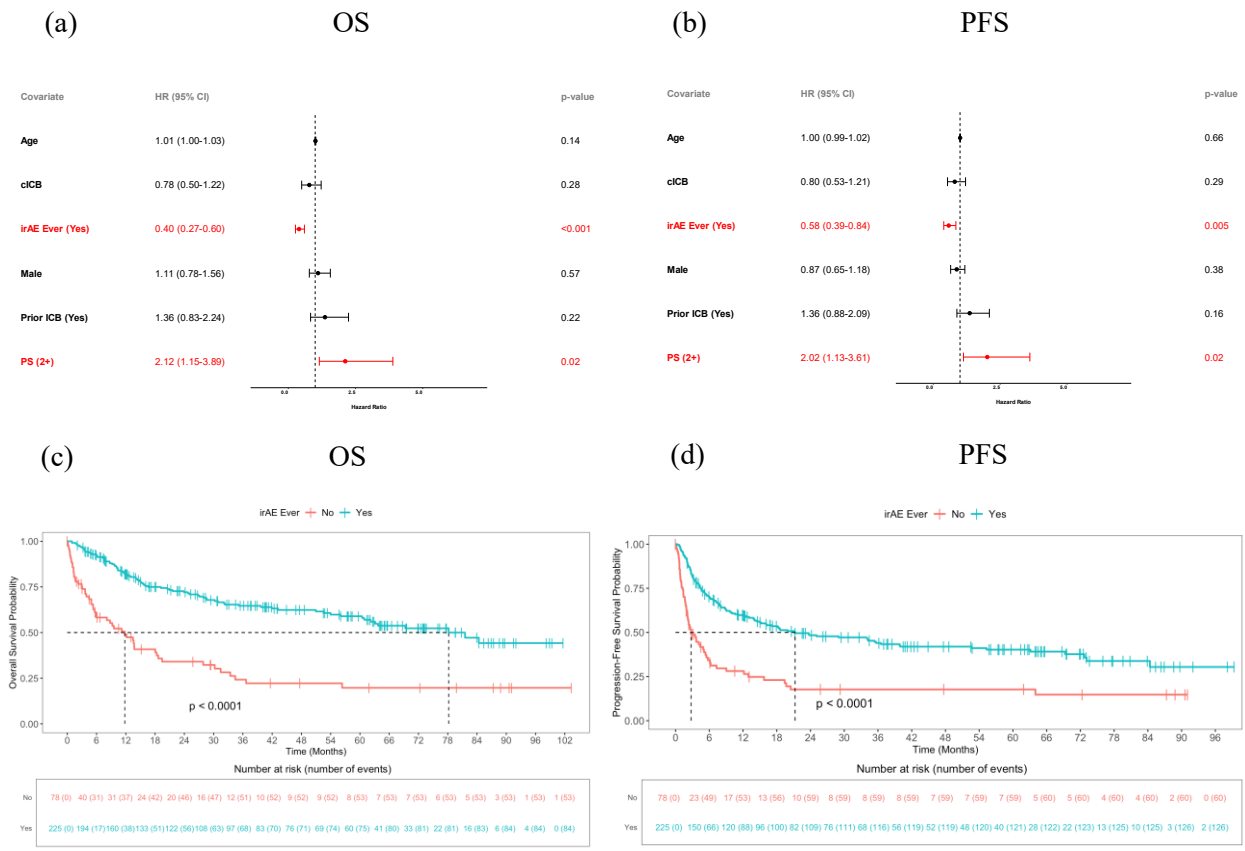


Figure 3.2: (a) Kaplan Meier analysis demonstrates significantly improved OS and (b) PFS in patients with any grade irAEs ($p < 0.0001$, log-rank test) (n = 303). (c) Time-dependent cox proportional hazards model indicates that the occurrence of any grade irAEs is associated with improved (c) OS and (d) PFS (n = 302). All multivariate analyses were performed adjusting for age, sex, ICB type, performance status and prior exposure to BRAF inhibitors or ICB.

Compared to patients without any irAEs, grade 1or 2 dermatologic toxicities were associated with reduced risk of death (HR = 0.51 (0.30 – 0.87), p = 0.01). Grade 1 or 2 gastrointestinal toxicities were also associated with a reduced risk of death with a marginal p-value (HR = 0.47 (0.22 – 1.01), p = 0.053) (Figure 3.3a and 3.3b). On the other hand, grade 3 or higher cardiac toxicities were associated with an increased risk of death (HR = 3.64 (1.29 – 10.30), p = 0.01) and progression (HR = 5.60, (2.21 – 14.20), p = <0.0001) (Figure 3.3c and 3.3d). The wide confidence interval is perhaps due to the low incidence of cardiac toxicities (2.2%). All toxicities involving the heart were at least grade 3 with case-fatality rate of 80% in the cohort. No reassuring association was seen between toxicities in other systems tested and patient outcome.

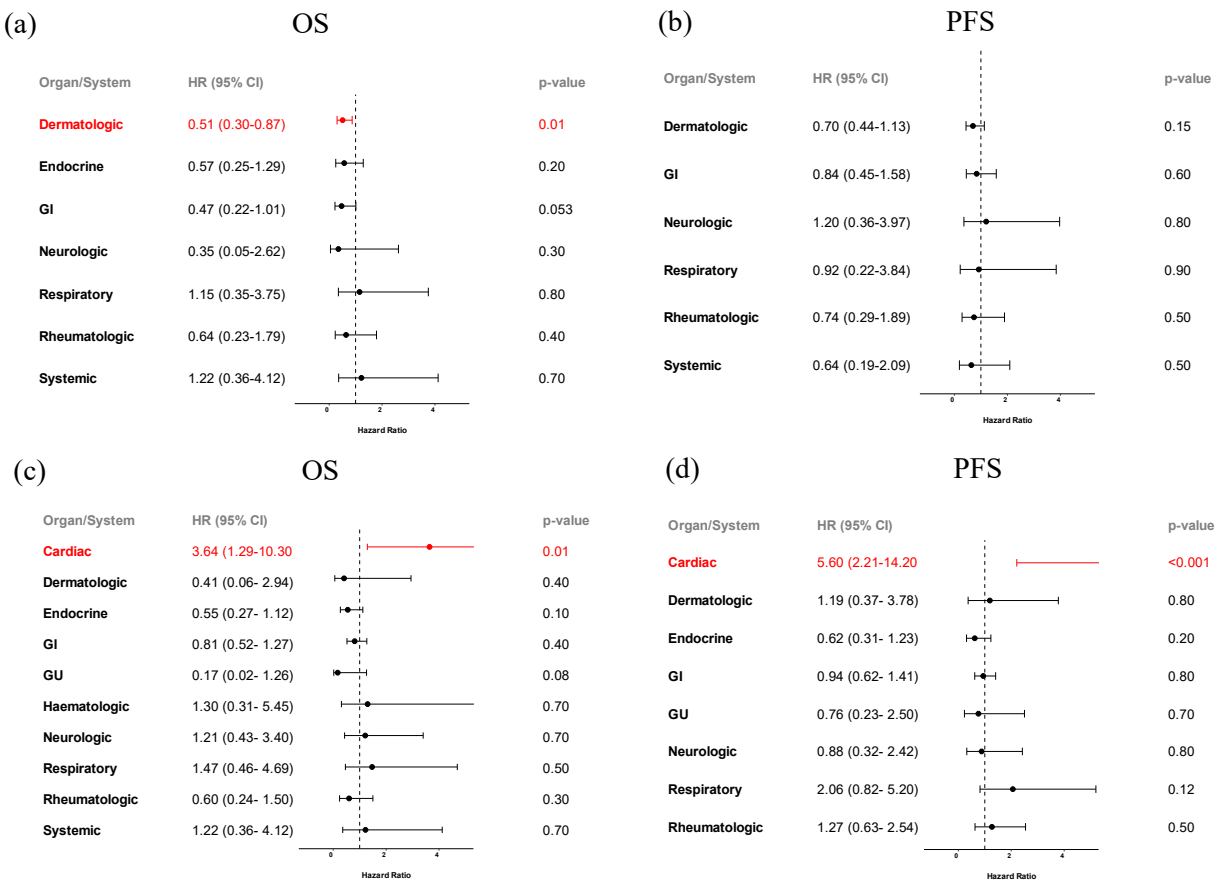


Figure 3.3: Time-dependent cox proportional hazard model showing the relationship between grade 1-2 system toxicities and impact on (a) overall survival and (b) progression-free survival (n = 162). Time-dependent cox proportional hazards showing the relationship between grade 3 or more system toxicities and impact on (c) overall survival and (d) progression-free survival (n = 214). Each system was tested while adjusting for age, sex, ICB type, performance status and prior exposure to BRAF inhibitors or ICB.

I was interested in exploring the relationship between the number of systems with irAEs and clinical outcome. Because most irAEs tend to occur within 3 months of commencing ICB[74], I therefore performed a 12-week landmark analysis to adjust for immortal time bias. When compared to patients without toxicities, the involvement of one or more systems was associated with improved patient outcome (Figure 3.4a and 3.4b). Interestingly, when I compared to patients with single system involvement, two or more systems with irAEs was associated with reduced risk of death (OS: HR for 2/3 = 0.48 (0.27 – 0.84), p = 0.010; HR for 4 or more = 0.42 (0.19 – 0.91), p = 0.027) (Figure 3.3c and 3.3d). This benefit of numerically more systems with irAEs was also observed on PFS with marginal significance for four or more systems involved. When I looked at the relationship between the maximum grade experienced by a patient and the impact on clinical outcome, benefit was only observed when comparing to patients without toxicities (Figure 3.5). There was no survival benefit of experiencing a grade 3 or more irAEs compared to grade 2 or less irAEs.

(a) OS

Characteristic	HR†	95% CI†	p-value
no_body_systems_affected			
No_tox	—	—	
1	0.60	0.36, 0.98	0.041
2-3	0.30	0.18, 0.51	<0.001
4+	0.28	0.14, 0.58	<0.001
age	1.00	0.99, 1.02	0.6
sex			
Female	—	—	
Male	1.13	0.77, 1.67	0.5
Prior_ICB			
No	—	—	
Yes	1.49	0.86, 2.59	0.2
PS			
0-1	—	—	
2+	1.24	0.53, 2.90	0.6
Rx_type			
cICB	—	—	
sICB	0.67	0.40, 1.11	0.12

† HR = Hazard Ratio, CI = Confidence Interval

(b) PFS

Characteristic	HR†	95% CI†	p-value
no_body_systems_affected			
No_tox	—	—	
1	0.71	0.46, 1.10	0.12
2-3	0.38	0.24, 0.60	<0.001
4+	0.39	0.22, 0.71	0.002
age	1.00	0.98, 1.01	0.6
sex			
Female	—	—	
Male	0.85	0.62, 1.17	0.3
Prior_ICB			
No	—	—	
Yes	1.51	0.96, 2.37	0.073
PS			
0-1	—	—	
2+	1.42	0.68, 2.96	0.4
Rx_type			
cICB	—	—	
sICB	0.66	0.43, 1.01	0.055

† HR = Hazard Ratio, CI = Confidence Interval

(c) OS

Characteristic	HR†	95% CI†	p-value
no_body_systems_affected			
1	—	—	
2-3	0.48	0.27, 0.84	0.010
4+	0.42	0.19, 0.91	0.027
age	1.00	0.98, 1.02	0.8
sex			
Female	—	—	
Male	1.20	0.75, 1.93	0.4
Prior_ICB			
No	—	—	
Yes	1.82	0.92, 3.59	0.084
PS			
0-1	—	—	
2+	0.77	0.18, 3.34	0.7
Rx_type			
cICB	—	—	
sICB	0.60	0.31, 1.16	0.13

† HR = Hazard Ratio, CI = Confidence Interval

(d) PFS

Characteristic	HR†	95% CI†	p-value
no_body_systems_affected			
1	—	—	
2-3	0.54	0.34, 0.84	0.006
4+	0.56	0.30, 1.02	0.056
age	1.0	0.98, 1.01	0.5
sex			
Female	—	—	
Male	0.95	0.65, 1.38	0.8
Prior_ICB			
No	—	—	
Yes	1.78	1.04, 3.06	0.036
PS			
0-1	—	—	
2+	1.07	0.37, 3.10	0.9
Rx_type			
cICB	—	—	
sICB	0.68	0.40, 1.15	0.15

† HR = Hazard Ratio, CI = Confidence Interval

Figure 3.4: 12-week landmark cox proportional hazard model shows relationship between number of systems with irAEs and (a) OS (b) PFS while including patients that did not experience any irAEs (n = 272). 12-week landmark cox proportional hazard model shows relationship between number of systems with irAEs and (c) OS (d) PFS in patients that experienced any irAEs (n = 217). All multivariate analyses were performed adjusting for age, sex, ICB type, performance status and prior exposure to BRAF inhibitors or ICB.

(a) OS

Characteristic	HR[†]	95% CI[†]	p-value
Grade			
No_tox	—	—	
1-2	0.39	0.23, 0.67	<0.001
3+	0.43	0.26, 0.71	0.001
age	1.00	0.99, 1.02	0.5
sex			
Female	—	—	
Male	1.15	0.78, 1.68	0.5
Prior_ICB			
No	—	—	
Yes	1.57	0.90, 2.74	0.11
PS			
0-1	—	—	
2+	1.18	0.51, 2.78	0.7
Rx_type			
cICB	—	—	
sICB	0.87	0.52, 1.44	0.6

[†] HR = Hazard Ratio, CI = Confidence Interval

(b) PFS

Characteristic	HR[†]	95% CI[†]	p-value
Grade			
No_tox	—	—	
1-2	0.50	0.32, 0.79	0.003
3+	0.51	0.33, 0.80	0.003
age	1.00	0.98, 1.01	0.7
sex			
Female	—	—	
Male	0.87	0.63, 1.19	0.4
Prior_ICB			
No	—	—	
Yes	1.59	1.01, 2.49	0.044
PS			
0-1	—	—	
2+	1.35	0.65, 2.83	0.4
Rx_type			
cICB	—	—	
sICB	0.80	0.52, 1.24	0.3

[†] HR = Hazard Ratio, CI = Confidence Interval

(c) OS

Characteristic	HR[†]	95% CI[†]	p-value
Grade			
1-2	—	—	
3+	1.11	0.65, 1.88	0.7
age	1.00	0.98, 1.02	0.8
sex			
Female	—	—	
Male	1.29	0.81, 2.04	0.3
Prior_ICB			
No	—	—	
Yes	2.16	1.10, 4.23	0.025
PS			
0-1	—	—	
2+	0.55	0.12, 2.44	0.4
Rx_type			
cICB	—	—	
sICB	0.95	0.51, 1.79	0.9

[†] HR = Hazard Ratio, CI = Confidence Interval

(d) PFS

Characteristic	HR[†]	95% CI[†]	p-value
Grade			
1-2	—	—	
3+	1.04	0.67, 1.59	0.9
age	1.0	0.98, 1.01	0.5
sex			
Female	—	—	
Male	0.98	0.68, 1.42	>0.9
Prior_ICB			
No	—	—	
Yes	1.98	1.16, 3.38	0.012
PS			
0-1	—	—	
2+	0.87	0.30, 2.53	0.8
Rx_type			
cICB	—	—	
sICB	0.91	0.54, 1.54	0.7

[†] HR = Hazard Ratio, CI = Confidence Interval

Figure 3.5: 12-week landmark cox proportional hazard model shows relationship between maximum grade of irAEs experienced by a patient and (a) OS (b) PFS while including patients that did not experience any irAEs (n = 272). 12-week landmark cox proportional hazard model shows relationship between maximum grade of irAEs experienced by a patient and (c) OS (d) PFS in patients that experienced any irAEs (n = 217). All multivariate analyses were performed adjusting for age, sex, ICB type, performance status and prior exposure to BRAF inhibitors or ICB.

Given the immunosuppressive effects of steroids and other medications used in the management of irAEs, I sought to look at the impact of these medications on outcome, limiting analysis to patients who experienced any grade toxicities. However, steroid use (OS: HR = 0.97, (0.60 – 1.57), p = 0.90; PFS: HR = 1.09, (0.69 – 1.73), p = 0.70) or use of other second

line medications (OS: HR = 0.74, (0.42 – 1.31), p = 0.30; PFS: HR = 0.99, (0.64 – 1.53), p = 0.90) for the management of irAEs had no significant impact on the outcome of patients (Figure 3.6).

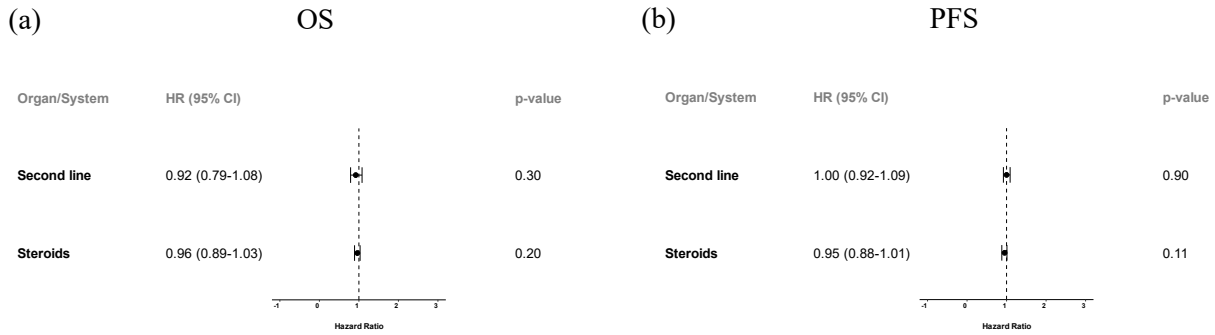


Figure 3.6: Cox proportional hazard model showing the relationship between the use of immunosuppressants for the management of irAEs and impact on (a) overall survival and (b) progression-free survival (n = 225). Each parameter was tested while adjusting for age, sex, ICB type, performance status and prior exposure to BRAF inhibitors or ICB.

3.1.4 irAEs and Patient outcome sub-section summary

In this section, I have shown that the occurrence of any grade irAEs is associated with good outcome in patients with metastatic melanoma managed with ICB, while adjusting for variability in the time to onset of irAEs. In addition, I showed that occurrence of dermatological irAEs is associated with good outcome, while the occurrence of cardiac irAEs is associated with poor outcome. These findings reinforce the urgent need for a biomarker for irAEs. Pre-emptive identification of patients who are more likely to have irAEs would enable patient-oriented management of irAEs and potentially lead to better outcomes in these patients.

3.1.5 Sub-section acknowledgements

The clinical data was prepared by Martin Little.

3.2 Induction of *IL7* in B cells

3.2.1 Introduction

While there is currently no biomarker to predict the occurrence of irAEs, previous work in our lab has identified that carriers of a single nucleotide polymorphism at rs16906115, intronic to *IL7* have increased likelihood of irAEs validating a similar observation in another independent study[103]. In addition to this, it was also shown that carriers of the SNP had significantly higher levels of *IL7* expression in their B cells compared to non-carriers and independent of the SNP and the ICB type administered, B cell *IL7* expression was predictive of irAEs. Suggestive of a causal link between B cell *IL7* and irAEs. Furthermore, carriers of the SNP, who expressed more *IL7* in their B cells, were characterized to have lesser naivety of both B and T cell repertoire and more lymphocyte stability compared to non-carriers[104]. However, the mechanism leading to *IL7* expression in B cells of metastatic melanoma patients remains unclear. Considering that *IL7* expression was observed in peripheral blood $CD19^+$ cells of patients with metastatic melanoma, we hypothesize that there is a cancer-derived soluble factor which induces *IL7* expression in B cells of metastatic melanoma patients. Therefore, to test this hypothesis, I cultured B cells from healthy donors in plasma from patients with metastatic melanoma as well as in conditioned media obtained from different metastatic melanoma cell lines. B cells used in culture were obtained from 4 healthy donor cones, numerically labelled donor 1 through 4.

3.2.2 Healthy B cells in Plasma

In order to increase the chances of identifying a response, patients in the discovery cohort with high expression of *IL7* at baseline were identified from bulk RNA data. Normalisation was performed using DESeq2 as described in section 2.8.1.3. The top 5 patients and their normalised B cell *IL7* expression values are displayed in table 3.2.

Patient ID	**Normalised *IL7* Expression**
49	10.25
38	10.08
159	10.06
66	9.98
54	9.95

Table 3.2: Normalised *IL7* expression of top 5 patients in the cohort

Healthy B cells were cultured in plasma from these patients. However, despite progressively increasing the number of healthy B cells cultured up to 3 x 10^5 cells/well, the RNA yield from B cells cultured in patients' plasma was persistently undetectable by fluorescence

quantification (Qubit) despite optimisation of the culture condition with stimulatory cytokines – IL-2, IL-21 and soluble CD40 ligand (details of optimisation can be found at Appendix A). To obtain detectable RNA values, approximately 6 x 10^5 cells were cultured per condition. RNA values recorded from this experiment are displayed in Figure 3.7. In-keeping with previous observation, RNA yield from B cells cultured in experimental (plasma) conditions were remarkably lesser compared to control (media alone). cDNA was generated and qPCR was performed for *IL7* quantification. Average delta Ct values are recorded in the table 3.3. Unsurprisingly, the average Ct values of both *IL7* and *GAPDH* were higher in the experimental conditions compared to the control condition which denotes a reduction in *IL7* and *GAPDH* transcript levels respectively. This is likely due to the low RNA yield from these conditions. However, given the large variation in the housekeeping gene, *GAPDH* between experimental conditions, I had limited confidence in this result. This experiment required the use of large number of resources and required further optimization of the conditions; however, I did not have time to explore this.

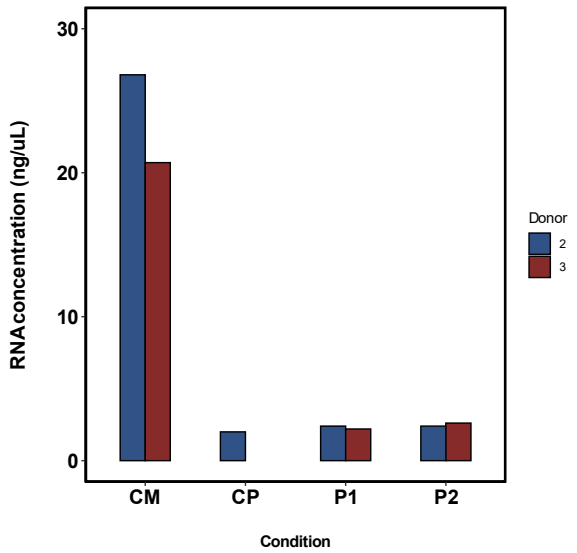


Figure 3.7: RNA concentrations measured by fluorescence quantification. CM – Control media; CP – Control plasma; P1 & P2 – plasma from 2 patients with metastatic melanoma (ID = 38 and 159).

Donor	Condition	IL7 average Ct	GAPDH average Ct
2	Control media (CM)	25.9	18.4
	Control Plasma (CP)	34.2	25.5
	Patient's plasma (P1)	35.82	28.6
	Patient's plasma (P2)	33.82	25.95
3	Control media (CM)	26.75	20.0
	Control Plasma (CP)	34.64	29.36
	Patient's plasma (P1)	34.69	29.27
	Patient's plasma (P2)	33.28	27.16

Table 3.3: Average Ct values of *IL7* and *GAPDH* from quantitative polymerase chain reaction. Approximately 6 x 10^5 healthy B cells were cultured.

3.2.3 B cell *IL7* expression by Melanoma Conditioned Media

Considering the hypothesis that B cell *IL7* is induced in the state of cancer, I tested to see if cancer cell lines might release factors that induced B cell *IL7*. Melanoma conditioned media (MCM) were produced from different melanoma cell lines. First, from four cell lines: A375P, 501Mel, CHL1, SKMEL28. B cells were then cultured in MCM for 72 hours. RNA yield from this experiment was robust across all conditions from approximately 3 x 10^5 B cells per condition. *IL7* quantification performed using SYBR green qPCR revealed a marked heterogeneity in *IL7* expression between healthy donor B cells (Figure 3.8a). Specifically, there was an increase in *IL7* transcripts levels in B cells from donor 1 cultured in MCM from all cell lines except A375P. A marginal increase in *IL7* transcript levels was observed for Donor 4 in 2 cell lines: A375P and SKMEL28. While an increase in *IL7* transcript levels was observed in Donor 2 by only 501Mel cell line, there was no increase in *IL7* levels in Donor 3 across all cell lines. To further investigate this heterogeneity and potentially identify a cell line that consistently induced *IL7* in all donor B cells, I produced MCM from 3 other melanoma cell lines (ME, Na8 and SKMEL2) and incubated healthy B cells in these. I again observed this heterogeneity in *IL7* expression between donor B cell samples (Figure 3.8b). Robust *IL7* induction was observed consistently in donor 1 B cell samples, marginal in donor 4 by Na8 and SKMEL2 cell lines and not at all in donor 2 and 3 samples. Attempt was made to evaluate the expression of a few other genes that were reported to correlate with *IL7* by Taylor *et al*[104]. However, I only observed a marginal increase in the transcription factors *IKZF3* and *TFE3* with heterogeneity between donor samples again observed. (Figure 3.8c).

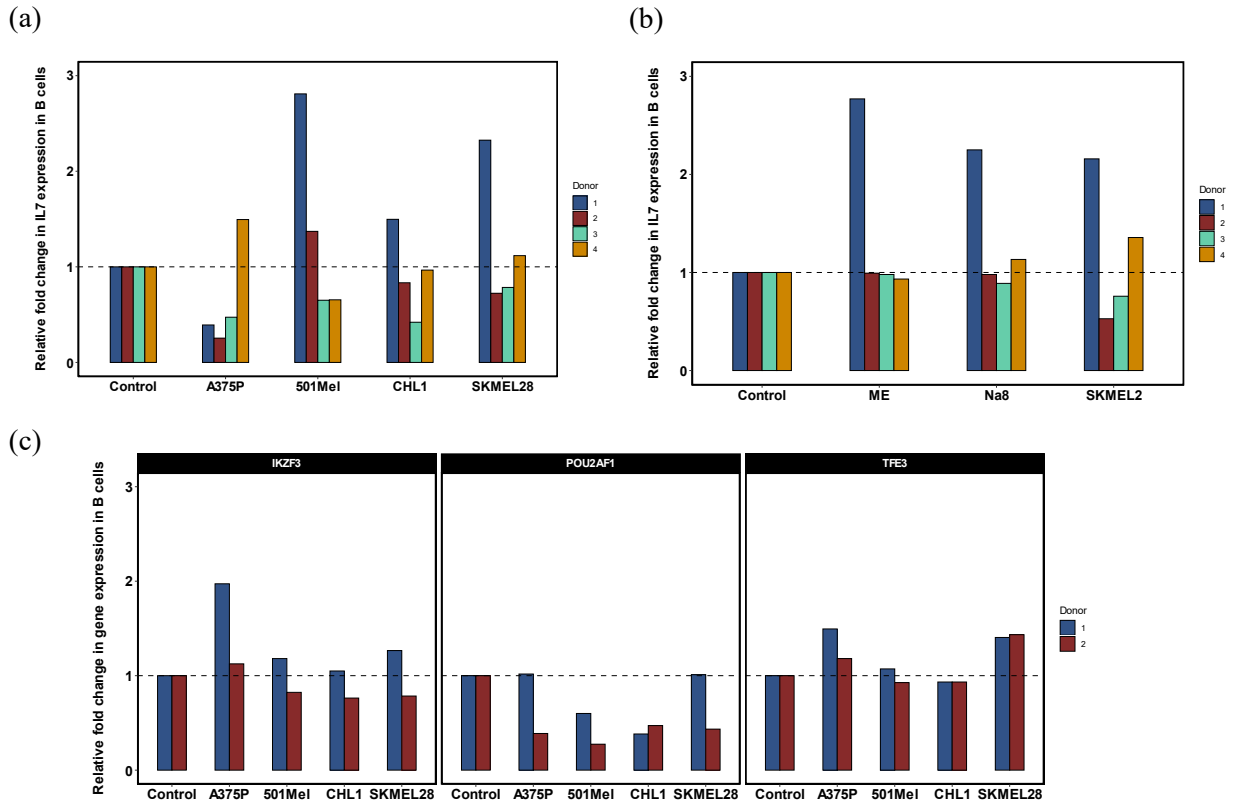


Figure 3.8: Bar plots showing relative fold change in *IL7* in A375P, 501-Mel, CHL-1 and SKMEL28 cell lines. (b) as in (a) but in ME, Na8 and SKMEL2 cell lines. (c) Bar plots showing relative fold change in the expression of *IKZF3*, *POU2AF1* and *TFE3* in B cells from 2 healthy donors cultured in conditioned media from 4 melanoma cancer cell lines: A375P, 501-Mel, CHL-1 and SKMEL28.

3.2.4 B cell *IL7* expression and Patient characteristics

The heterogeneity observed in the B cell response between donors suggest that there is a donor intrinsic factor involved in the expression of *IL7* in B cells. While I had no information on the characteristics of the donors of the blood cones, I explored the relationship between B cell *IL7* expression and patient characteristics in the discovery cohort. However, asides from the previously reported association showing that carriers of the *IL7* SNP had significantly higher *IL7* expression in their B cells compared to non-carriers, I observed no relationship with age (R = 0.11, p = 0.22) or sex (p = 0.57) (Figure 3.8a and 3.8b). No difference was also observed based on BRAF mutational status (Wilcox test, p = 0.79) or disease metastatic state (Wilcox test, p = 0.55) (Figure 3.8c and 3.8d). At a minor allele frequency (MAF) of 8%, it is unlikely that the carriage of the SNP alone would explain the heterogeneity in the *IL7* response in donor B cells. Although, due to time constraints, the carriage of the *IL7* SNP is yet to be tested in donor B cells.

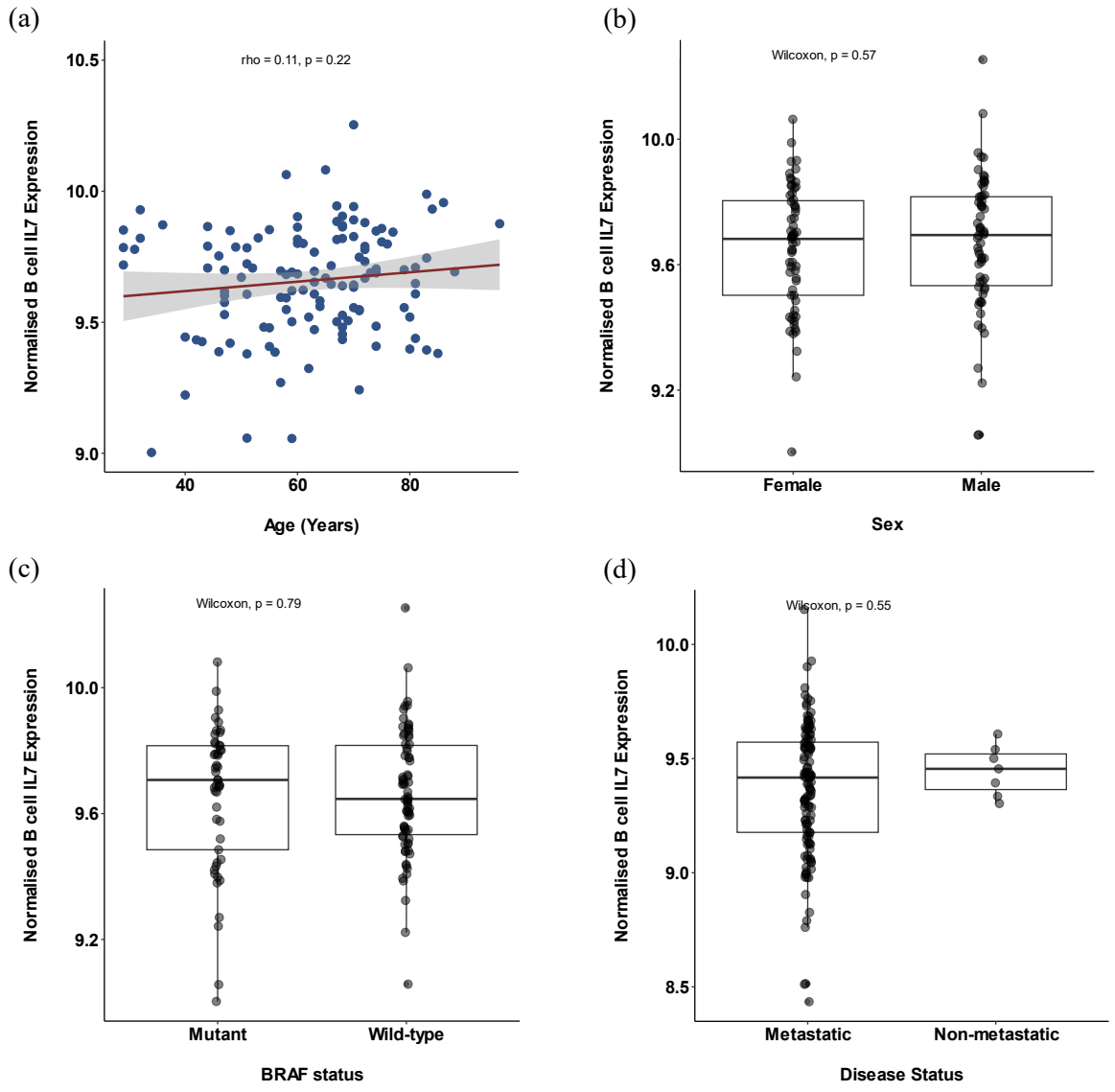


Figure 3.9 (previous page): (a) Normalised *IL7* expression correlated with age (in years) at diagnosis (Spearman Rank Correlation test). Boxplots of normalised *IL7* expression and (b) Sex, (c) BRAF mutational status and (d) disease stage. Statistics computed using Wilcoxon rank sum test.

3.2.5 Induction of *IL7* sub-section summary

Here, I showed that melanoma secretome is able to induce *IL7* expression in B cells, albeit heterogeneously, depending on the donor B cell sample and cancer cell line. The low RNA yield from B cells cultured in plasma compared to those cultured in control media suggests the absence of key nutrients required by B cells for survival or less likely, the presence of a growth inhibitor in plasma.

3.3 Plasma Proteins and B cell *IL7* expression

3.3.1 Introduction

Taking a different approach, I employed the services of Olink technology, which uses a technique called proximity-extension assay, a dual-antibody based system combined with qPCR that enables the simultaneous measurement of several analytes in the plasma. A pre-defined panel called 'Olink Target 96 Immuno-oncology' was selected. The panel contains 92 carefully curated proteins biomarkers with reported role in the immunological response to cancers. Plasma concentrations are reported as normalised protein expression (NPX) values which represents the relative quantification of proteins. I then evaluated the relationship between B cell *IL7* expression and expression values of the 92 plasma proteins.

3.3.2 Normalisation and Quality control

Plasma samples from 57 patients were sent in 2 batches. First batch had two plates and the second batch had one plate. Results were provided in an excel spreadsheet and combined into a single document in R. Uniform manifold approximation and projection (UMAP) plot showed significant batch effects between plates (Figure 3.10a and Supplementary Figure B.2a). Intensity normalisation was performed using a wrapper function which performs the following steps sequentially: first for each assay, the overall median value for all samples and plates is calculated, then for each plate and assay, the plate-specific median value is calculated, next, for each assay, the plate specific median value is subtracted from each value and finally the overall median value is then added for each assay. UMAP plot following normalisation shows the successful removal of batch effects, evidenced by overlap of samples between plates and no differences in median of assays between plates (Figure 3.10b and Supplementary Figure B.2b).

As part of the olink workflow, internal controls are added to each sample. These were used to perform quality control analysis. Samples that deviate less than 0.3 NPX from the plate median are deemed to pass quality control. Samples that do not pass i.e. deviate more than 0.3 NPX are tagged with a 'warning' label (highlighted in red in Figure 3.10c). These samples were filtered out before normalisation and downstream analysis.

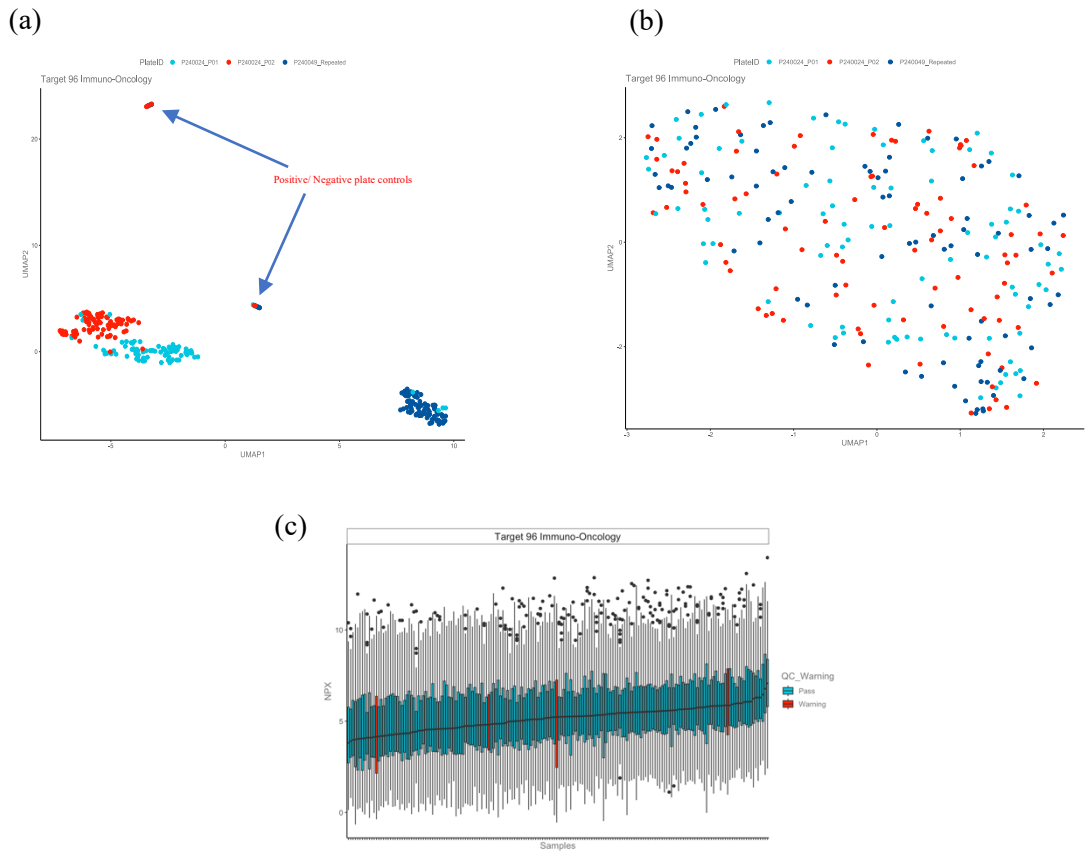


Figure 3.10: (a) UMAP plots showing significant batch effects between plates. (b) UMAP plot shows resolution of batch effects following intensity normalisation. (c) Boxplots of normalised expression of 92 plasma proteins per sample, coloured by quality assessment (blue = pass, red = warning/fail).

3.3.3 Plasma IL-6 and IL-10 concentration anti-correlates with B cell *IL7* expression

To get a sense of how different plasma protein concentrations modulate B cell *IL7* expression, batch-corrected normalised protein expression values were correlated with B cell *IL7* expression. Results showed a significant correlation between B cell *IL7* expression and concentrations of 9 plasma proteins: IL-6, TIE2, LAMP3, ANGPT2, TNFRS4, PD-L2, ADGRG1, GZMB, IL-10 (Figure 3.11). The most significant of these was the association with Interleukin 6 (IL-6) ($R = -0.4$, $p = 0.0021$). To further explore the potential interaction of these ligands with B cells, the expression values of B cell genes coding the receptors of the most significant proteins identified, were correlated with *IL7* expression. Receptors with low expression values (i.e. sum of gene count across samples is less than 10) were filtered out. Interestingly, a significant negative correlation was observed between *IL6R* and *IL7* ($R = 0.53$, $p = 2.2 \times 10^{-10}$) and between the expression value of the gene coding the alpha subunit of IL-10 receptor, *IL10RA* and *IL7* in B cells (Figure 3.12). Further suggestive of a modulatory role of the IL-6 and IL-10 cytokines on *IL7* expression in B cells.

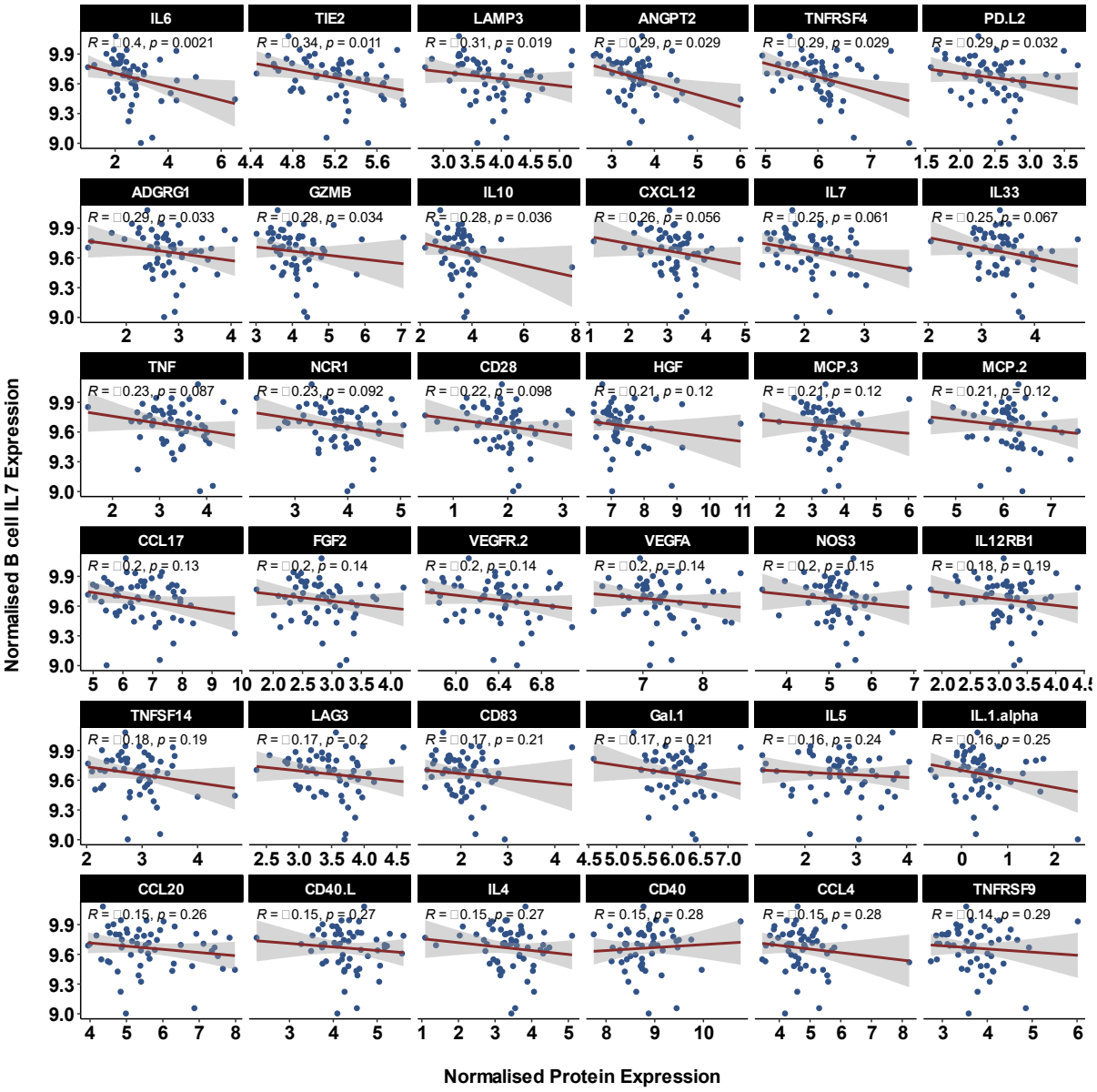


Figure 3.11: Correlation between normalised expression of *IL7* in B cells and normalised expression of proteins in plasma, ordered by level of statistical significance (First 36 (out of 92) proteins displayed). Statistics computed by Spearman correlation (n = 57).

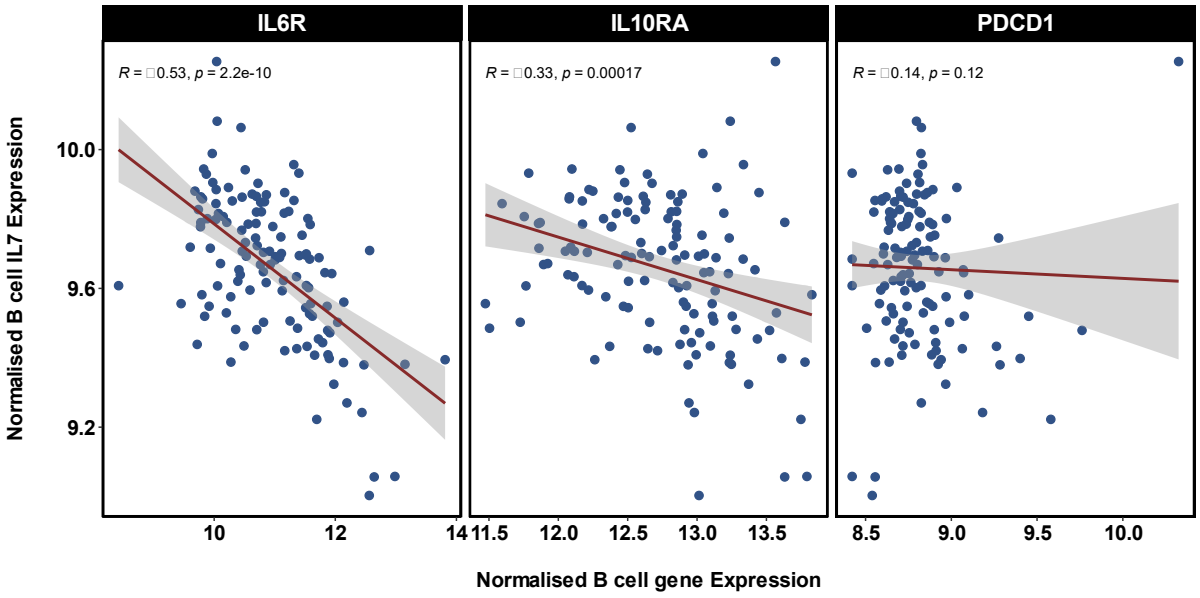


Figure 3.12: Correlation between normalised expression of *IL7* and normalised expression of *IL6R*, *IL10RA*, and *PDCD1* in B cells. Statistics computed by Spearman correlation (n = 125).

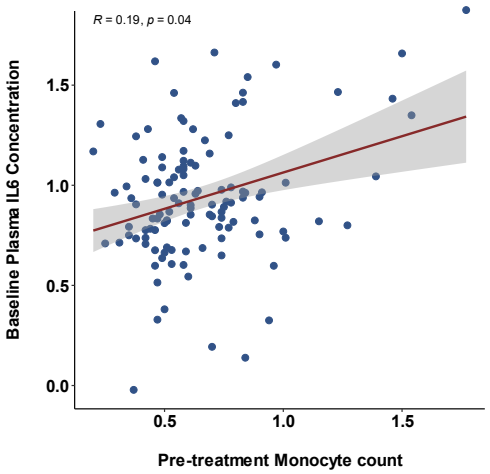
3.3.4 Pre-treatment monocyte count interacts with B cell *IL7*

Monocytes are the most important source of IL-6 at inflammatory sites[157], in line with this, I observed a significant correlation between pre-treatment monocyte count, obtained from routine hospital blood test and plasma IL-6 concentration (R = 0.19, 0.04) (Figure 3.13a). With the weak correlation suggestive of other determinants of plasma IL-6 concentrations. In addition, the population of monocytes and monocyte-derived cells such as TAMs and MDSCs have been described to modulate the activity of other immune cells in the TME and in turn the anti-tumour response[158]. Therefore, I sought to understand the relationship between monocytes and B cell *IL7*. Pre-treatment monocyte count was found to negatively correlate with B cell *IL7* expression (R = -0.2, p = 0.042) (figure 3.13b). I did not observe any significant correlation between B cell *IL7* expression and the baseline count of other immune cells (Neutrophils, Basophils, Eosinophils, Lymphocytes), nor with other published peripheral blood count derived markers of irAEs such as neutrophil-lymphocyte ratio (NLR) or lymphocyte-monocyte ratio (LMR) (Supplementary Figure B.3).

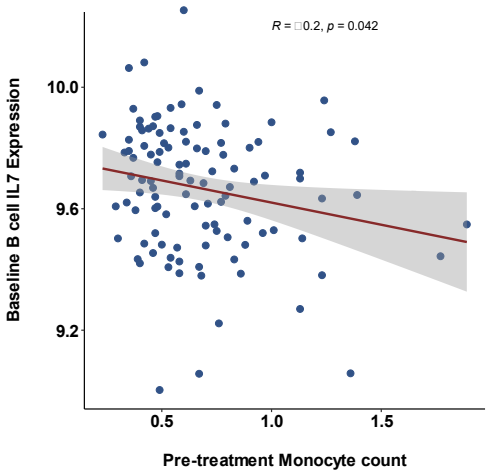
Interestingly, using a linear regression, I observed that when controlling for IL-6, this resolves the association between pre-treatment monocyte count and B cell *IL7* expression, however, independent of monocyte count, the effect of IL-6 on B cell *IL7* expression is preserved, although with marginal p-value (figure 3.13c). This suggests that IL-6 might be confounding the relationship between monocyte count and B cell *IL7* expression. Furthermore, while adjusting for IL-6, IL-10 and monocyte count, *IL6R* expression and *IL10RA* expression were

independently predictive of B cell *IL7* expression (figure 3.13d). This suggests that these are two independent pathways modulating *IL7* expression in B cells.

(a)



(b)



(c)

Characteristic	Beta	95% CI[1]	p-value
age	0.01	0.00, 0.01	0.017
sex			
Female	—	—	
Male	0.04	-0.08, 0.16	0.5
IL6	-0.06	-0.12, 0.00	0.056
Mono_pre	0.00	-0.22, 0.22	>0.9

[1] CI = Confidence Interval

(d)

Characteristic	Beta	95% CI[1]	p-value
age	0.00	0.00, 0.01	0.12
sex			
Female	—	—	
Male	0.08	-0.02, 0.18	0.12
IL6	-0.04	-0.10, 0.02	0.2
IL10	-0.02	-0.09, 0.05	0.6
Mono_pre	0.05	-0.14, 0.23	0.6
IL10RA_expression	-0.13	-0.22, -0.05	0.003
IL6R_expression	-0.09	-0.16, -0.03	0.006

[1] CI = Confidence Interval

Figure 3.13: Scatterplot showing correlation between pre-treatment monocyte and (a) Plasma IL-6 concentration and (b) B cell *IL7* expression (computed using spearman correlation test) (n = 108) (c) Linear regression model exploring the effect of IL-6 and pre-treatment monocyte count (Mono_pre) on B cell *IL7* (d) Linear regression model shows *IL6R* and *IL10RA* are independent predictors of *IL7* expression in B cells while adjusting for age, sex, pre-treatment monocyte count, plasma IL-6 and IL10 concentrations

I then fit pre-treatment monocyte count onto B cell expression using DESeq2 to explore B cell genes modulated by monocytosis. 1366 genes were observed to be differentially expressed (Figure 3.14a). Amongst the set of positively correlated genes (1215 genes), there was enrichment of myeloid derived genes such *MPO*, *AZU1*, *ARG1* which might suggest contamination of the B cell RNA. Pathway analysis of these gene set revealed enrichment of pathways such as 'wound healing', 'phagocytosis', and 'myeloid leukocyte differentiation' in-keeping with monocyte function (Figure 3.14b). Indeed, correcting for *MPO* in the DESeq2 design resolved most of these differentially expressed genes (Figure 3.14c). I hypothesize that this might represent an increase in B cell – Monocyte interactions associated with monocytosis, however, this is yet to be explored.

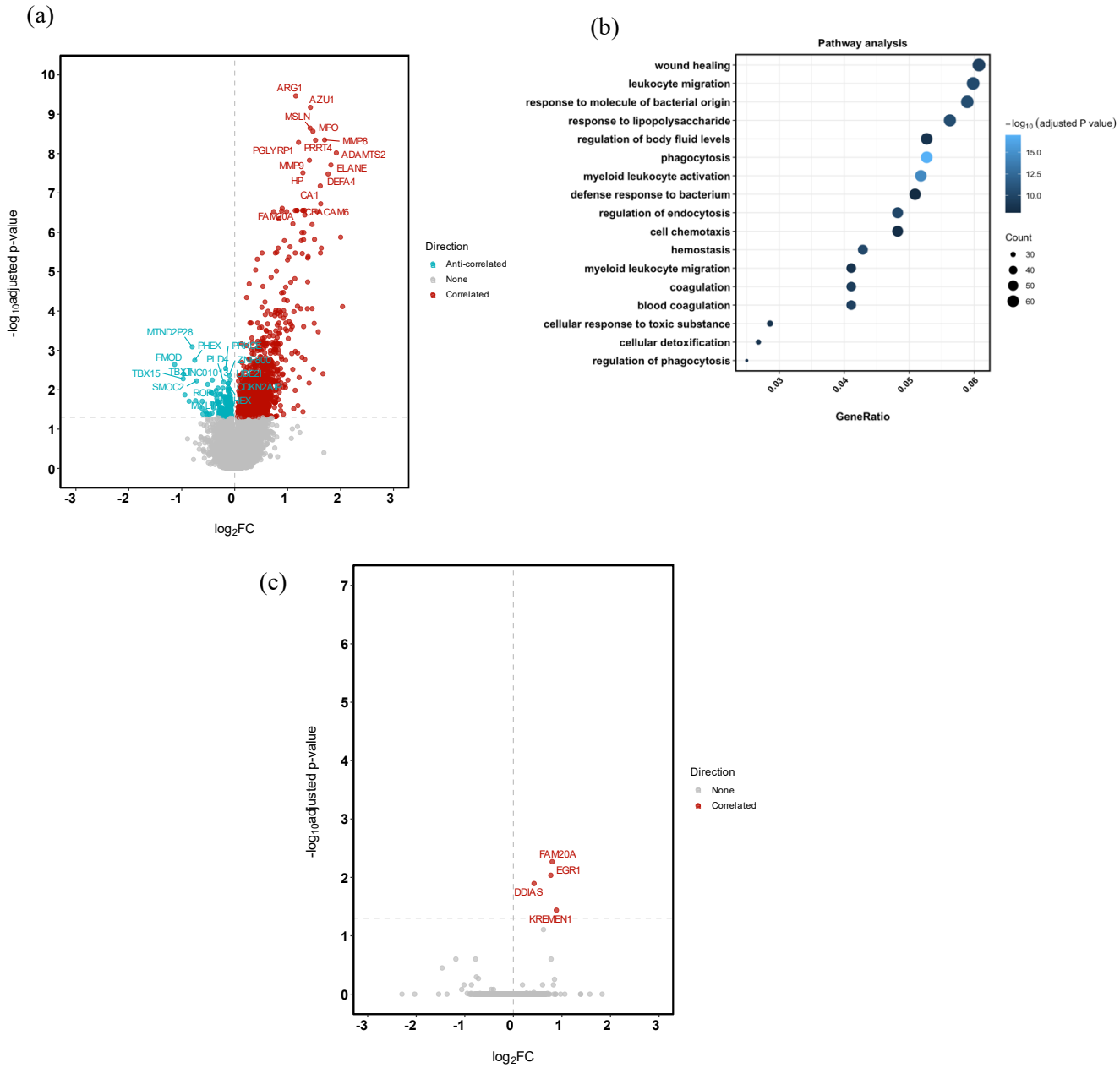


Figure 3.14: (a) Volcano plot demonstrating B cell genes correlated with pre-treatment monocyte count from routine clinical test (n = 108) using DESeq2. Age, sex, library RNA input and sequencing batch were included as controls in the design argument (b) Gene Ontology Biological Process (GOPB) analysis of genes positively correlated with pre-treatment monocyte count. (c) Volcano plot as in (a) in addition to controlling for *MPO* expression in the design argument. Statistics were calculated using the negative binomial distribution and adjusted for multiple testing using the Benjamini-Hochberg procedure in DESeq2

3.3.5 Sub-section summary

In summary, in this section, I have shown that the cytokines IL-6 and IL-10 pathway might be involved in the regulation of *IL7* expression in B cells. In addition, monocytes possibly through the production of IL-6 might also be involved in the regulation of *IL7* expression.

3.3.6 Sub-section acknowledgements

Bench work and Normalisation was performed by Dylan Muldoon. Images of the normalisation were generated by him and used with his permission.

3.4 Cell-cell Interaction using NicheNet

3.4.1 Introduction

The activity of B cells is known to be modulated by other cells of the immune system. Particularly, interactions with $CD4^+$ T cells are critical in the formation of memory B cells. Therefore, I wanted to explore how other cells in the B cell microenvironment impact on its gene expression changes. NicheNet is a novel bioinformatic tool which predicts ligand-receptor-target pathways using gene expression data of cells and prior information of ligand-target interactions. The tool is built on three databases which contain current information on ligand-receptor pathway, intracellular signalling and gene regulatory interactions. Using this prior knowledge, NicheNet generates a regulatory potential score for each ligand-target link, denoting how well prior knowledge supports that a ligand may regulate the expression of a target gene. A potential ligand activity score is also calculated using the area under the precision recall curve denoting the likelihood of the ligand interacting with the receiver cell. This ligand activity score is mainly used to rank the ligands in order of potential activity on the cell of interest. The tool provides two modes of analysis: a sender-agnostic and a sender-focused approach. While the sender focused approach considers ligands from only the cells in the single cell data, the sender-agnostic approach considers ligands from other potential cells or sources not present in the single cell data. The single cell experiment and data pre-processing was performed by Rob, a previous DPhil student in the laboratory. In this experiment, PBMCs from 14 patients with metastatic melanoma were sequenced.

3.4.2 Selection of gene set of interest and background genes

A critical step in NicheNet analysis is defining the gene set of interest. Here, to define the gene set, differential gene expression analysis was performed between B cells with at least one single copy of *IL7* (*IL7*+) versus B cells with no copy of the *IL7* transcript (*IL7*-). 573 transcripts (290 upregulated, 283 downregulated) were observed to be differentially expressed (Figure 3.15a). Approximately 97% of these genes have been previously reported to correlate with *IL7*[104]. Pathway analysis of the upregulated genes revealed enrichment of pathways involved in B cell activation and differentiation (Figure 3.15b). I therefore selected the first 30 upregulated genes as the genes of interest.

3.4.3 Sender Agnostic Method

In the sender-agnostic (SA) method, potential ligands were defined as ligands whose cognate receptor is expressed by B cells. 158 receptors were identified to be expressed by B cells and 497 ligands were identified to potentially interact with these receptors based on prior knowledge. Ligands were then ranked based on their predicted activity in B cells and figure 3.16a shows the top 30 ligands with highest ligand activity. The receptors these ligands bind to were identified using NicheNet (Figure 3.16b). Ligand-target analysis of the first 30 ligands were identified and CD40LG, Interferon-gamma (IFNG) and IL-13 were identified as potential ligands modulating the expression of *IL7* in B cells (Figure 3.17). In addition, IFNG was also predicted to regulate the expression of key *IL7* correlated genes involved in antigen presentation *HLA-DRA* and *HLA-DPA1*.

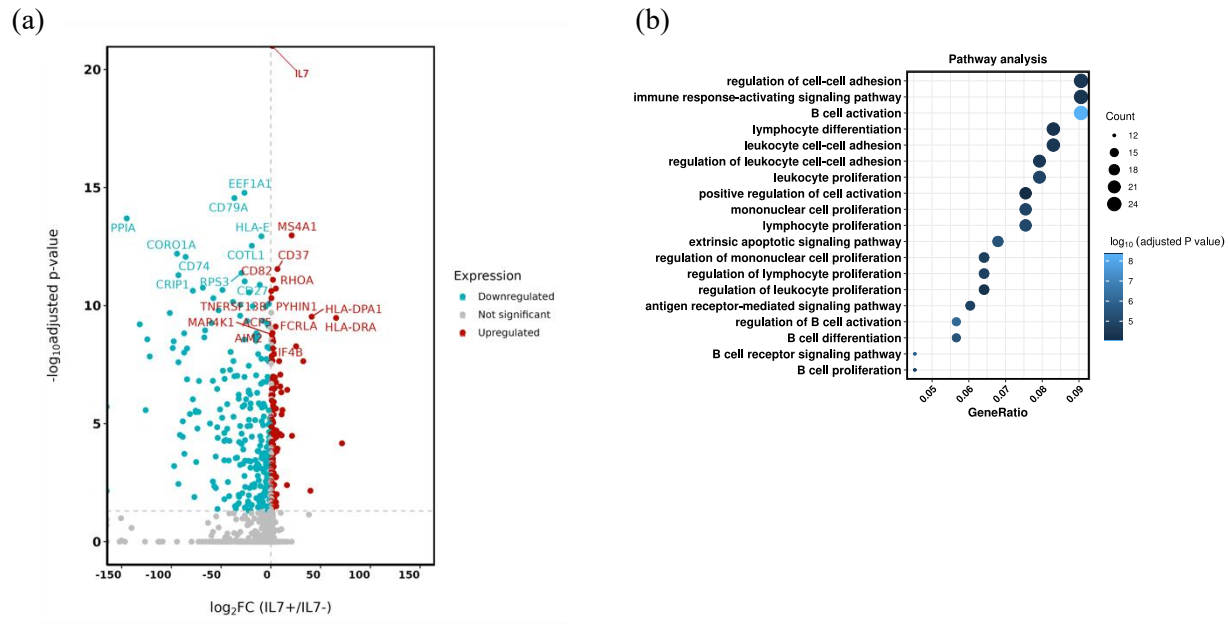


Figure 3.15: (a) Volcano plot showing differentially expressed genes between *IL7*+ and *IL7*- B cells in single cell data of patients with metastatic melanoma (n = 14). Statistics was computed using non-parametric Wilcoxon rank sum test, p-value adjusted for multiple testing using Bonferroni correction. (b) Pathway analysis of upregulated genes in *IL7*+ cells.

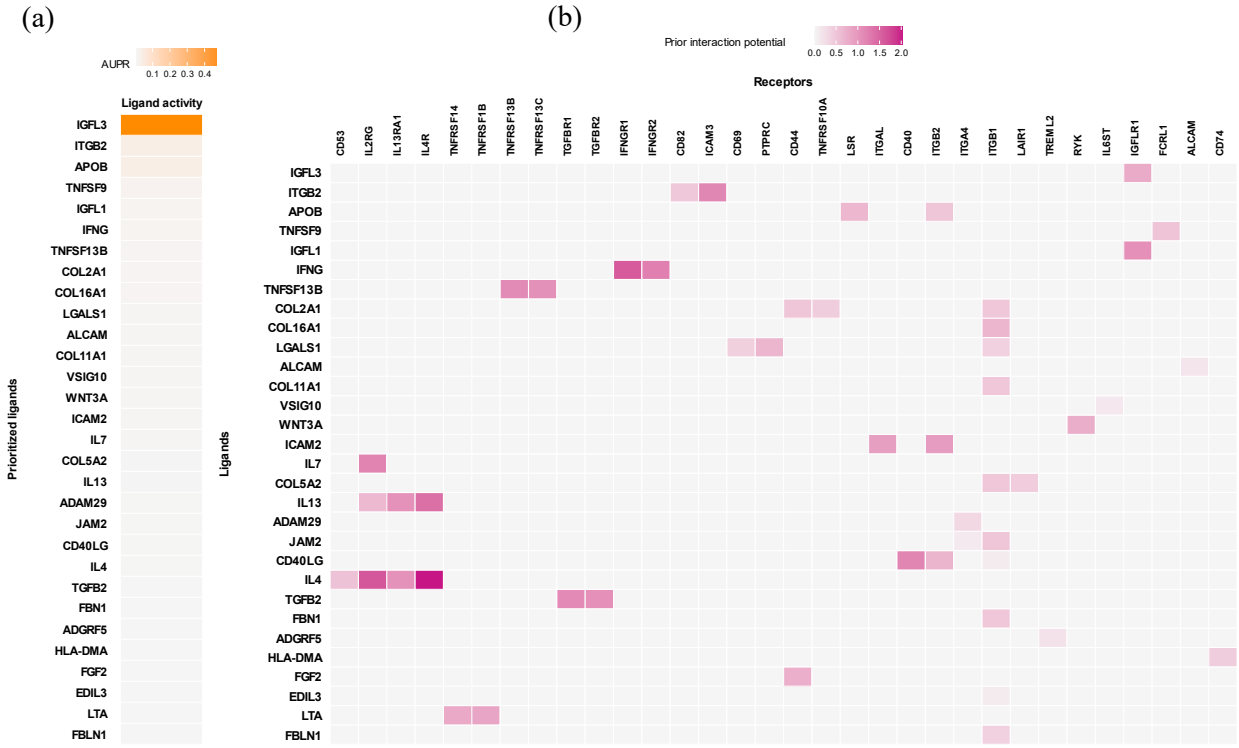


Figure 3.16: Sender Agnostic analysis. (a) Heatmap showing the predicted activity of the top 30 (out of 497) ligands on B cells. Ligand activity metric is the area under the precision recall curve (AUPR) (b) Ligand-receptor heatmap showing the top 30 ligands and the receptor(s) they interact with based on prior interaction potential.

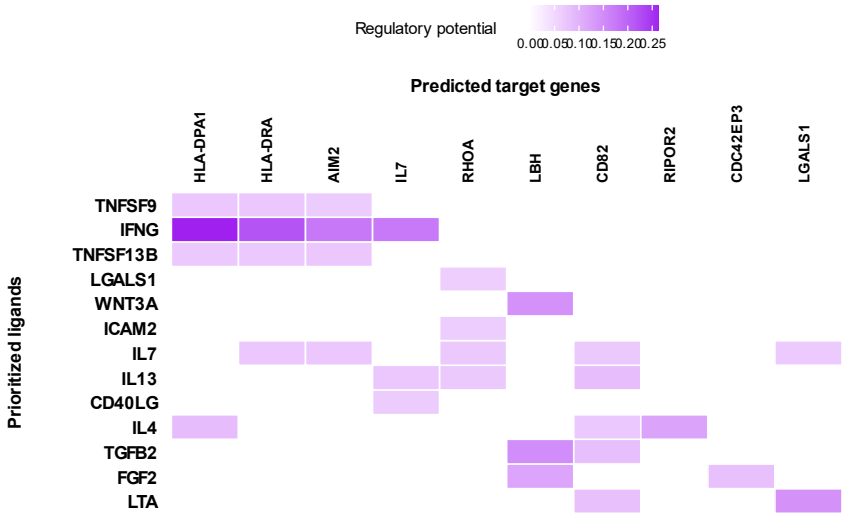


Figure 3.17: Heatmap showing ligand-target pairs with highest regulatory potential (> 0.05) as predicted by NicheNet). *IL7* expression predicted to be regulated by IFNG, IL-13 and CD40LG.

3.4.4 Sender Focused Method

All cells – B cells, $CD4^+$ T cells, $CD8^+$ T cells, Monocytes – were identified as a potential 'sender' cells in the sender-focused (SF) approach. Here potential ligands were defined as the ligands expressed by at least one of the sender cells whose cognate receptor is expressed by the receiver cell (B cells). A total of 132 potential ligands met this inclusion criteria and ligand activity analysis was performed. The first 30 ligands with the highest activity on B cells and the receptor they bind to are shown in Figure 3.18a and 3.18b. Ligand-target analysis again identified CD40LG as a potential ligand modulating *IL7* expression in B cells (Figure 3.18c). In addition, $CD4^+$ T cells were predicted as the source of the ligand, CD40LG (Figure 3.18d). Interestingly, B cells were predicted as a source of *IL7* and regulating the expression of *HLA-DRA* and *AIM2*, suggesting that *IL7* produced by B cells might be acting in an autocrine fashion to regulate antigen presentation and the humoral response.

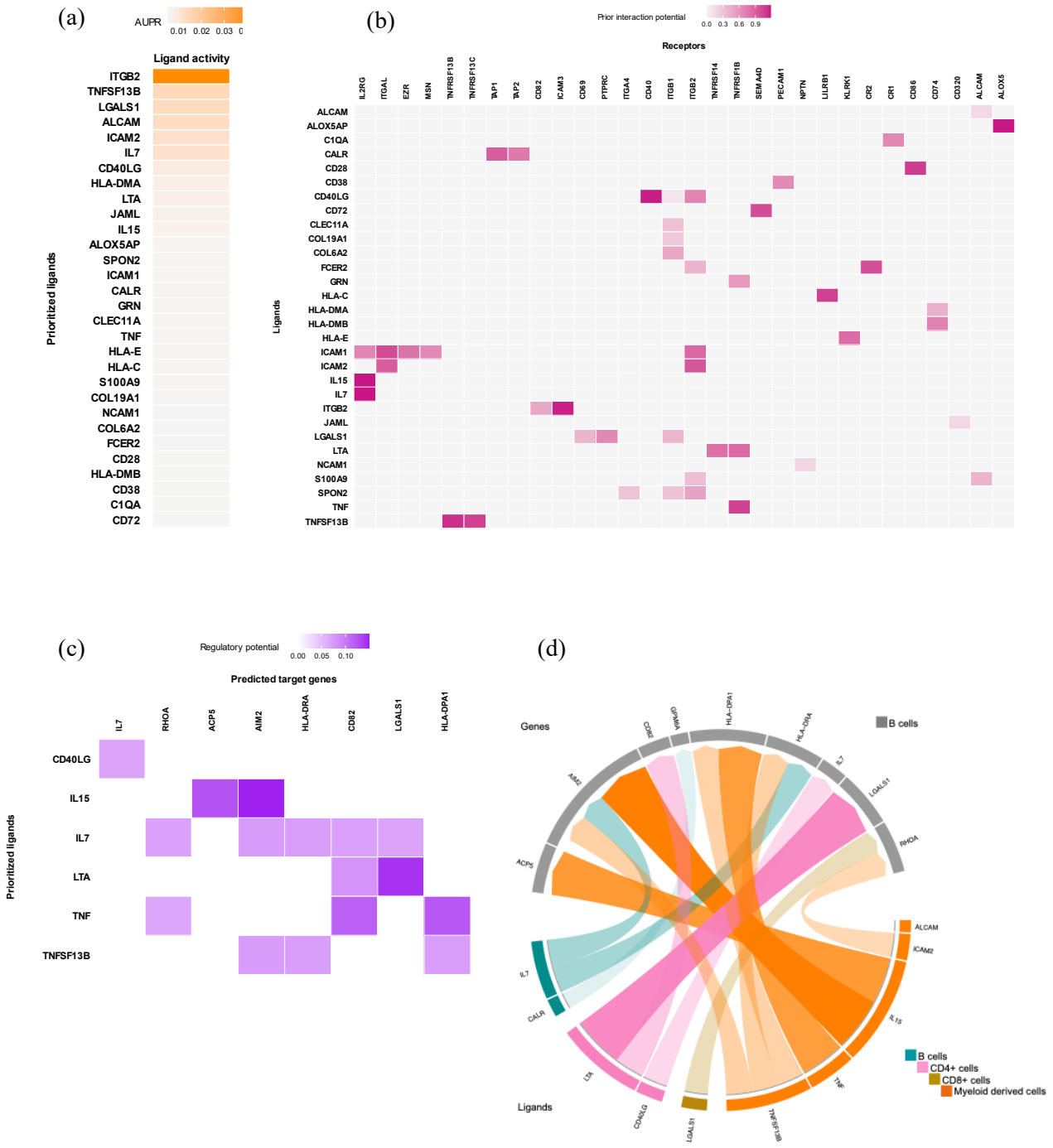


Figure 3.18: Sender Focused Analysis. (a) Heatmap showing the predicted activity of the top 30 (out of 132) ligands on *IL7* and *IL7* correlates (b) Ligand-receptor heatmap showing the top 30 ligands and the receptor(s) they interact with based on prior interaction potential. (c) Heatmap showing ligand-target pairs with highest regulatory potential (> 0.05) as predicted by NicheNet. (d) Circus plot showing cell source of ligands and B cell genes being modulated. Coloured by sender cell. Strength of regulatory potential represented by opacity of lines.

3.4.5 *CD40LG/CD40* correlates with B cell *IL7* in single cell and bulk RNA data

While NicheNet is able to predict the regulatory role of a ligand on a gene or set of genes, the bioinformatic tool does not inform on the direction of the effect. Therefore, I explored the relationship between $CD4^+$ T cell *CD40LG* expression and B cell *IL7* expression. First in single cell, I aggregated the expression values per individual of *CD40LG* and *IL7* from $CD4^+$ T cells and B cells respectively. I observed a significant positive correlation between $CD4^+$ T cell *CD40LG* expression and B cell *IL7* expression (R = 0.66, p = 0.011) (Figure 3.19a). I also observed a significant positive correlation between the expression value of the CD40LG receptor, *CD40* and *IL7* in B cells both in single cell data after aggregation of expression values (R = 0.89, p = 1.8 x 10^5) and in bulk RNA data (R = 0.46, p = 6.9 x 10^8) (Figure 3.19b and 3.19c). Further suggestive of a potential regulatory role of CD40LG on B cell *IL7* expression.

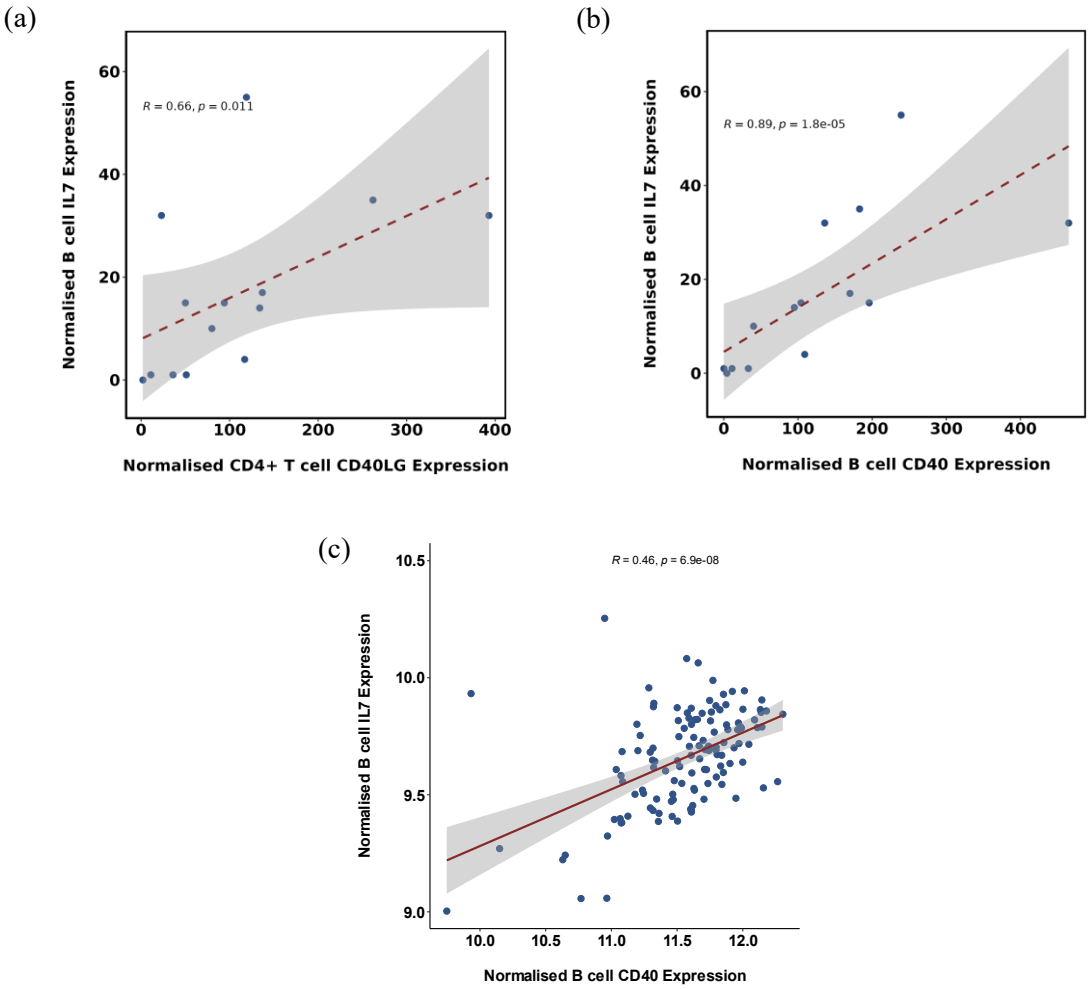


Figure 3.19: Scatter plot showing correlation between (a) Normalised $CD4^+$ T cell *C40LG* expression and Normalised B cell *IL7* expression in single cell after pseudobulking (n = 14) (b) Normalised B cell *CD40* expression and Normalised B cell *IL7* expression in single cell after pseudobulking (n = 14) (c) Normalised B cell *IL7* expression and Normalised B cell *CD40* expression in bulk RNA data (n = 125). Statistics were computed using Spearman correlation test.

3.4.6 NicheNet sub-section summary

Here, I have shown a potential contributory role of $CD4^+$ T cells to the modulation of *IL7* gene expression in B cells via CD40LG/CD40 interactions. In addition, IFN and IL13 were shown to potentially modulate the expression of *IL7*.

3.4.7 Sub-section acknowledgements

Single cell experiment including sample preparation, data pre-processing, clustering and annotation were performed by Robert Watson and used with his permission.

3.5 *IL7* dynamics in Durable Responders

3.5.1 Introduction

Based on the hypothesis that B cell *IL7* expression is being mediated by a cancer-derived factor, I reasoned that in the absence of the tumour, there should perhaps be a reduction in *IL7* expression of B cells. To evaluate this, we identified patients in the cohort with the following inclusion criteria:

- clinically and radiologically cancer-free;
- had at least 5 years of follow-up post-ICB and;
- previously had RNA sequencing performed at baseline

I was able to obtain blood samples from five patients who met these criteria. Four of these patients were managed with combination anti-PD1/anti-CTLA4 (cICB) therapy and one patient got only Pembrolizumab (sICB). B cells were then isolated from these samples, RNA was extracted and sent for sequencing. To address batch effects, six patients on the previous sequencing run for which we had RNA samples remaining were included on the new sequencing run. Such that, variations between these two samples would be accounted to batch effects. In total, eleven samples were sequenced (Table 3.3).

	Sample ID
5-year Samples	61, 64, 98, 103, 104
Intersecting Samples (all C2)	53, 61, 64, 106, 108, 134

Table 3.3: Sample ID of patients sequenced. C2 refers to blood sample after one cycle of immunotherapy

3.5.2 Batch Effects Correction

Following mapping of fastq files to reference genome and generation of count data, samples were checked for the presence of batch effects. Two batches were observed following principal component analysis, denoting the differences in time the sequencing was performed (Figure 3.20a). Batch effects were removed using *combat_seq*[159] and Figure 3.20b shows the distribution of the data after batch effects removal. Significant clustering was observed between the intersecting samples suggesting the successful removal of batch effects.

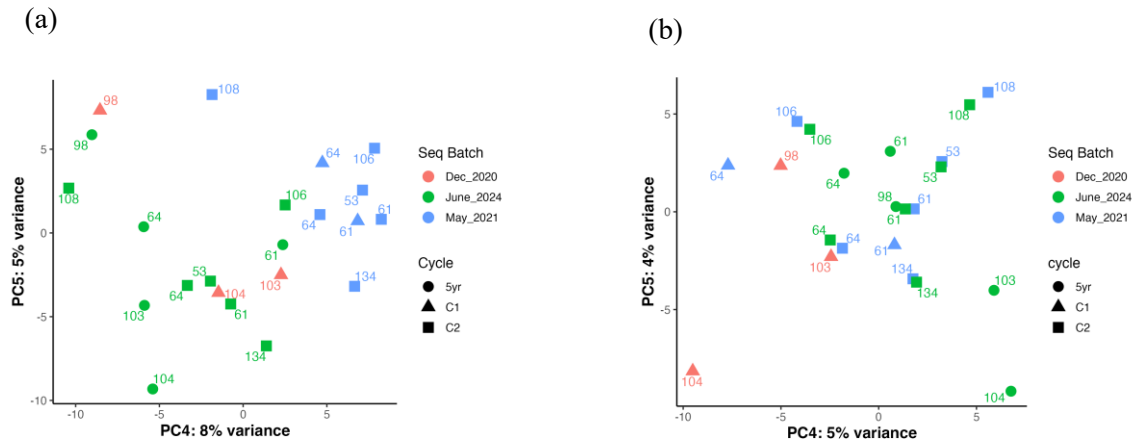


Figure 3.20: Principal component analysis showing samples (a) prior to correction of batch effects and (b) following batch effects removal using combat_seq. C1 represents patient sample prior to commencement of treatment; C2 – patient sample after one sample of ICB; 5yr – patient sample after at least 5 years of follow-up post ICB.

3.5.3 Long term B cell transcriptomic changes

After batch effects were removed, differential gene expression analysis was performed on five paired samples. I observed differential expression of 1298 genes. Upregulated genes include *IL10RA*, *IGHE*, *IGHG2*, and *BCL2* (figure 3.21a and 3.21b). Pathway analysis of genes upregulated in the 5-year post-treatment samples demonstrated enrichment of several mitochondrial pathways such as 'aerobic respiration', 'ATP biosynthetic process', 'electron transport chain' (figure 3.21c). In keeping with upregulation of mitochondrial genes associated with aging. Pathway analysis of genes downregulated revealed enrichment of pathways associated with response to type I interferon and defence response to virus (figure 3.21d). Suggesting a resolution of the anti-tumour response. Normalised *IL7* expression values were compared between the two time points. However, I did not observe any significant difference in *IL7* expression (figure 3.22). This lack of difference might perhaps be due to small sample size or change in B cell composition in the blood over this time period.

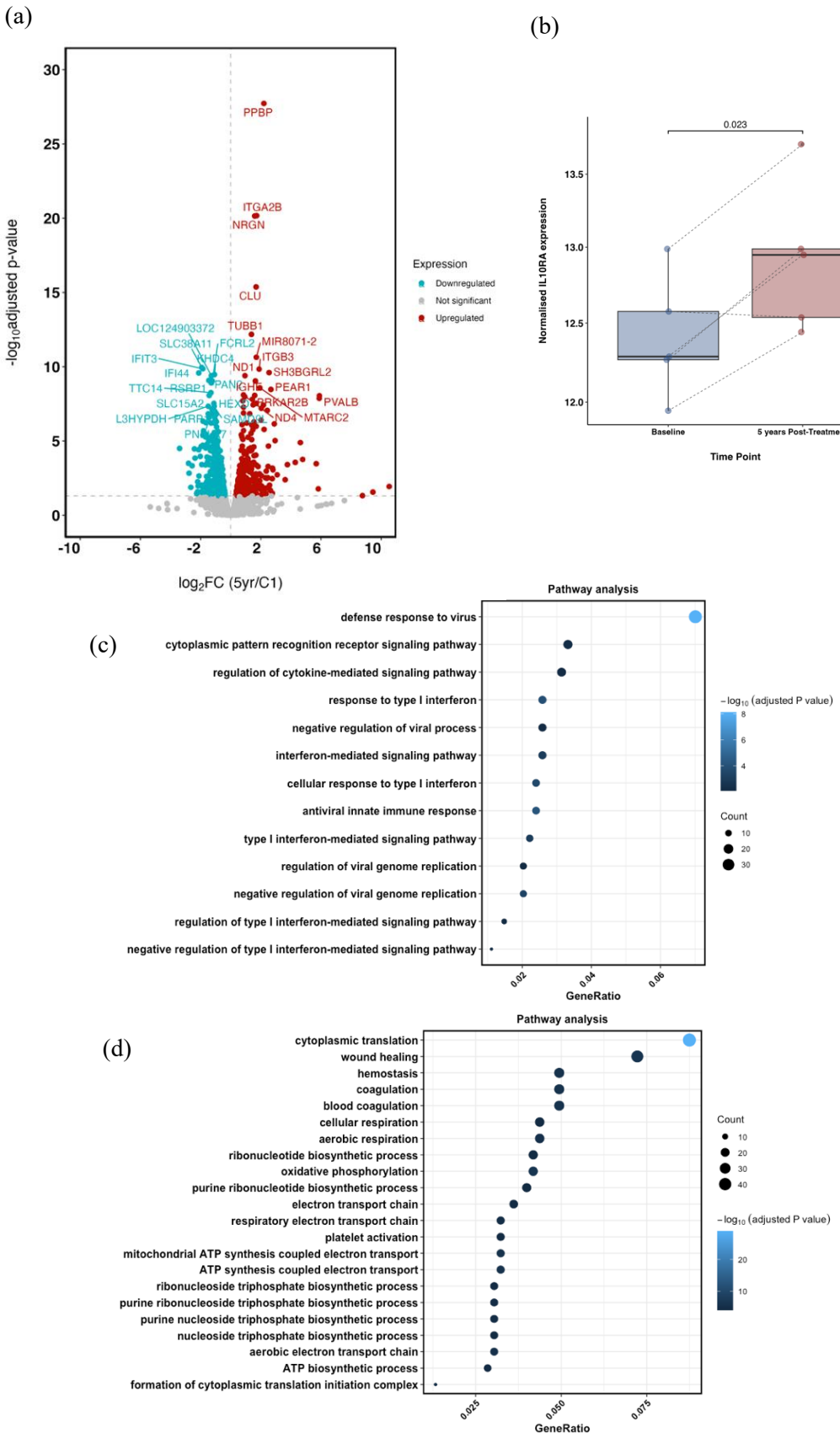


Figure 3.21: Differential gene expression analysis in durable responders. (a) Five paired CD19^{+} C1/5yr samples were compared for gene expression pre-ICB and 5 years post ICB using DESeq2. Patient ID was included as control in the design argument. Genes significantly enriched are in blue and those significantly downregulated are in red. The $\log_2$ fold change for each gene is visualised on the x-axis with the significance of this difference displayed on the y-axis. Statistics were computed using the negative binomial distribution and adjusted for

multiple testing using Benjamini-Hochberg procedure in DESeq2. (b) Comparison of normalised expression of *IL10RA* at baseline and 5 years post (Statistics computed using paired t-test). (c) Gene Ontology Biological Process (GOPB) analysis of genes downregulated at 5-years Post ICB (d) Gene Ontology Biological Process (GOPB) analysis of genes upregulated at 5-years post ICB.

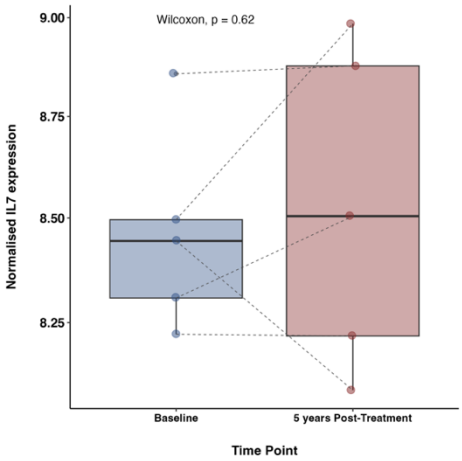


Figure 3.22: Boxplot showing comparisons between normalised *IL7* expression at baseline and 5-years post-ICB. Statistics computed using Wilcoxon signed-rank test (n = 5).

3.5.4 Sub-section acknowledgements

Informed consents were taken by Martin Little. Bulk RNA library preparation was performed by Dylan Muldoon and Sophie Mackay. Pre-processing of fastq files and generation of count data were performed by Guangyi Niu.

3.6 The Humoral response and impact on outcome in patients with metastatic melanoma

3.6.1 Introduction

The role of B cells in the anti-tumour response is increasingly being recognised. B cells in response to antigen exposure produce a wide variety of antibodies, such as IgG, IgA, IgM, IgD, and IgE[160]. In addition to their role in clearing invaders, these antibodies can also have diagnostic and prognostic purposes[161]. In line with evaluating the B cell response to melanoma, I sought to explore the relationship between plasma antibody concentrations and patient outcome. A bead-based technology was used to determine the concentrations of eight antibody subtypes – IgG1, IgG2, IgG3, IgG4, IgA, IgM, IgD, IgE – in plasma (more details in method section). Plasma concentrations at baseline and after one cycle of immunotherapy were measured in 112 patients with metastatic melanoma and this data was integrated with patient outcome data, bulk RNA and flow cytometry data of the patients.

3.6.2 Immunoglobulin concentration and Patient Outcome

First, I looked at the relationship between baseline immunoglobulin (Ig) concentration and patient outcome. Strikingly, pre-treatment IgD concentrations was predictive of worse overall survival (HR = 1.31 (1.02 – 1.70), p = 0.04) and progression-free survival (HR = 1.28 (1.05 – 1.57), p = 0.02) However, pre-treatment concentrations of IgG3 had the opposite effect on OS (HR = 0.45 (0.27 – 0.77), p = 0.004) and PFS (0.62 (0.42 – 0.92), p = 0.02). Pretreatment concentration of IgG1 was associated with increased risk of progression (HR = 1.78 (1.07 – 2.95), p = 0.03) but no significant relationship was observed with overall survival (1.51 (0.80 – 2.86), p = 0.2) (Figure 3.23a and 3.23b). Following one cycle of immunotherapy, the concentration of IgD and IgG4 were independently associated with poor patient outcome (Figure 3.24a and 3.24b). In addition, an increase in IgD concentration, defined as a fold change (post-cycle 1 concentration/pre-treatment concentration) was observed to be predictive of poor outcome in patients (Figure 3.25a and 3.25b).

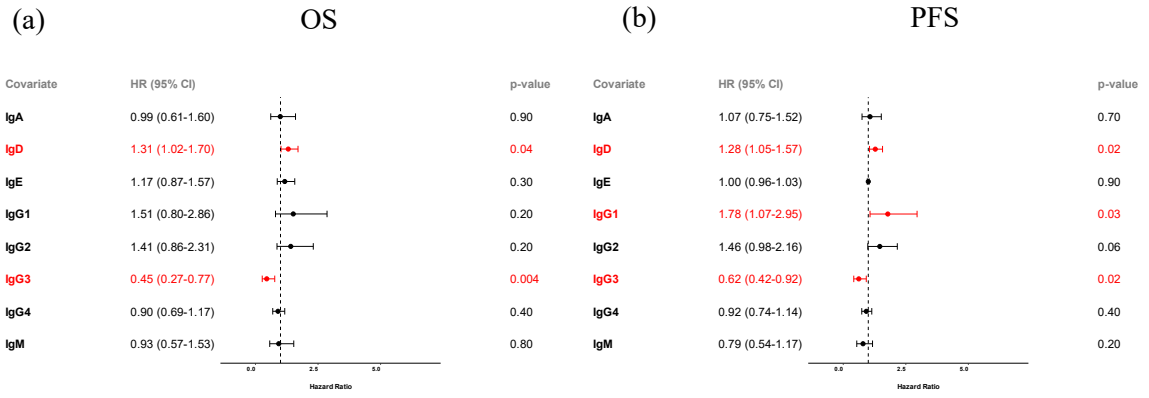


Figure 3.23: Cox Proportional hazard model showing the relationship between plasma immunoglobulin concentration (log_{10} transformed) at baseline (C1) and (a) Overall survival and (b) Progression-free survival (n = 112). Each model was controlled for age, sex, performance status, treatment type, prior exposure to ICB or BRAF inhibitors.

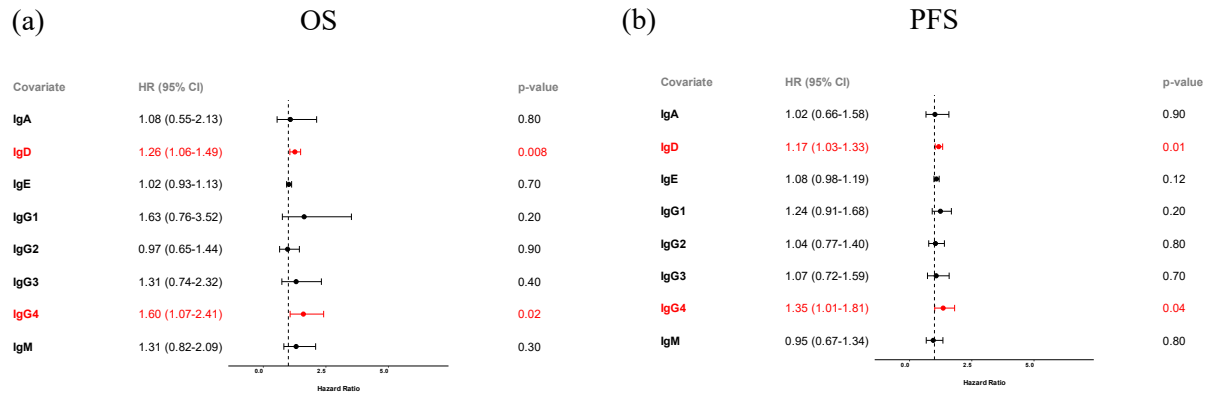


Figure 3.24: Cox Proportional hazard model showing the relationship between plasma immunoglobulin concentration (log_{10} transformed) after one cycle of ICB (C2) and (a) Overall survival and (b) Progression-free survival (n = 90). Each model was controlled for age, sex, performance status, treatment type, prior exposure to ICB or BRAF inhibitors.

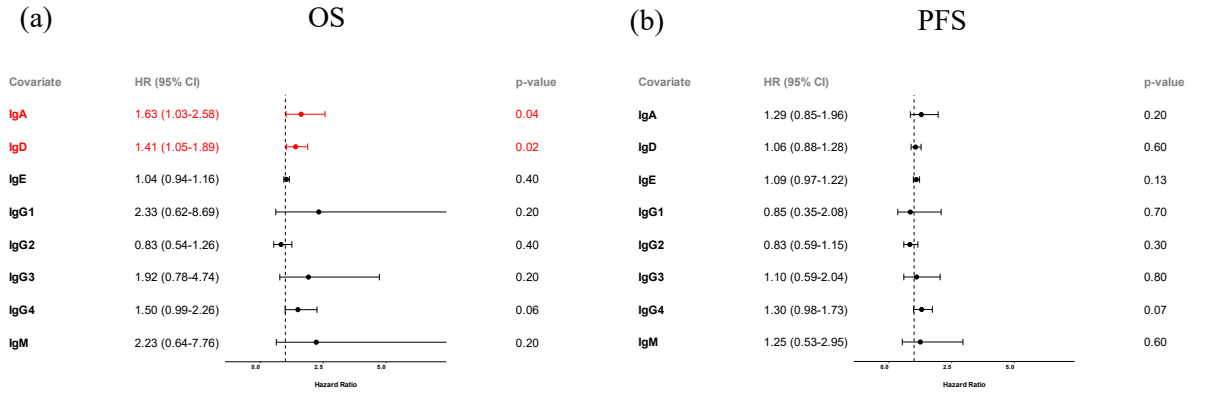


Figure 3.25: Cox Proportional hazard model showing the relationship between fold change (C2/C1) in plasma immunoglobulin concentration (log_{10} transformed) and (a) Overall survival and (b) Progression-free survival (n = 90). Each model was controlled for age, sex, performance status, treatment type, prior exposure to ICB or BRAF inhibitors.

3.6.3 B cell *IL7* and Plasma Immunoglobulin concentration

I was curious to understand the mechanism behind the relationship between plasma immunoglobulin D concentrations and patient outcome. Considering the reported relationship between B cell *IL7* and *IGHD* expression in B cells, and *IL7* being associated with somatic hypermutation[104], I correlated B cell *IL7* expression with plasma concentrations of all immunoglobulin subtypes at baseline. However, I only observed a significant negative association with plasma IgA concentration (R = -0.38, p = 0.0013). No significant correlation was observed between plasma IgD concentration and B cell *IL7* expression (Figure 3.26).

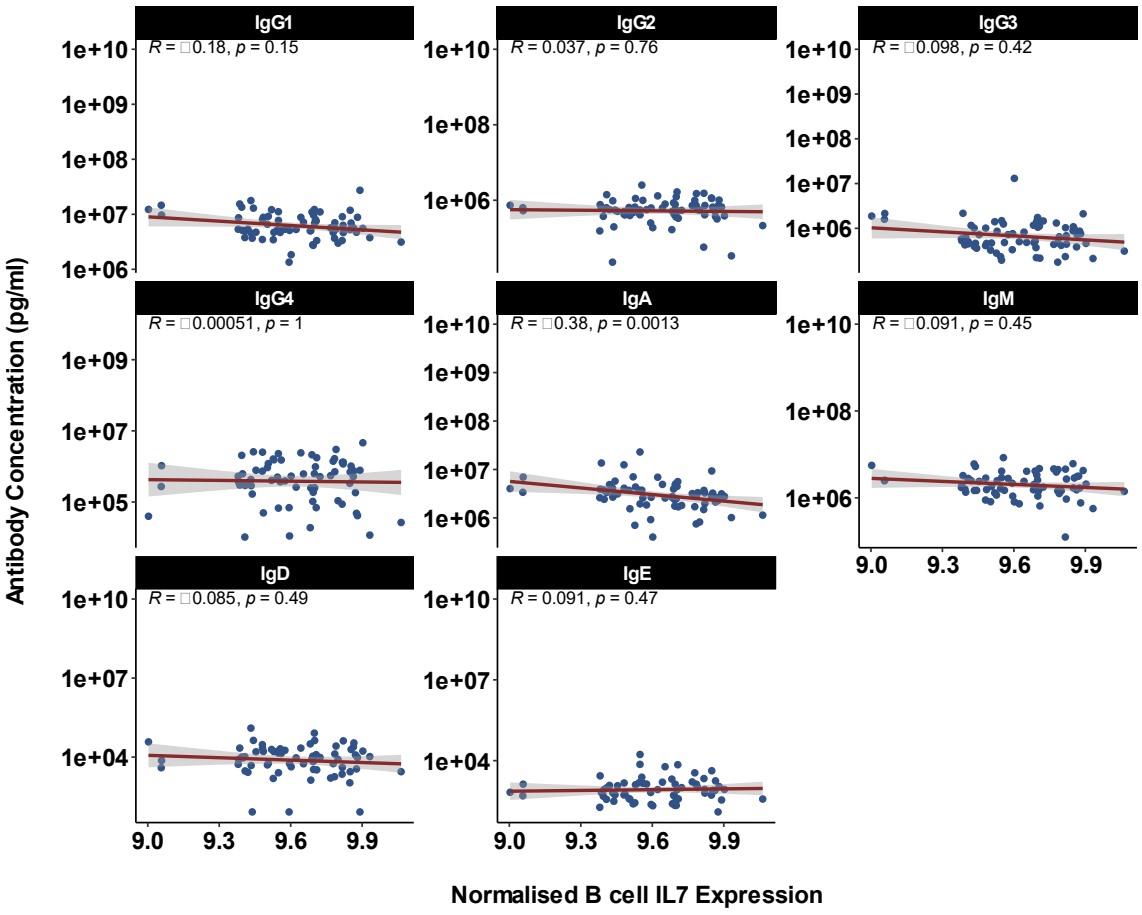


Figure 3.26: (a) Correlation between plasma immunoglobulin concentration (log_{10} transformed) and normalised B cell *IL7* expression. Statistics computed using spearman correlation test (n = 69).

3.6.4 Differences in Immune cell composition by Plasma Immunoglobulin D concentration

Immunoglobulin D is generally referred to as a marker of naivety. I therefore sought to explore the relationship between immune cell composition and plasma immunoglobulin concentration. I obtained flow cytometry data on the patient cohort and integrated it with patients' data on plasma immunoglobulin concentration. This experiment was performed by Chelsea Taylor, a previous DPhil student in the laboratory. I dichotomised the cohort using cut point value determined using maximally rank statistics provided by the function *surv_cutpoint* from the survival package (Figure 3.27a). This identifies the highest value of Immunoglobulin D associated with overall survival.

While I did not find any significant differences in B cell subsets between those that were IgD high compared to those that were IgD low (Figure 3.27b), I observed that in T cells, those with low IgD had a greater proportion of their T cells occupied by $CD8^+$ T cells (Figure 3.27c). Within the $CD8^+$ population, individuals with low IgD had significantly lesser proportion of naïve cells and a greater proportion of terminally differentiated effector memory T cells (TEMRA) (Figure 3.27d). This trend was also observed in $CD4^+$ T cells, with marginal p-value (Figure 3.27e).

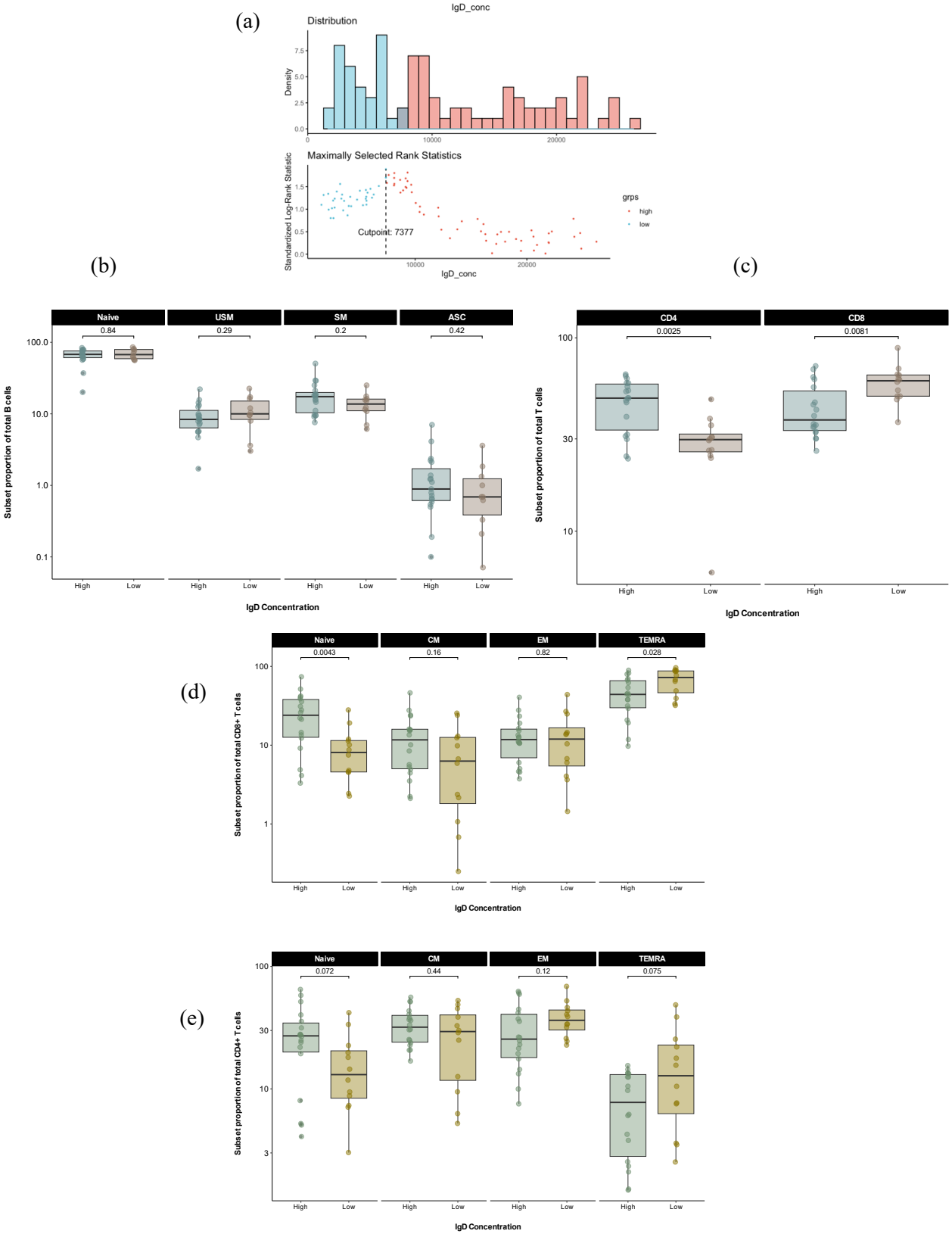


Figure 3.27: (a) Histogram showing the distribution of baseline plasma immunoglobulin concentration and cut-point value identified using maximally ranked statistics from the *surv_cutpoint* function in R. Subset proportion of (b) total B cells; (c) total T cells; (d) total $CD8^+$ T cells; and (e) total $CD4^+$ cells by baseline plasma

IgD concentration (n = 30). Statistics computed using Wilcoxon rank-sum test. USM – Unswitched memory B cell; SM – Switched memory B cell; ASC – Antibody-secreting cells; CM – Central memory T cell; EM – Effector memory T cell; TEMRA – effector memory T cell re-expressing CD45RA.

3.6.5 Low Immunoglobulin D correlates with genes in CD8$^+$ T cell involved in the production of pro-inflammatory cytokines

I then performed differential gene expression analysis between IgD high and IgD low patients on CD19$^+$ cells, CD14$^+$ cells and CD8$^+$ cells. There were no differentially expressed genes between IgD high and IgD low patients in CD14$^+$ cells (data not shown). In CD19$^+$ cells, I observed the differential expression of *MSLN* and *PIP* (figure 3.28a). In CD8$^+$ cells, 594 genes were differentially expressed between IgD high and IgD low (figure 3.28b). Pathway analysis of CD8$^+$ T cell genes upregulated with low IgD revealed enrichment of pathways involved in the production of pro-inflammatory cytokines, tumour necrosis factor (TNF) and IL-6 (figure 3.28c).

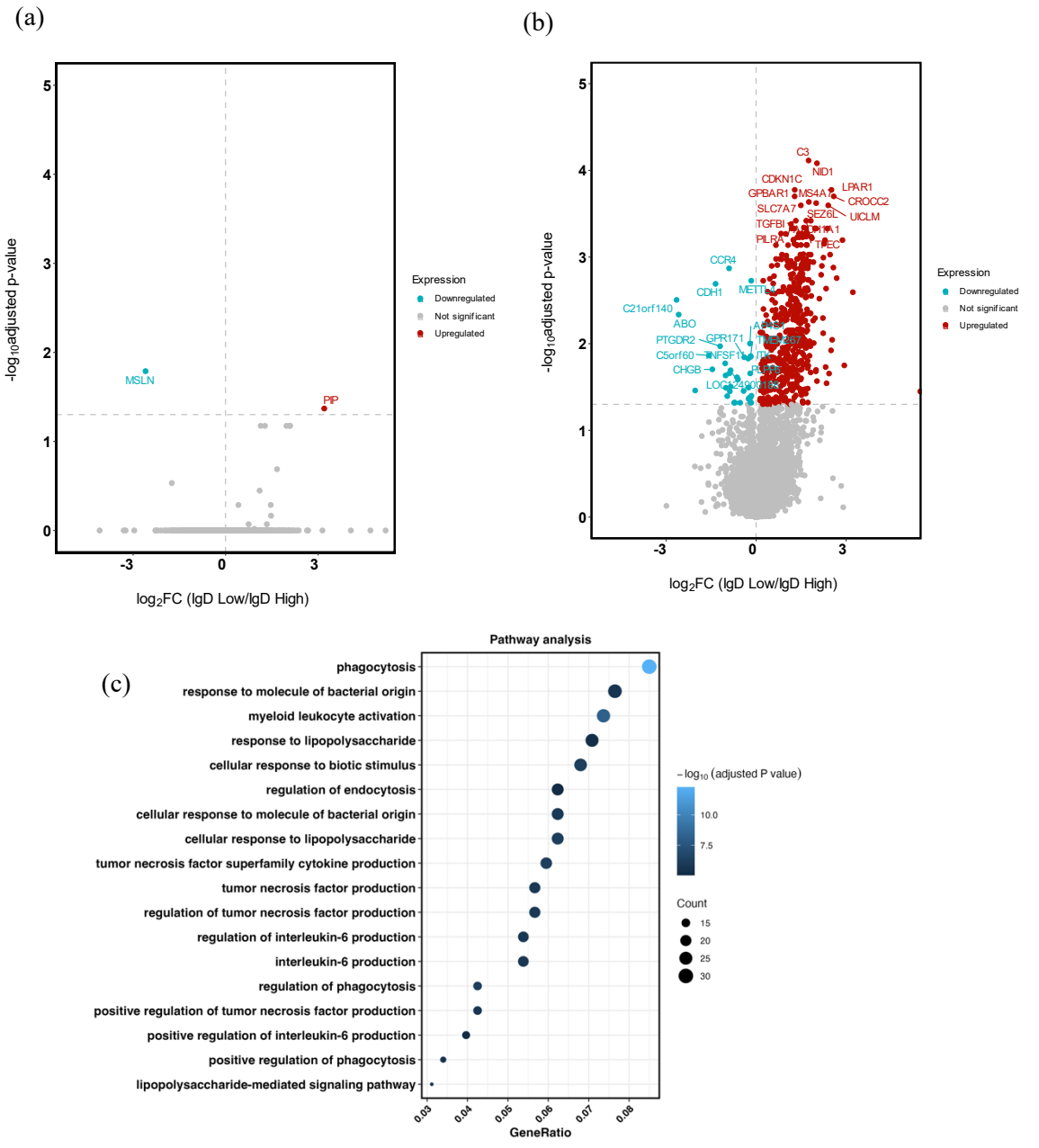


Figure 3.28 (previous page): Volcano plots comparing (a) $CD19^+$ B cell expression (n = 69) and (b) $CD8^+$ T cell expression (n = 94) of metastatic melanoma patients with low plasma IgD concentration to patients with high plasma IgD concentration. Age, sex, library RNA input and sequencing batch were controlled for in the design. Upregulated genes are coloured red and downregulated genes are coloured blue. The log_2 fold change for each gene is visualised on the x-axis with the significance of this difference displayed on the y-axis. Statistics were computed using the negative binomial distribution and adjusted for multiple testing using Benjamini-Hochberg procedure in DESeq2 (c) Gene ontology biological process of $CD8^+$ T cell genes upregulated in low IgD patients.

3.6.6 Sub-section summary

In this section, I have examined the relationship between the plasma concentration of eight antibody isotypes and the clinical outcome of patients. I observed that the baseline concentration of IgD was predictive of poor outcome in metastatic melanoma patients. I then attempted to offer some mechanistic insights into how IgD concentration was driving poor outcome. I showed that patients with low IgD concentration had a higher proportion of their T cells occupied by $CD8^+$ T cells with less naïve subsets and higher effector cells re-expressing CD45RA. Patients with low IgD also had upregulation of genes involved in pro-inflammatory cytokine production in $CD8^+$ T cells. This highlights a significant role of secreted IgD in the immune response which hitherto hasn't been recognised.

3.6.7 Sub-section acknowledgements

Initial batches of antibody isotype measurements and flow cytometry were performed by Chelsea Taylor.

Chapter 4: Discussion

4.1 Discussion

The occurrence and mechanism behind irAEs remain poorly understood. In addition, it remains yet to be discovered a reassuring biomarker for irAEs. The main aim of this thesis was to identify determinants of *IL7* expression, a published genetic biomarker of irAEs, in B cells of metastatic melanoma patients. To address this, I employed a multi-pronged approach. Here I summarize briefly the key findings from each approach taken, the impact of these findings and potential directions.

I started by replicating the association between irAEs and patient outcome while adjusting for the immortal time bias of irAEs i.e. patients that develop irAEs are those who have received ICB treatment for a longer period and hence have a better prognosis than patients that do not develop toxicities. Here, I observed that the occurrence of any grade irAEs was associated with favourable outcome. These findings are in line with several other studies that have reported an association between irAEs and good clinical outcome[162-165]. Dermatological, Endocrine and Gastro-intestinal irAEs are usually the most commonly encountered irAEs irrespective of tumour type[74, 166-169]. I suspect that the association between low-grade dermatological toxicities and patient outcome might be related to their high incidence in this cohort. The association between multi-system involvement and irAEs is in-keeping with previous report that a widespread immune system activation is critical for the anti-tumour response and alludes to the response-dependent theory of irAEs. Given the absence of a relationship between the administration of immunosuppressives for the management of irAEs and clinical outcome, one can interpret this to mean that patients that develop irAEs should be promptly managed as these are the patients that would most benefit from ICB. Indeed, the factors responsible for the heterogeneity in the anti-tumour immune response should be promptly identified. In addition, there are a subset of patients who do not develop irAEs and still have a good outcome, suggesting that the "anti-tumour" response is separate from the "anti-self" response. Identifying the factors responsible for *IL7* expression in B cells of metastatic melanoma patients might be critical in answering these questions.

In the first approach taken to identify the determinants of *IL7* expression in B cells of metastatic melanoma patients, I cultured healthy B cells in plasma from patients with metastatic melanoma, however, the RNA yield from this experiment was poor, likely suggestive of reduced concentrations of key nutrients required for B cells survival. I then produced conditioned media from seven different melanoma cell lines and cultured B cells in these media. Results here showed that melanoma secretome induces *IL7* expression in B cells. Although this response was highly variable depending on the cell line and healthy donor B cell used. While a previous study[104] has shown differences in the *IL7* expression by carriage of the *IL7* SNP, the low MAF of the SNP (approximately 8%) makes it less likely the factor responsible for the heterogeneity observed here. Differences in donor B cell composition and in antigenic response are potential factors at play. In addition, technical differences cannot be entirely ruled out.

In the second approach, I showed a potential relationship between B cell *IL7* expression and plasma concentration of IL-6 and IL-10. On the background of this, I showed that normalised expression of the *IL6R* and *IL10RA,* independently predict a reduction in B cell *IL7* expression. The combination of these findings suggests that these might be two independent pathways

involved in the regulation of *IL7* expression in B cells. IL-6 is a pleiotropic cytokine produced by several cells of the immune system. IL-6 has been reported to have a stimulatory effect on B cells, inducing the differentiation of activated B cells into antibody secreting cells (ASCs)[170]. IL-10 on the other hand is a known anti-inflammatory cytokine, although its effect on B cells has not been fully defined. However, it has been proposed to increase immunoglobulin production from the differentiation of B cells into plasma cells[171-173]. Based on this knowledge, I hypothesize that IL-6 might not have a direct inhibitory effect on *IL7,* but might be associated with a B cell subset with reduced *IL7* expression. Indeed, Taylor *et al* reported that *IL7* expression was highest in memory B cells and least expressed by ASCs[104].

In the third approach, using single cell data, I was able to show a potential modulatory role of $CD4^+$ T cells on *IL7* expression in B cells, through the interaction between CD40LG from $CD4^+$ T cells and potentially CD40 on B cells. CD40LG directs the differentiation of B cells into memory B cells and in the absence of CD40LG, B cells differentiate into plasma-like cells[122, 172, 174]. Griss *et al* observed differentiation of B cells into plasmablast-like cells following culture in melanoma-conditioned media. Strikingly, *IL7* was observed to be downregulated in B cells cultured in melanoma conditioned media compared to control[127]. Ultimately, this suggests that differentiation into different B cell subsets might be critical in regulating the levels of *IL7* expression in B cells with signals associated with an increase in memory B cell production associated with higher levels of *IL7* expression.

In the next part, attempt was made to explore the change in *IL7* expression over time in durable responders. Although, I found no difference in *IL7* expression between the two time points. I suspect this might be due to the low sample size. In addition, there might also be a change in peripheral blood B cell composition after resolution of the inflammatory response. Indeed, following the resolution of inflammation, memory B cells usually reside in the lymph nodes[175]. However, I observed a transcriptomic change in B cells with a trend towards resolution of genes involved in the B cell adaptive immune response.

Finally, I showed that concentration of IgD at baseline and after one cycle of immunotherapy was predictive of worse outcome. I then tried to provide some mechanistic explanations for how secreted IgD plasma concentration was influencing poor outcomes. While I did not observe any correlations between plasma IgD concentration and B cell *IL7* expression, I demonstrated that individuals with low plasma IgD levels had a greater proportion of their T cells occupied by $CD8^+$ T cells with fewer naïve subsets and a higher number of effector cells re-expressing CD45RA. Individuals with low IgD levels also exhibited increased expression of genes involved in producing pro-inflammatory cytokines in $CD8^+$ T cells. The combination of these findings suggests that plasma concentration of antibodies could serve as potential biomarkers of anti-tumour response in metastatic melanoma. While more is known about the function of membrane bound IgD, little is known about the function of secreted IgD. Several studies have identified IgD receptors on T cells and ligation of this receptors by soluble or membrane bound IgD led to increase effector functions in T cells and facilitated antigen presentation by B cells[176, 177]. Wu *et al* had previously reported that ligation of the IgD receptor on T cells led to an increase in antigen-specific clonal expansion[178]. This might represent a potential regulatory mechanism of IgD on the anti-tumour response, however, the details of this mechanism are yet to be clarified.

4.2 Limitations

Perhaps a major limitation of this study is the absence of validation of these key findings. While I was able to show that melanoma secretome induces *IL7* expression in B cells, I was unable to find a condition that consistently led to the expression of this observation. This would have served as a positive control and one can then explore the potential stimulatory or inhibitory role of the cytokines proposed to affect *IL7* expression. Another limitation affecting several areas of this study is small sample size. Critically, I have only explored the induction of *IL7* in B cells from four healthy donor. This might not be representative of the *IL7* expression at a population level. Evaluating this response in more donor samples might be informative. Finally, this is a relatively new research area and hence there are few publications available to consider other perspectives.

While the current standard is the use of CTCAE for the evaluation and diagnosis of irAEs, this does not provide a definite diagnosis. Definite diagnosis is provided by histopathological examination of tissues for evidence of inflammation, especially $CD8^+$ T cell infiltration. However, due to safety reasons or technical issues with obtaining tissue biopsy samples, this is not routinely done[179]. This is especially true for grade 2 or less irAEs. While the clinical context and timing are factors considered in the diagnosis or irAEs, it is not possible to diagnose with 100% certainty that an adverse event is immune-related without a biopsy being done. Hence, this can lead to overdiagnosis or underdiagnosis irAEs.

4.3 Future directions

First optimizing the plasma experiment would be a nice place to start. I suspect that reducing the plasma to media ratio from 1:2 to 1:4 might provide B cells with more survival nutrients which seemed to be absent from patient plasma. Another option would be to use resilient cells in terms of virally transformed B cells, however the risk of altering the expression profile should be considered. Although Maurer *et al* had reported that immortalised peripheral blood B cells can effectively recapitulate the response of fresh healthy B cells when exposed to melanoma conditioned media[127, 180]. Furthermore, given the heterogeneity in the response observed between healthy donor B cells, it would be reasonable to explore this response in a larger number of healthy B cell donors and also test for the carriage of the *IL7* SNP in these cells. This would permit the selection of conditions that optimally leads to the expression of B cell *IL7* expression and further experiments to determine the inducers and inhibitors of this response can then be performed. Given the pleiotropic effects of B cell *IL7* on both B cells and T cells and *IL7* found greatly expressed in memory B cells compared to other B cell subsets, and *IL7* being predictive of irAEs, the ability to generate these *IL7* high memory B cells might be a critical determinant of the response to ICB. Identifying optimal conditions that lead to preferential differentiation of B cells into memory B cells should be explored. Finally, the mechanism behind the relationship between IgD and T cells is not fully described. An area of interest is how the cross-talk between T cells and B cells regulate the production of IgD and how plasma IgD concentration regulate T cell effector function. Exploring the IgD receptor on T cells and its interaction with soluble IgD might clarify this.

4.4 Executive Summary

The expression of *IL7* in B cells of patients with metastatic melanoma is regulated potentially by factors responsible for the differentiation of B cells into various subsets. Signals associated with increase in memory B cell production such as CD40LG/CD40 interaction, are associated

with a higher *IL7* expression. On the other hand, signals associated with differentiation of B cells into antibody secreting cells such as IL-6 and IL-10 interactions are associated with reduced *IL7* expression (Figure 4.1a). Plasma IgD concentration is associated with notable variations in the composition of T cell subsets and leads to increased production of pro-inflammatory cytokines such as TNF and IL-6 in patients with metastatic melanoma (Figure 4.1b).

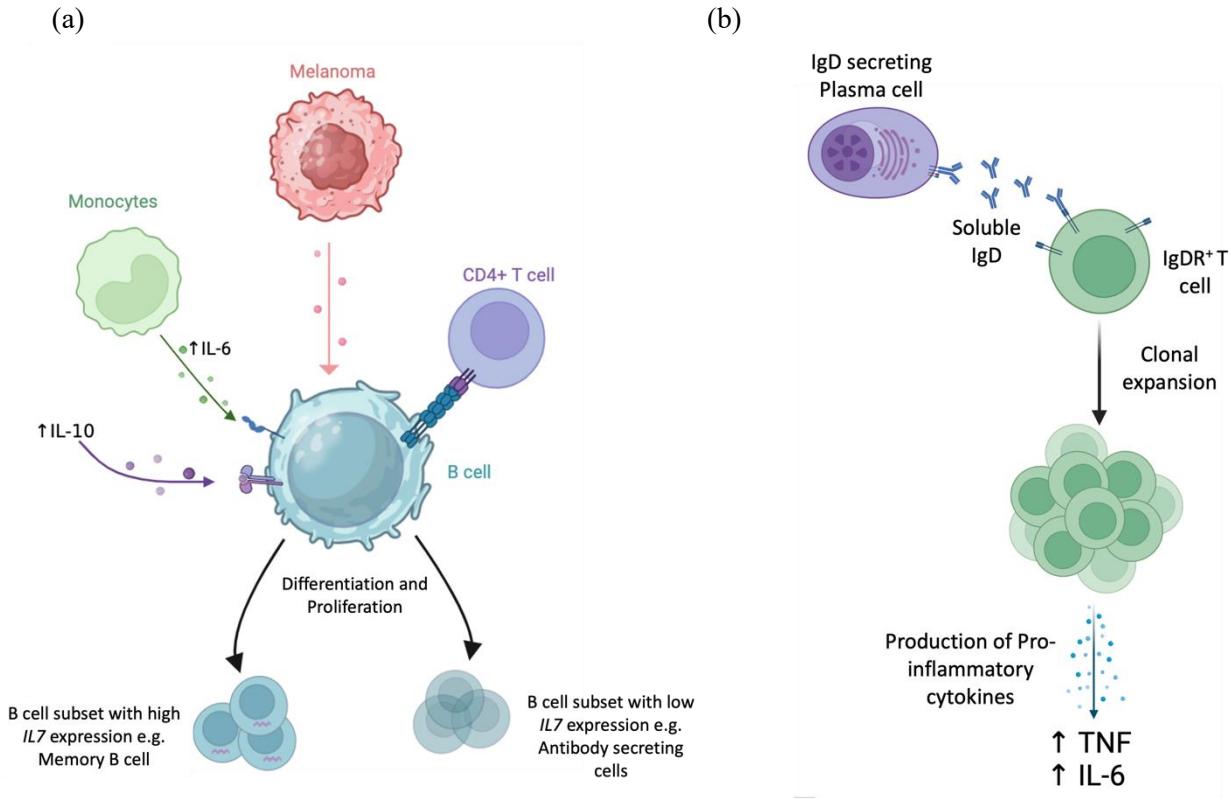


Figure 4.1: (a) Cartoon of proposed mechanism of *IL7* expression in B cells of patients with metastatic melanoma. (b) Cartoon of proposed mechanism of interaction between secreted IgD and T cells in patients with metastatic melanoma. Illustrations created using Biorender.com.

Appendix A – Optimizing the B cell culture conditions

Background: While attempting to culture B cells in plasma, initially B cells were cultured with B cell medium (containing RPMI supplemented with 10% FCS) and plasma in 1:1 ratio. However, the RNA yield from this experiment was persistently undetectable by fluorescence detection even in the B cell media alone condition. I suspected that the cells were dying in culture, hence I performed flow cytometry primarily to assess the viability of these cells following 72 hours in culture with and without the addition of cytokines and also evaluate the change in B cell subsets in response to plasma from patients with metastatic melanoma.

Methods: PBMCs from healthy donors were thawed at 37°C after recovery from liquid nitrogen. PBMCs were counted and approximately 1 – 3 x 10^5 cells were then cultured in 100% B cell media (consisting of RPMI supplemented with 10% FCS) or 50% B cell media and 50% plasma from healthy donor or 50% plasma stock (made by combining plasma from 3 patients with metastatic melanoma in equal proportions). Cells were cultured for 72 hours with 50% of the media replaced every 24 hours with fresh media or media with plasma. Flow cytometry was performed at baseline, at 24 hours and at 72 hours for viability of B cell proportions. Briefly, cells were spun down at 300 g for 5 minutes at 4°C. Cells were then incubated for 30 minutes with Zombie Green (ZG) diluted in HBSS 1:1000. Cells were spun down and washed in 200 µL of FACS buffer (PBS supplemented with 1mM EDTA, 0.1% BSA, 0.1% Sodium Azide). Antibody mix was prepared according to table A1. To ensure uniformity, enough antibody mix was made for the entire experiment. The cells were re-suspended in 50 µL of antibody mix and incubated for 30 minutes at 4°C in the dark. Compensation controls for each fluorochrome-conjugated antibody were prepared by adding equal volume of positive and negative compensation beads to 2 µL of the antibody followed by incubation for 10 minutes at 4°C in the dark. The cells and compensation beads were washed twice in HBSS and then re-suspended in 200 µL of fix buffer. Flow cytometry was performed on Attune NxT flow cytometer (Thermo Fisher Scientific) and results analysed on FlowJo version 10.10. Single lymphocytes were identified on the basis of their forward and side scatter. B cells were then identified as $CD19^+$ cells, live $CD19^+$ cells were identified as negative for the viability dye (ZG). B cell subsets were then defined as follows: $CD27^-IgD^+$ (Naïve), $CD27^+IgD^+$ (USM), $CD27^+IgD^-$ (SM), $CD27^-IgD^-$ (DN), $CD24^{hi}CD38^{hi}$ (Transitional B cells), $CD38^{hi}CD27^{hi}CD138^+$ (Plasma cells), $CD38^{hi}CD27^{hi}CD138^+$ (Plasmablasts).

Marker	Fluorochrome	Clone	Dilution	Source
Viability dye (Zombie Green)	n/a	n/a	1/1000	BioLegend
CD3	BV711	UCHT1	1/40	BioLegend
IgD	BV421	IA6-2	1/50	BioLegend
CD19	BV510	HIB19	1/20	BioLegend
CD38	PE/Cy7	HB-7	1/50	BioLegend
CD138	PE	DL-101	1/50	BioLegend
CD27	APC	M-T271	1/25	BioLegend
CD24	PerCP/Cy5.5	ML5	1/50	BioLegend

Table A1: Multi-colour flow cytometry panel showing fluorochrome-conjugated antibodies and dilutions used.

Results: In the first instance, PBMCs from healthy donors were revived from liquid nitrogen and cultured in plasma and plasma stock without cytokines. Here I observed a decline in the

proportion of $CD19^+$ cells over time with over 95% the cells dead after 72 hours in culture. I then obtained fresh PBMCs (from < 24-hour old blood cones) and cultured with IL-2, IL-21 and soluble CD40 ligand (sCD40L), cytokines that have been reported to stimulate B cell proliferation and survival[181-183]. This had a profound effect on the B cells with a greater proportion alive after 72 hours in culture. However, I did not observe any significant changes in B cell subsets after 72 hours in culture. Hence, I performed subsequent B cell cultures with this cocktail of cytokines.

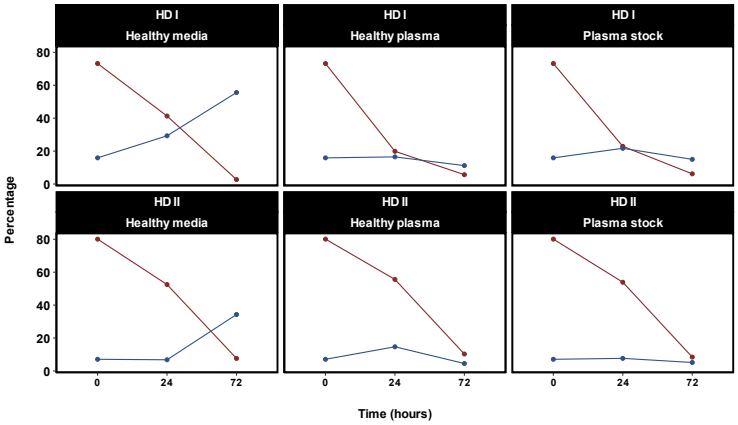


Figure A.1: B cells from healthy donors cultured in different experimental conditions without cytokines added. Trend lines: Red – proportion of live cells in $CD19^+$ population; Blue – Proportion of $CD19^+$ population of total lymphocyte population.

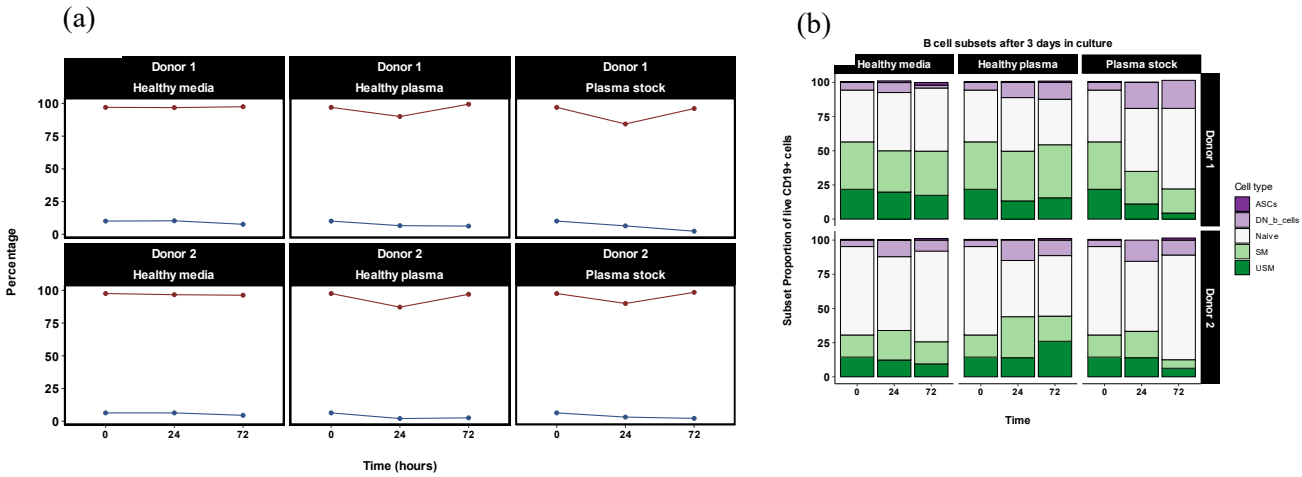


Figure A.2: (a) B cells from healthy donor blood cones cultured in different experimental conditions with IL-2, IL-21 and sCD40L added. Trend lines: Red – proportion of live cells in $CD19^+$ population; Blue – Proportion of $CD19^+$ population of total lymphocyte population. (b) Subset proportion of B cell subsets in live $CD19^+$ population. ASCs – Antibody-secreting cells, DN_b_cells – Double negative B cells; SM – Switched memory B cells; USM – Unswitched memory B cells

Appendix B – Supplementary Images

(a) (b)

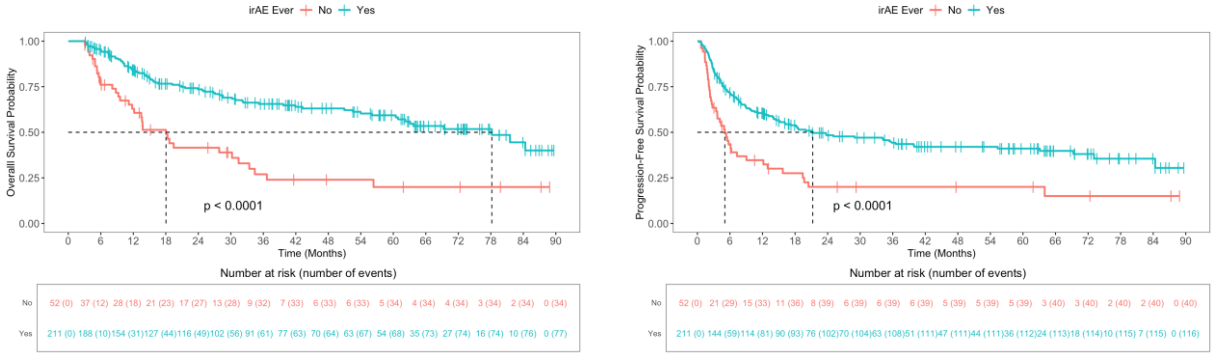
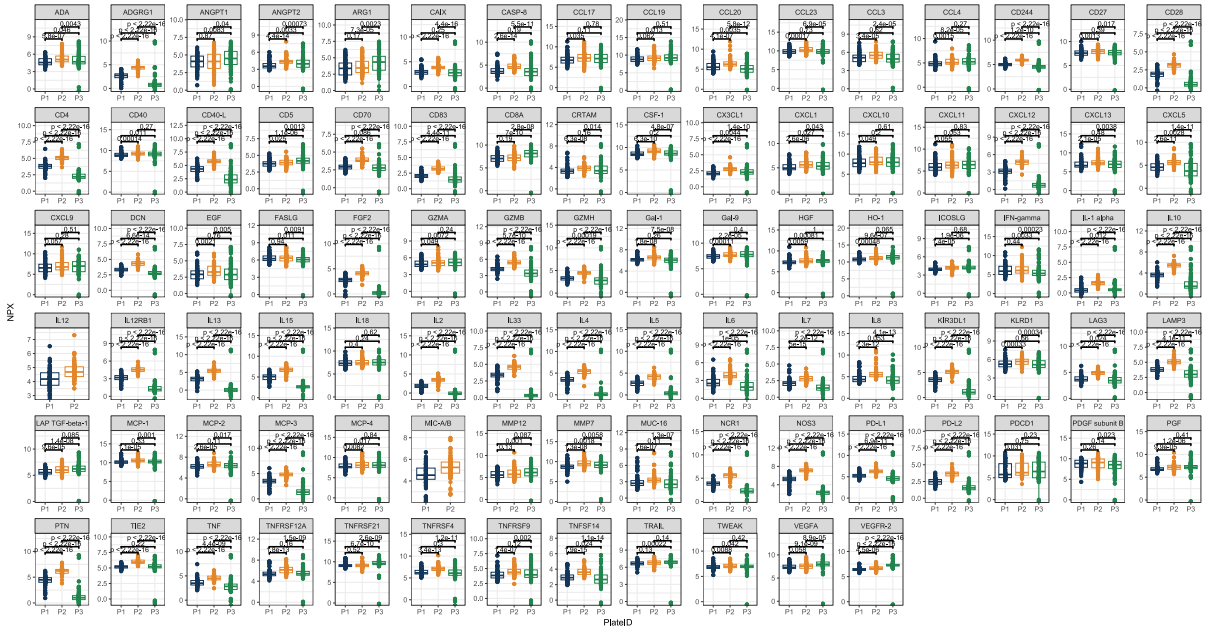


Figure B.1: 12-week Kaplan Meier analysis demonstrates significantly improved (a) OS and (b) PFS in patients with any grade irAEs ($p < 0.0001$, log-rank test) ($n = 263$).

(a)



(b)

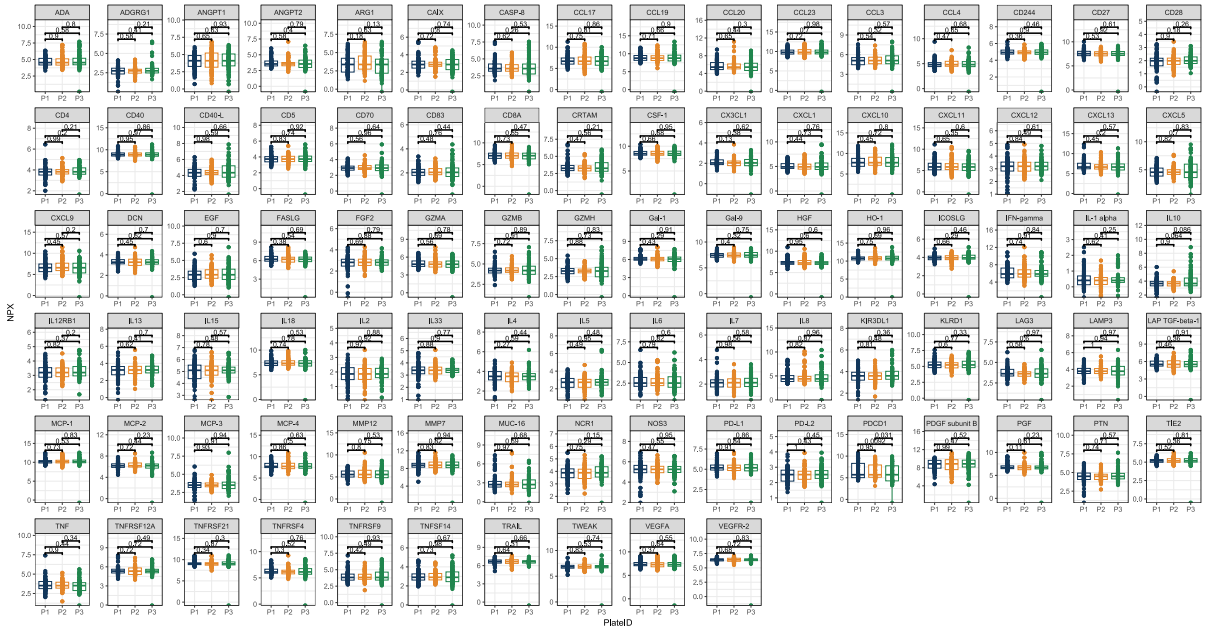
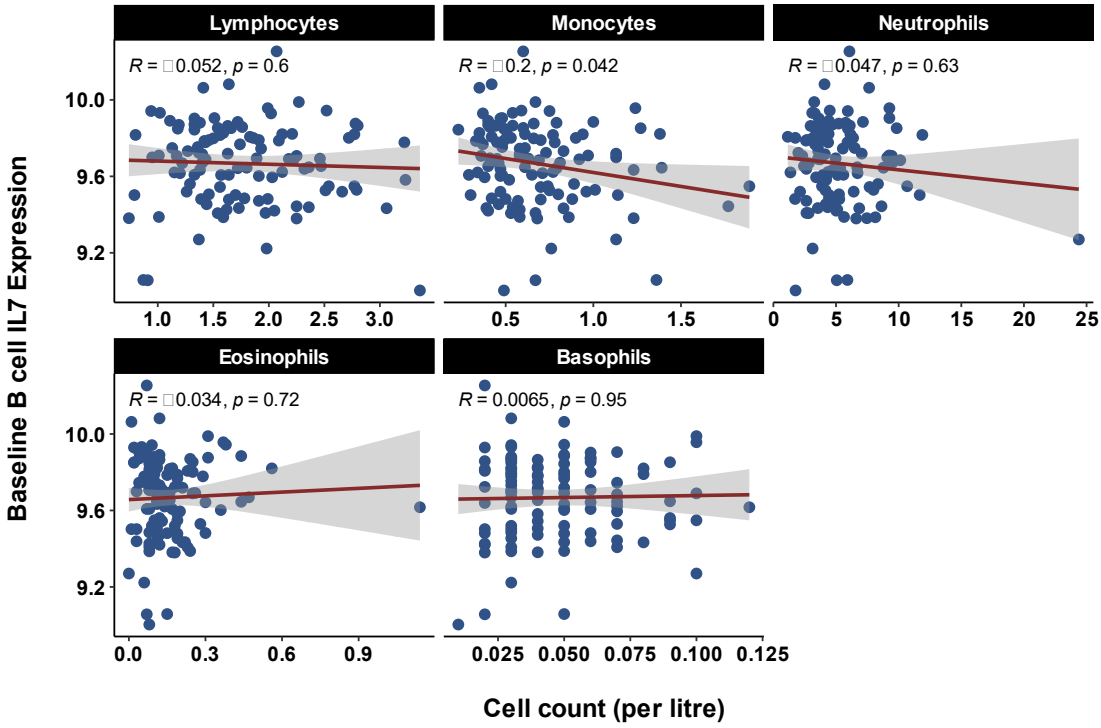


Figure B.2: Boxplots showing normalised expression of 92 proteins in plasma by plate (a) prior to and (b) after batch effects removal. Each dot represents a patient sample (n = 255). Statistics computed using Wilcoxon rank sum test.

(a)



(b)

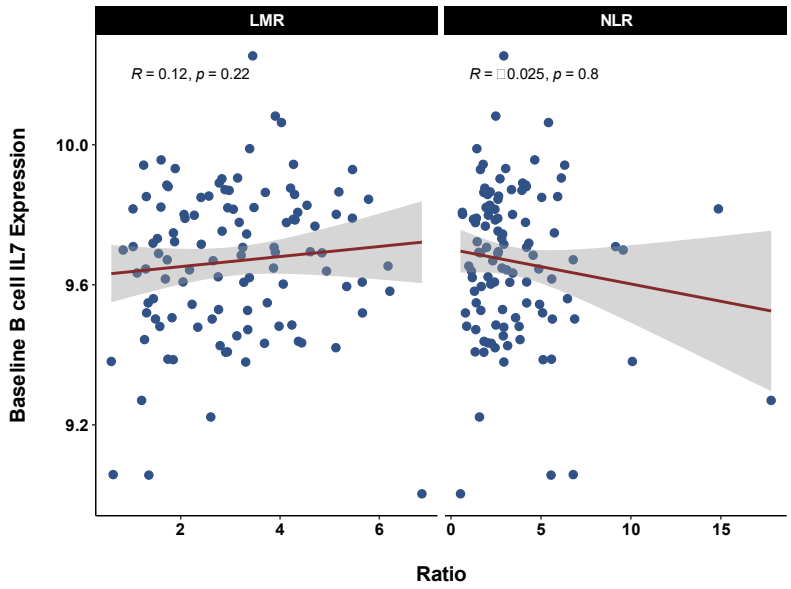


Figure B.3: (a) Scatter plots showing correlation between normalised B cell *IL7* expression and pre-treatment count of immune cells obtained from routine clinical laboratory test (n = 108). (b) Scatter plots showing correlation between normalised B cell *IL7* expression and peripheral blood-derived ratios. LMR =Lymphocyte-monocyte ratio; NLR – Neutrophil-lymphocyte ratio. Statistics computed using spearman correlation test.

Bibliography

1. Schadendorf D, Fisher DE, Garbe C, Gershenwald JE, Grob J-J, Halpern A, et al. Melanoma. Nature Reviews Disease Primers. 2015;1(1):15003.
2. Cichorek M, Wachulska M, Stasiewicz A, Tymińska A. Skin melanocytes: biology and development. Postepy Dermatol Alergol. 2013;30(1):30-41.
3. Feller L, Masilana A, Khammissa RA, Altini M, Jadwat Y, Lemmer J. Melanin: the biophysiology of oral melanocytes and physiological oral pigmentation. Head Face Med. 2014;10:8.
4. Plonka PM, Passeron T, Brenner M, Tobin DJ, Shibahara S, Thomas A, et al. What are melanocytes really doing all day long...? Exp Dermatol. 2009;18(9):799-819.
5. Tachibana M. Sound needs sound melanocytes to be heard. Pigment Cell Res. 1999;12(6):344-54.
6. De Pinto G, Mignozzi S, La Vecchia C, Levi F, Negri E, Santucci C. Global trends in cutaneous malignant melanoma incidence and mortality. Melanoma Research. 2024;34(3):265-75.
7. Matthews NH, Li WQ, Qureshi AA, Weinstock MA, Cho E. Epidemiology of Melanoma. In: Ward WH, Farma JM, editors. Cutaneous Melanoma: Etiology and Therapy. Brisbane (AU): Codon Publications

The Authors.; 2017.
8. Liu Y, Sheikh MS. Melanoma: Molecular Pathogenesis and Therapeutic Management. Mol Cell Pharmacol. 2014;6(3):228.
9. Hasan N, Nadaf A, Imran M, Jiba U, Sheikh A, Almalki WH, et al. Skin cancer: understanding the journey of transformation from conventional to advanced treatment approaches. Mol Cancer. 2023;22(1):168.
10. Cooper BR, Krishnamurthy K. Overview of Environmental Skin Cancer Risks. StatPearls. Treasure Island (FL): StatPearls Publishing

Copyright © 2024, StatPearls Publishing LLC.; 2024.
11. Sandri A, Tessari A, Giannetti D, Cetti A, Lleo MM, Boschi F. UV-A Radiation: Safe Human Exposure and Antibacterial Activity. Int J Mol Sci. 2023;24(9).
12. Ravanat J-L, Douki T. UV and ionizing radiations induced DNA damage, differences and similarities. Radiation Physics and Chemistry. 2016;128:92-102.
13. D'Orazio J, Jarrett S, Amaro-Ortiz A, Scott T. UV radiation and the skin. Int J Mol Sci. 2013;14(6):12222-48.
14. Murray HC, Maltby VE, Smith DW, Bowden NA. Nucleotide excision repair deficiency in melanoma in response to UVA. Exp Hematol Oncol. 2015;5:6.
15. Leung AK, Barankin B, Lam JM, Leong KF, Hon KL. Xeroderma pigmentosum: an updated review. Drugs Context. 2022;11.
16. Marteijn JA, Lans H, Vermeulen W, Hoeijmakers JHJ. Understanding nucleotide excision repair and its roles in cancer and ageing. Nature Reviews Molecular Cell Biology. 2014;15(7):465-81.
17. Videira IF, Moura DF, Magina S. Mechanisms regulating melanogenesis. An Bras Dermatol. 2013;88(1):76-83.
18. Chakraborty AK, Funasaka Y, Slominski A, Ermak G, Hwang J, Pawelek JM, et al. Production and release of proopiomelanocortin (POMC) derived peptides by human melanocytes and keratinocytes in culture: regulation by ultraviolet B. Biochim Biophys Acta. 1996;1313(2):130-8.
19. Lourenço GJ, Oliveira C, Carvalho BS, Torricelli C, Silva JK, Gomez GVB, et al. Inherited variations in human pigmentation-related genes modulate cutaneous melanoma risk and clinicopathological features in Brazilian population. Scientific Reports. 2020;10(1):12129.
20. Rodríguez CI, Setaluri V. Cyclic AMP (cAMP) signaling in melanocytes and melanoma. Archives of Biochemistry and Biophysics. 2014;563:22-7.
21. Lin JY, Fisher DE. Melanocyte biology and skin pigmentation. Nature. 2007;445(7130):843-50.
22. Maranduca MA, Branisteanu D, Serban DN, Branisteanu DC, Stoleriu G, Manolache N, et al. Synthesis and physiological implications of melanic pigments. Oncol Lett. 2019;17(5):4183-7.

23. Sturm RA. Skin colour and skin cancer - MC1R, the genetic link. Melanoma Res. 2002;12(5):405-16.
24. Sturm RA, Duffy DL, Box NF, Chen W, Smit DJ, Brown DL, et al. The Role of Melanocortin-1 Receptor Polymorphism in Skin Cancer Risk Phenotypes. Pigment Cell Research. 2003;16(3):266-72.
25. Brenner M, Hearing VJ. The protective role of melanin against UV damage in human skin. Photochem Photobiol. 2008;84(3):539-49.
26. Landi MT, Bishop DT, MacGregor S, Machiela MJ, Stratigos AJ, Ghiorzo P, et al. Genome-wide association meta-analyses combining multiple risk phenotypes provide insights into the genetic architecture of cutaneous melanoma susceptibility. Nature Genetics. 2020;52(5):494-504.
27. Guo Y, Chen Y, Zhang L, Ma L, Jiang K, Yao G, et al. TERT Promoter Mutations and Telomerase in Melanoma. J Oncol. 2022;2022:6300329.
28. Huang FW, Hodis E, Xu MJ, Kryukov GV, Chin L, Garraway LA. Highly Recurrent TERT Promoter Mutations in Human Melanoma. Science. 2013;339(6122):957-9.
29. Horn S, Figl A, Rachakonda PS, Fischer C, Sucker A, Gast A, et al. TERT Promoter Mutations in Familial and Sporadic Melanoma. Science. 2013;339(6122):959-61.
30. Potrony M, Puig-Butille JA, Ribera-Sola M, Iyer V, Robles-Espinoza CD, Aguilera P, et al. POT1 germline mutations but not TERT promoter mutations are implicated in melanoma susceptibility in a large cohort of Spanish melanoma families. Br J Dermatol. 2019;181(1):105-13.
31. Sargen MR, Calista D, Elder DE, Massi D, Chu EY, Potrony M, et al. Histologic features of melanoma associated with germline mutations of CDKN2A, CDK4, and POT1 in melanoma-prone families from the United States, Italy, and Spain. J Am Acad Dermatol. 2020;83(3):860-9.
32. Aoude LG, Pritchard AL, Robles-Espinoza CD, Wadt K, Harland M, Choi J, et al. Nonsense mutations in the shelterin complex genes ACD and TERF2IP in familial melanoma. J Natl Cancer Inst. 2015;107(2).
33. Gandini S, Sera F, Cattaruzza MS, Pasquini P, Abeni D, Boyle P, et al. Meta-analysis of risk factors for cutaneous melanoma: I. Common and atypical naevi. Eur J Cancer. 2005;41(1):28-44.
34. Institute NC. Adolescents and Young Adults with Cancer 2024 [Available from: https://www.cancer.gov/types/aya.
35. Stott FJ, Bates S, James MC, McConnell BB, Starborg M, Brookes S, et al. The alternative product from the human CDKN2A locus, p14(ARF), participates in a regulatory feedback loop with p53 and MDM2. Embo j. 1998;17(17):5001-14.
36. Guo W, Wang H, Li C. Signal pathways of melanoma and targeted therapy. Signal Transduction and Targeted Therapy. 2021;6(1):424.
37. Glaviano A, Foo ASC, Lam HY, Yap KCH, Jacot W, Jones RH, et al. PI3K/AKT/mTOR signaling transduction pathway and targeted therapies in cancer. Molecular Cancer. 2023;22(1):138.
38. Cheng L, Lopez-Beltran A, Massari F, MacLennan GT, Montironi R. Molecular testing for BRAF mutations to inform melanoma treatment decisions: a move toward precision medicine. Mod Pathol. 2018;31(1):24-38.
39. Zengarini C, Mussi M, Veronesi G, Alessandrini A, Lambertini M, Dika E. BRAF V600K vs. BRAF V600E: a comparison of clinical and dermoscopic characteristics and response to immunotherapies and targeted therapies. Clin Exp Dermatol. 2022;47(6):1131-6.
40. Randic T, Kozar I, Margue C, Utikal J, Kreis S. NRAS mutant melanoma: Towards better therapies. Cancer Treatment Reviews. 2021;99:102238.
41. Sensi M, Nicolini G, Petti C, Bersani I, Lozupone F, Molla A, et al. Mutually exclusive NRASQ61R and BRAFV600E mutations at the single-cell level in the same human melanoma. Oncogene. 2006;25(24):3357-64.
42. Petti C, Molla A, Vegetti C, Ferrone S, Anichini A, Sensi M. Coexpression of NRASQ61R and BRAFV600E in human melanoma cells activates senescence and increases susceptibility to cell-mediated cytotoxicity. Cancer Res. 2006;66(13):6503-11.
43. Kiuru M, Busam KJ. The NF1 gene in tumor syndromes and melanoma. Lab Invest. 2017;97(2):146-57.

44. Seminog OO, Goldacre MJ. Risk of benign tumours of nervous system, and of malignant neoplasms, in people with neurofibromatosis: population-based record-linkage study. Br J Cancer. 2013;108(1):193-8.
45. Wiesner T, Kiuru M, Scott SN, Arcila M, Halpern AC, Hollmann T, et al. NF1 Mutations Are Common in Desmoplastic Melanoma. Am J Surg Pathol. 2015;39(10):1357-62.
46. Akbani R, Akdemir Kadir C, Aksoy BA, Albert M, Ally A, Amin Samirkumar B, et al. Genomic Classification of Cutaneous Melanoma. Cell. 2015;161(7):1681-96.
47. Iida Y, Salomon MP, Hata K, Tran K, Ohe S, Griffiths CF, et al. Predominance of triple wild-type and IGF2R mutations in mucosal melanomas. BMC Cancer. 2018;18(1):1054.
48. Hayward NK, Wilmott JS, Waddell N, Johansson PA, Field MA, Nones K, et al. Whole-genome landscapes of major melanoma subtypes. Nature. 2017;545(7653):175-80.
49. Wu H, Goel V, Haluska FG. PTEN signaling pathways in melanoma. Oncogene. 2003;22(20):3113-22.
50. Kong Y, Kumar SM, Xu X. Molecular pathogenesis of sporadic melanoma and melanoma-initiating cells. Arch Pathol Lab Med. 2010;134(12):1740-9.
51. Li C, Kuai L, Cui R, Miao X. Melanogenesis and the Targeted Therapy of Melanoma. Biomolecules. 2022;12(12):1874.
52. Lawrence MS, Stojanov P, Polak P, Kryukov GV, Cibulskis K, Sivachenko A, et al. Mutational heterogeneity in cancer and the search for new cancer-associated genes. Nature. 2013;499(7457):214-8.
53. Alexandrov LB, Nik-Zainal S, Wedge DC, Aparicio SA, Behjati S, Biankin AV, et al. Signatures of mutational processes in human cancer. Nature. 2013;500(7463):415-21.
54. Davis LE, Shalin SC, Tackett AJ. Current state of melanoma diagnosis and treatment. Cancer Biol Ther. 2019;20(11):1366-79.
55. Chudnovsky Y, Khavari PA, Adams AE. Melanoma genetics and the development of rational therapeutics. The Journal of Clinical Investigation. 2005;115(4):813-24.
56. Keung EZ, Gershenwald JE. The eighth edition American Joint Committee on Cancer (AJCC) melanoma staging system: implications for melanoma treatment and care. Expert Rev Anticancer Ther. 2018;18(8):775-84.
57. Heistein J.B. AU, Mukkamalla SHR. Malignant Melanoma. StatPearls. 2024;[Internet].
58. Bhatia S, Tykodi SS, Thompson JA. Treatment of metastatic melanoma: an overview. Oncology (Williston Park). 2009;23(6):488-96.
59. Costanza ME, Nathanson L, Costello WG, Wolter J, Brunk SF, Colsky J, et al. Results of a randomized study comparing DTIC with TIC mustard in malignant melanoma. Cancer. 1976;37(4):1654-9.
60. Eggermont AMM, Kirkwood JM. Re-evaluating the role of dacarbazine in metastatic melanoma: what have we learned in 30 years? European Journal of Cancer. 2004;40(12):1825-36.
61. Jiang G, Li RH, Sun C, Liu YQ, Zheng JN. Dacarbazine combined targeted therapy versus dacarbazine alone in patients with malignant melanoma: a meta-analysis. PLoS One. 2014;9(12):e111920.
62. Wolchok JD, Chiarion-Sileni V, Gonzalez R, Grob JJ, Rutkowski P, Lao CD, et al. Long-Term Outcomes With Nivolumab Plus Ipilimumab or Nivolumab Alone Versus Ipilimumab in Patients With Advanced Melanoma. J Clin Oncol. 2022;40(2):127-37.
63. Shiravand Y, Khodadadi F, Kashani SMA, Hosseini-Fard SR, Hosseini S, Sadeghirad H, et al. Immune Checkpoint Inhibitors in Cancer Therapy. Curr Oncol. 2022;29(5):3044-60.
64. Pardoll DM. The blockade of immune checkpoints in cancer immunotherapy. Nat Rev Cancer. 2012;12(4):252-64.
65. Rowshanravan B, Halliday N, Sansom DM. CTLA-4: a moving target in immunotherapy. Blood. 2018;131(1):58-67.

66. Qureshi OS, Zheng Y, Nakamura K, Attridge K, Manzotti C, Schmidt EM, et al. Trans-endocytosis of CD80 and CD86: a molecular basis for the cell-extrinsic function of CTLA-4. Science. 2011;332(6029):600-3.
67. Waldman AD, Fritz JM, Lenardo MJ. A guide to cancer immunotherapy: from T cell basic science to clinical practice. Nature Reviews Immunology. 2020;20(11):651-68.
68. Han Y, Liu D, Li L. PD-1/PD-L1 pathway: current researches in cancer. Am J Cancer Res. 2020;10(3):727-42.
69. Su J, Fu Y, Cui Z, Abidin Z, Yuan J, Zhang X, et al. Relatlimab: a novel drug targeting immune checkpoint LAG-3 in melanoma therapy. Front Pharmacol. 2023;14:1349081.
70. Tawbi HA, Schadendorf D, Lipson EJ, Ascierto PA, Matamala L, Gutiérrez EC, et al. Relatlimab and Nivolumab versus Nivolumab in Untreated Advanced Melanoma. New England Journal of Medicine. 2022;386(1):24-34.
71. Morad G, Helmink BA, Sharma P, Wargo JA. Hallmarks of response, resistance, and toxicity to immune checkpoint blockade. Cell. 2021;184(21):5309-37.
72. Conroy M, Naidoo J. Immune-related adverse events and the balancing act of immunotherapy. Nat Commun. 2022;13(1):392.
73. Schneider BJ, Naidoo J, Santomasso BD, Lacchetti C, Adkins S, Anadkat M, et al. Management of Immune-Related Adverse Events in Patients Treated With Immune Checkpoint Inhibitor Therapy: ASCO Guideline Update. Journal of Clinical Oncology. 2021;39(36):4073-126.
74. Martins F, Sofiya L, Sykiotis GP, Lamine F, Maillard M, Fraga M, et al. Adverse effects of immune-checkpoint inhibitors: epidemiology, management and surveillance. Nature Reviews Clinical Oncology. 2019;16(9):563-80.
75. Sullivan RJ, Weber JS. Immune-related toxicities of checkpoint inhibitors: mechanisms and mitigation strategies. Nature Reviews Drug Discovery. 2022;21(7):495-508.
76. Johnson DB, Nebhan CA, Moslehi JJ, Balko JM. Immune-checkpoint inhibitors: long-term implications of toxicity. Nat Rev Clin Oncol. 2022;19(4):254-67.
77. Paderi A, Gambale E, Botteri C, Giorgione R, Lavacchi D, Brugia M, et al. Association of Systemic Steroid Treatment and Outcome in Patients Treated with Immune Checkpoint Inhibitors: A Real-World Analysis. Molecules. 2021;26(19).
78. Skribek M, Rounis K, Afshar S, Grundberg O, Friesland S, Tsakonas G, et al. Effect of corticosteroids on the outcome of patients with advanced non–small cell lung cancer treated with immune-checkpoint inhibitors. European Journal of Cancer. 2021;145:245-54.
79. Mouri A, Kaira K, Yamaguchi O, Hashimoto K, Miura Y, Shiono A, et al. Effect of Systemic Steroid Use for Immune-Related Adverse Events in Patients with Non-Small Cell Lung Cancer Receiving PD-1 Blockade Drugs. J Clin Med. 2021;10(16).
80. SHIMOMURA K, YAMAGUCHI T, OYA Y, UCHIDA K, MUROTANI K. Impact of Corticosteroids for IrAEs on the Clinical Outcome of Immunotherapy in Patients With NSCLC. Anticancer Research. 2022;42(12):5961-9.
81. Fan Y, Xie W, Huang H, Wang Y, Li G, Geng Y, et al. Association of Immune Related Adverse Events With Efficacy of Immune Checkpoint Inhibitors and Overall Survival in Cancers: A Systemic Review and Meta-analysis. Front Oncol. 2021;11:633032.
82. Romão R, Mendes AS, Ranchor R, Ramos MJ, Coelho J, Pichel RC, et al. Impact of Immune-Related Adverse Events on Immune Checkpoint Inhibitors Treated Cancer Patients' Survival: Single Center Experience and Literature Review. Cancers (Basel). 2023;15(3).
83. Fukushima T, Kobayashi S, Ueno M. The correlation between immune-related adverse events and efficacy of immune checkpoint inhibitors. Japanese Journal of Clinical Oncology. 2024.
84. Group F-NBW. BEST (Biomarkers, EndpointS, and other Tools) Resource [Internet]. Silver Spring (MD): Food and Drug Administration (US). Co-published by National Institutes of Health (US), Bethesda (MD); 2016 [Available from: https://www.ncbi.nlm.nih.gov/books/NBK326791/
85. Les I, Martínez M, Pérez-Francisco I, Cabero M, Teijeira L, Arrazubi V, et al. Predictive Biomarkers for Checkpoint Inhibitor Immune-Related Adverse Events. Cancers (Basel). 2023;15(5).

86. Liu W, Liu Y, Ma F, Sun B, Wang Y, Luo J, et al. Peripheral Blood Markers Associated with Immune-Related Adverse Effects in Patients Who Had Advanced Non-Small Cell Lung Cancer Treated with PD-1 Inhibitors. Cancer Manag Res. 2021;13:765-71.
87. Egami S, Kawazoe H, Hashimoto H, Uozumi R, Arami T, Sakiyama N, et al. Absolute Lymphocyte Count Predicts Immune-Related Adverse Events in Patients With Non-Small-Cell Lung Cancer Treated With Nivolumab Monotherapy: A Multicenter Retrospective Study. Frontiers in Oncology. 2021;11.
88. Diehl A, Yarchoan M, Hopkins A, Jaffee E, Grossman SA. Relationships between lymphocyte counts and treatment-related toxicities and clinical responses in patients with solid tumors treated with PD-1 checkpoint inhibitors. Oncotarget. 2017;8(69):114268-80.
89. Michailidou D, Khaki AR, Morelli MP, Diamantopoulos L, Singh N, Grivas P. Association of blood biomarkers and autoimmunity with immune related adverse events in patients with cancer treated with immune checkpoint inhibitors. Scientific Reports. 2021;11(1):9029.
90. Zhang W, Tan Y, Li Y, Liu J. Neutrophil to Lymphocyte ratio as a predictor for immune-related adverse events in cancer patients treated with immune checkpoint inhibitors: a systematic review and meta-analysis. Front Immunol. 2023;14:1234142.
91. Chu X, Zhao J, Zhou J, Zhou F, Jiang T, Jiang S, et al. Association of baseline peripheral-blood eosinophil count with immune checkpoint inhibitor-related pneumonitis and clinical outcomes in patients with non-small cell lung cancer receiving immune checkpoint inhibitors. Lung Cancer. 2020;150:76-82.
92. Ma Y, Ma X, Wang J, Wu S, Wang J, Cao B. Absolute eosinophil count may be an optimal peripheral blood marker to identify the risk of immune-related adverse events in advanced malignant tumors treated with PD-1/PD-L1 inhibitors: a retrospective analysis. World J Surg Oncol. 2022;20(1):242.
93. Nakamura Y, Tanaka R, Maruyama H, Ishitsuka Y, Okiyama N, Watanabe R, et al. Correlation between blood cell count and outcome of melanoma patients treated with anti-PD-1 antibodies. Jpn J Clin Oncol. 2019;49(5):431-7.
94. Valpione S, Pasquali S, Campana LG, Piccin L, Mocellin S, Pigozzo J, et al. Sex and interleukin-6 are prognostic factors for autoimmune toxicity following treatment with anti-CTLA4 blockade. J Transl Med. 2018;16(1):94.
95. Callahan MK, Yang A, Tandon S, Xu Y, Subudhi SK, Roman RA, et al. Evaluation of serum IL-17 levels during ipilimumab therapy: Correlation with colitis. Journal of Clinical Oncology. 2011;29(15_suppl):2505-.
96. Maekura T, Naito M, Tahara M, Ikegami N, Kimura Y, Sonobe S, et al. Predictive Factors of Nivolumab-induced Hypothyroidism in Patients with Non-small Cell Lung Cancer. In Vivo. 2017;31(5):1035-9.
97. Osorio JC, Ni A, Chaft JE, Pollina R, Kasler MK, Stephens D, et al. Antibody-mediated thyroid dysfunction during T-cell checkpoint blockade in patients with non-small-cell lung cancer. Ann Oncol. 2017;28(3):583-9.
98. Kimbara S, Fujiwara Y, Iwama S, Ohashi K, Kuchiba A, Arima H, et al. Association of antithyroglobulin antibodies with the development of thyroid dysfunction induced by nivolumab. Cancer Sci. 2018;109(11):3583-90.
99. Chennamadhavuni A, Abushahin L, Jin N, Presley CJ, Manne A. Risk Factors and Biomarkers for Immune-Related Adverse Events: A Practical Guide to Identifying High-Risk Patients and Rechallenging Immune Checkpoint Inhibitors. Front Immunol. 2022;13:779691.
100. Borgers JSW, van Wesemael TJ, Gelderman KA, Rispens T, Verdegaal EME, Moes DJAR, et al. Autoantibody-positivity before and seroconversion during treatment with anti-PD-1 is associated with immune-related adverse events in patients with melanoma. Journal for ImmunoTherapy of Cancer. 2024;12(6):e009215.
101. Giannicola R, D'Arrigo G, Botta C, Agostino R, Del Medico P, Falzea AC, et al. Early blood rise in auto-antibodies to nuclear and smooth muscle antigens is predictive of prolonged survival and

autoimmunity in metastatic-non-small cell lung cancer patients treated with PD-1 immune-check point blockade by nivolumab. Mol Clin Oncol. 2019;11(1):81-90.
102. Chin IS, Khan A, Olsson-Brown A, Papa S, Middleton G, Palles C. Germline genetic variation and predicting immune checkpoint inhibitor induced toxicity. NPJ Genom Med. 2022;7(1):73.
103. Groha S, Alaiwi SA, Xu W, Naranbhai V, Nassar AH, Bakouny Z, et al. Germline variants associated with toxicity to immune checkpoint blockade. Nature Medicine. 2022;28(12):2584-91.
104. Taylor CA, Watson RA, Tong O, Ye W, Nassiri I, Gilchrist JJ, et al. IL7 genetic variation and toxicity to immune checkpoint blockade in patients with melanoma. Nature Medicine. 2022;28(12):2592-600.
105. Jiang Q, Li WQ, Aiello FB, Mazzucchelli R, Asefa B, Khaled AR, et al. Cell biology of IL-7, a key lymphotrophin. Cytokine & Growth Factor Reviews. 2005;16(4):513-33.
106. Winer H, Rodrigues GOL, Hixon JA, Aiello FB, Hsu TC, Wachter BT, et al. IL-7: Comprehensive review. Cytokine. 2022;160:156049.
107. Rivière E, Pascaud J, Virone A, Dupré A, Ly B, Paoletti A, et al. Interleukin-7/Interferon Axis Drives T Cell and Salivary Gland Epithelial Cell Interactions in Sjögren's Syndrome. Arthritis & Rheumatology. 2021;73(4):631-40.
108. Weitzmann MN, Cenci S, Rifas L, Brown C, Pacifici R. Interleukin-7 stimulates osteoclast formation by up-regulating the T-cell production of soluble osteoclastogenic cytokines. Blood. 2000;96(5):1873-8.
109. Tang J, Nuccie BL, Ritterman I, Liesveld JL, Abboud CN, Ryan DH. TGF-beta down-regulates stromal IL-7 secretion and inhibits proliferation of human B cell precursors. The Journal of Immunology. 1997;159(1):117-25.
110. Mackall CL, Fry TJ, Gress RE. Harnessing the biology of IL-7 for therapeutic application. Nature Reviews Immunology. 2011;11(5):330-42.
111. Grenningloh R, Tai T-S, Frahm N, Hongo T, Chicoine A, Brander C, et al. Ets-1 Maintains IL-7 Receptor Expression in Peripheral T Cells. Journal of immunology (Baltimore, Md : 1950). 2011;186:969-76.
112. Lundström W, Fewkes NM, Mackall CL. IL-7 in human health and disease. Semin Immunol. 2012;24(3):218-24.
113. Fry TJ, Connick E, Falloon J, Lederman MM, Liewehr DJ, Spritzler J, et al. A potential role for interleukin-7 in T-cell homeostasis. Blood. 2001;97(10):2983-90.
114. Chen D, Tang TX, Deng H, Yang XP, Tang ZH. Interleukin-7 Biology and Its Effects on Immune Cells: Mediator of Generation, Differentiation, Survival, and Homeostasis. Front Immunol. 2021;12:747324.
115. Sammicheli S, Ruffin N, Lantto R, Vivar N, Chiodi F, Rethi B. IL-7 modulates B cells survival and activation by inducing BAFF and CD70 expression in T cells. Journal of Autoimmunity. 2012;38(4):304-14.
116. Rosenberg SA, Sportès C, Ahmadzadeh M, Fry TJ, Ngo LT, Schwarz SL, et al. IL-7 administration to humans leads to expansion of CD8+ and CD4+ cells but a relative decrease of CD4+ T-regulatory cells. J Immunother. 2006;29(3):313-9.
117. Pellegrini M, Calzascia T, Elford AR, Shahinian A, Lin AE, Dissanayake D, et al. Adjuvant IL-7 antagonizes multiple cellular and molecular inhibitory networks to enhance immunotherapies. Nature Medicine. 2009;15(5):528-36.
118. Fu C, Zhang X, Zhang X, Wang D, Han S, Ma Z. Advances in IL-7 Research on Tumour Therapy. Pharmaceuticals. 2024;17(4):415.
119. Chiaruttini G, Mele S, Opzoomer J, Crescioli S, Ilieva KM, Lacy KE, et al. B cells and the humoral response in melanoma: The overlooked players of the tumor microenvironment. Oncoimmunology. 2017;6(4):e1294296.
120. Sanz I, Wei C, Jenks SA, Cashman KS, Tipton C, Woodruff MC, et al. Challenges and Opportunities for Consistent Classification of Human B Cell and Plasma Cell Populations. Front Immunol. 2019;10:2458.

121. Cano RLE, Lopera, H.D.E. Introduction to T and B lymphocytes. 2013. In: Autoimmunity: From Bench to Bedside [Internet]. El Rosario University Press. Available from: https://www.ncbi.nlm.nih.gov/books/NBK459471/.
122. Akkaya M, Kwak K, Pierce SK. B cell memory: building two walls of protection against pathogens. Nature Reviews Immunology. 2020;20(4):229-38.
123. Rodgers CB, Mustard CJ, McLean RT, Hutchison S, Pritchard AL. A B-cell or a key player? The different roles of B-cells and antibodies in melanoma. Pigment Cell Melanoma Res. 2022;35(3):303-19.
124. Anderson NM, Simon MC. The tumor microenvironment. Curr Biol. 2020;30(16):R921-r5.
125. Milardi G, Lleo A. Tumor-Infiltrating B Lymphocytes: Promising Immunotherapeutic Targets for Primary Liver Cancer Treatment. Cancers (Basel). 2023;15(7).
126. Fridman WH, Petitprez F, Meylan M, Chen TW, Sun CM, Roumenina LT, et al. B cells and cancer: To B or not to B? J Exp Med. 2021;218(1).
127. Griss J, Bauer W, Wagner C, Simon M, Chen M, Grabmeier-Pfistershammer K, et al. B cells sustain inflammation and predict response to immune checkpoint blockade in human melanoma. Nature Communications. 2019;10(1):4186.
128. Cabrita R, Lauss M, Sanna A, Donia M, Skaarup Larsen M, Mitra S, et al. Tertiary lymphoid structures improve immunotherapy and survival in melanoma. Nature. 2020;577(7791):561-5.
129. Helmink BA, Reddy SM, Gao J, Zhang S, Basar R, Thakur R, et al. B cells and tertiary lymphoid structures promote immunotherapy response. Nature. 2020;577(7791):549-55.
130. de Jonge K, Tillé L, Lourenco J, Maby-El Hajjami H, Nassiri S, Racle J, et al. Inflammatory B cells correlate with failure to checkpoint blockade in melanoma patients. OncoImmunology. 2021;10(1):1873585.
131. Henze J, Maintz D, Persigehl T. RECIST 1.1, irRECIST 1.1, and mRECIST: How to Do. Current Radiology Reports. 2016;4.
132. Therneau TM. A Package for Survival Analysis in R R package version 3.7-0 2024 [Available from: https://cran.r-project.org/package=survival.
133. Therneau TM, Grambsch PM, Therneau TM, Grambsch PM. The cox model: Springer; 2000.
134. Ye J, Coulouris G, Zaretskaya I, Cutcutache I, Rozen S, Madden TL. Primer-BLAST: a tool to design target-specific primers for polymerase chain reaction. BMC Bioinformatics. 2012;13:134.
135. Kuhn RM, Haussler D, Kent WJ. The UCSC genome browser and associated tools. Brief Bioinform. 2013;14(2):144-61.
136. Livak KJ, Schmittgen TD. Analysis of relative gene expression data using real-time quantitative PCR and the 2(-Delta Delta C(T)) Method. Methods. 2001;25(4):402-8.
137. Nevola K SM, Guess J, Forsberg S, Cambronero C, Pucholt P, Zhang B, Sheikhi M, Diamanti K, Kar A, Conze L, Chin K, Topouza D. OlinkAnalyze: Facilitate Analysis of Proteomic Data from Olink. R package version 4.0.1 2024 [Available from: https://github.com/olink-proteomics/olinkrpackage.
138. Kim D, Paggi JM, Park C, Bennett C, Salzberg SL. Graph-based genome alignment and genotyping with HISAT2 and HISAT-genotype. Nature Biotechnology. 2019;37(8):907-15.
139. Anders S, Pyl PT, Huber W. HTSeq--a Python framework to work with high-throughput sequencing data. Bioinformatics. 2015;31(2):166-9.
140. Barnett DW, Garrison EK, Quinlan AR, Strömberg MP, Marth GT. BamTools. Bioinformatics. 2011;27(12):1691–2.
141. Institute B. Picard toolkit 2019 [Available from: http://broadinstitute.github.io/picard.
142. Love MI, Huber W, Anders S. Moderated estimation of fold change and dispersion for RNA-seq data with DESeq2. Genome Biol. 2014;15(12):550.
143. Pagès H CM, Falcon S, Li N. AnnotationDbi: Manipulation of SQLite-based annotations in Bioconductor. R package version 1.66.0, 2024 [Available from: https://bioconductor.org/packages/AnnotationDbi.
144. Yu G, Wang LG, Han Y, He QY. clusterProfiler: an R package for comparing biological themes among gene clusters. Omics. 2012;16(5):284-7.

145. Wu T, Hu E, Xu S, Chen M, Guo P, Dai Z, et al. clusterProfiler 4.0: A universal enrichment tool for interpreting omics data. The Innovation. 2021;2(3):100141.
146. M C. org.Hs.eg.db: Genome wide annotation for Human. R package version 3.8.2. 2019 [Available from: https://doi.org/doi:10.18129/B9.bioc.org.Hs.eg.db.
147. v6.0.1 xGCR. [
148. Lun ATL, Riesenfeld S, Andrews T, Dao TP, Gomes T, Marioni JC, et al. EmptyDrops: distinguishing cells from empty droplets in droplet-based single-cell RNA sequencing data. Genome Biology. 2019;20(1):63.
149. Huang X, Huang Y. Cellsnp-lite: an efficient tool for genotyping single cells. Bioinformatics. 2021;37(23):4569-71.
150. Wolock SL, Lopez R, Klein AM. Scrublet: Computational Identification of Cell Doublets in Single-Cell Transcriptomic Data. Cell Syst. 2019;8(4):281-91.e9.
151. Lopez R, Regier J, Cole MB, Jordan MI, Yosef N. Deep generative modeling for single-cell transcriptomics. Nature Methods. 2018;15(12):1053-8.
152. Gayoso A, Lopez R, Xing G, Boyeau P, Valiollah Pour Amiri V, Hong J, et al. A Python library for probabilistic analysis of single-cell omics data. Nature Biotechnology. 2022;40(2):163-6.
153. Lotfollahi M, Naghipourfar M, Luecken MD, Khajavi M, Büttner M, Wagenstetter M, et al. Mapping single-cell data to reference atlases by transfer learning. Nat Biotechnol. 2022;40(1):121-30.
154. Browaeys R, Saelens W, Saeys Y. NicheNet: modeling intercellular communication by linking ligands to target genes. Nature Methods. 2020;17(2):159-62.
155. Hao Y, Stuart T, Kowalski MH, Choudhary S, Hoffman P, Hartman A, et al. Dictionary learning for integrative, multimodal and scalable single-cell analysis. Nature Biotechnology. 2024;42(2):293-304.
156. Wolchok JD, Chiarion-Sileni V, Gonzalez R, Rutkowski P, Grob JJ, Cowey CL, et al. Overall Survival with Combined Nivolumab and Ipilimumab in Advanced Melanoma. N Engl J Med. 2017;377(14):1345-56.
157. Gabay C. Interleukin-6 and chronic inflammation. Arthritis Research & Therapy. 2006;8(2):S3.
158. Schmidt H, Bastholt L, Geertsen P, Christensen IJ, Larsen S, Gehl J, et al. Elevated neutrophil and monocyte counts in peripheral blood are associated with poor survival in patients with metastatic melanoma: a prognostic model. British Journal of Cancer. 2005;93(3):273-8.
159. Zhang Y, Parmigiani G, Johnson WE. ComBat-seq: batch effect adjustment for RNA-seq count data. NAR Genom Bioinform. 2020;2(3):lqaa078.
160. Marshall JS, Warrington R, Watson W, Kim HL. An introduction to immunology and immunopathology. Allergy, Asthma & Clinical Immunology. 2018;14(2):49.
161. Pollak TA, Rogers JP, Nagele RG, Peakman M, Stone JM, David AS, et al. Antibodies in the Diagnosis, Prognosis, and Prediction of Psychotic Disorders. Schizophr Bull. 2019;45(1):233-46.
162. Wang J, Han X, Chen Y, Xie H, Zhang Y, Cui Y, et al. Organ-specific immune-related adverse events and survival in patients with cancer with immune checkpoint inhibitors. Journal of Clinical Oncology. 2024;42(16_suppl):12124-.
163. Downey SG, Klapper JA, Smith FO, Yang JC, Sherry RM, Royal RE, et al. Prognostic Factors Related to Clinical Response in Patients with Metastatic Melanoma Treated by CTL-Associated Antigen-4 Blockade. Clinical Cancer Research. 2007;13(22):6681-8.
164. Freeman-Keller M, Kim Y, Cronin H, Richards A, Gibney G, Weber JS. Nivolumab in Resected and Unresectable Metastatic Melanoma: Characteristics of Immune-Related Adverse Events and Association with Outcomes. Clinical Cancer Research. 2016;22(4):886-94.
165. Indini A, Di Guardo L, Cimminiello C, Prisciandaro M, Randon G, De Braud F, et al. Immune-related adverse events correlate with improved survival in patients undergoing anti-PD1 immunotherapy for metastatic melanoma. Journal of Cancer Research and Clinical Oncology. 2019;145(2):511-21.

166. Villa-Crespo L, Podlipnik S, Anglada N, Izquierdo C, Giavedoni P, Iglesias P, et al. Timeline of Adverse Events during Immune Checkpoint Inhibitors for Advanced Melanoma and Their Impacts on Survival. Cancers (Basel). 2022;14(5).
167. Arnaud-Coffin P, Maillet D, Gan HK, Stelmes J-J, You B, Dalle S, et al. A systematic review of adverse events in randomized trials assessing immune checkpoint inhibitors. International Journal of Cancer. 2019;145(3):639-48.
168. Zhou X, Yao Z, Yang H, Liang N, Zhang X, Zhang F. Are immune-related adverse events associated with the efficacy of immune checkpoint inhibitors in patients with cancer? A systematic review and meta-analysis. BMC Medicine. 2020;18(1):87.
169. Choi J, Lee SY. Clinical Characteristics and Treatment of Immune-Related Adverse Events of Immune Checkpoint Inhibitors. Immune Netw. 2020;20(1):e9.
170. Tanaka T, Narazaki M, Kishimoto T. IL-6 in inflammation, immunity, and disease. Cold Spring Harb Perspect Biol. 2014;6(10):a016295.
171. Banchereau J, Blanchard D, Brière F, Galizzi JP, Garrone P, Hermann P, et al. Role of cytokines in human B lymphocyte growth and differentiation. Nouv Rev Fr Hematol (1978). 1993;35(1):61-6.
172. Arpin C, Déchanet J, Van Kooten C, Merville P, Grouard G, Brière F, et al. Generation of Memory B Cells and Plasma Cells in Vitro. Science. 1995;268(5211):720-2.
173. Agematsu K, Nagumo H, Oguchi Y, Nakazawa T, Fukushima K, Yasui K, et al. Generation of plasma cells from peripheral blood memory B cells: synergistic effect of interleukin-10 and CD27/CD70 interaction. Blood. 1998;91(1):173-80.
174. Syeda MZ, Hong T, Huang C, Huang W, Mu Q. B cell memory: from generation to reactivation: a multipronged defense wall against pathogens. Cell Death Discovery. 2024;10(1):117.
175. Janeway C.A Jr. TP, Walport M., et al. Immunological memory. 2001. In: Immunobiology: The Immune System in Health and Disease [Internet]. Available from: Available from: https://www.ncbi.nlm.nih.gov/books/NBK27158/.
176. Coico RF, Finkelman F, Swenson CD, Siskind GW, Thorbecke GJ. Exposure to crosslinked IgD induces receptors for IgD on T cells in vivo and in vitro. Proceedings of the National Academy of Sciences. 1988;85(2):559-63.
177. Coico RF, Xue B, Wallace D, Pernis B, Siskind GW, Thorbecke GJ. T cells with receptors for IgD. Nature. 1985;316(6030):744-6.
178. Wu Y, Lakshmi Tamma SM, Lima V, Coico R. Facilitated Antigen Presentation by B Cells Expressing IgD when Responding T Cells Express IgD-Receptors. Cellular Immunology. 1999;192(2):194-202.
179. Reynolds KL, Arora S, Elayavilli RK, Louv WC, Schaller TH, Khandelwal A, et al. Immune-related adverse events associated with immune checkpoint inhibitors: a call to action for collecting and sharing clinical trial and real-world data. Journal for ImmunoTherapy of Cancer. 2021;9(7):e002896.
180. Maurer M, Müller AC, Parapatics K, Pickl WF, Wagner C, Rudashevskaya EL, et al. Comprehensive Comparative and Semiquantitative Proteome of a Very Low Number of Native and Matched Epstein–Barr-Virus-Transformed B Lymphocytes Infiltrating Human Melanoma. Journal of Proteome Research. 2014;13(6):2830-45.
181. Kuchen S, Robbins R, Sims GP, Sheng C, Phillips TM, Lipsky PE, et al. Essential role of IL-21 in B cell activation, expansion, and plasma cell generation during CD4+ T cell-B cell collaboration. J Immunol. 2007;179(9):5886-96.
182. Zarnegar B, He JQ, Oganesyan G, Hoffmann A, Baltimore D, Cheng G. Unique CD40-mediated biological program in B cell activation requires both type 1 and type 2 NF-κB activation pathways. Proceedings of the National Academy of Sciences. 2004;101(21):8108-13.
183. Mingari MC, Gerosa F, Carra G, Accolla RS, Moretta A, Zubler RH, et al. Human interleukin-2 promotes proliferation of activated B cells via surface receptors similar to those of activated T cells. Nature. 1984;312(5995):641-3.